

ANALYSIS OF
MULTILAYER SANDWICH BEAMS
AND
MULTIPLIER SHEAR WALLS

ANALYSIS OF
MULTILAYER SANDWICH BEAMS
AND
MULTIPLIER SHEAR WALLS

by

Hans Benninghoven, Dipl.-Ing. (TH Darmstadt, W. Germany)

A Project Report
-Submitted to the Faculty of Graduate Studies
in Partial Fulfilment of the Requirements
for the Degree
Master of Engineering

McMaster University

March 1978

ACKNOWLEDGEMENTS:

I would like to thank Dr. Robinson for his instructions and his helpful understanding during the preparation of this thesis.

Also many thanks to the Department of Civil Engineering and Engineering Mechanics of McMaster University and the Canadian people for their generous support and hospitality.

TABEL OF CONTENTS

<u>Chapter</u>	<u>Page</u>
1. <u>Introduction</u>	1
1.1 Introduction	1
1.2 Research on multiplier shear walls	1
1.3 Object and Scope	3
2. <u>Development of the basic differential equations for the multiplier shear wall problem and the multilayer sandwich beam problem</u>	5
2.1 Real and continuous system	5
2.2 Assumptions	8
2.3 Equilibrium	9
2.4 Compatibility	13
2.5 System of differential equations for the multiplier shear wall problem	19
3. <u>Solution of the system of differential equations for the multiplier shear wall problem</u>	23
3.1 Boundary conditions	23
3.2 Solution of the system of differential equations by means of Fourier series	24
3.3 Reactions and deflection	30
3.4 Forces in discrete connecting beams	38
3.5 Some special loadcases	40
3.6 Examples	46

<u>Chapter</u>	<u>Page</u>
4. <u>Stiffness parameter ρ_m</u>	52
4.1 Derivation of the stiffness parameter ρ_m	52
4.2 Comparison of ρ_m -parameters and $\bar{\alpha}$ -parameters for symmetrical ^m two-pier shear walls	55
4.3 Examples for the significance of the ρ_m -parameters	59
5. <u>The multilayer sandwich beam</u>	69
5.1 Mathematical formulation of the multilayer sandwich beam problem for simple supporting and symmetrical loading	69
5.2 Example	71
5.3 Discussion of the results of chapter 5.2	78
6. <u>Development of programs</u>	80
6.1 The multilayer sandwich beam program	80
6.2 The shear wall program with piecewise trapezoidal load	82
7. <u>Conclusions</u>	86
7.1 Conclusions	86
7.2 Future developments	87
Appendix A: Computer program listing, input and output data for multilayer sandwich beam program	89
Appendix B: Computer program listing, input and output data for shear wall program with piecewise trapezoidal load	97
Bibliography	107

Notation

Note: Other symbols are defined when used, suffices m refer to pier (layer) m or interface m

I_{B_m}	moment of inertia of connecting beams
AB_m	effective cross-sectional shear area of connecting beams
I_m	moment of inertia of pier (layer)
A_m	cross-sectional area of pier (layer)
K_m	shear modulus of laminas
ρ_m	stiffness parameter defined in Eq. (4.1.6)
E	modulus of elasticity
G	shear modulus
μ	= G/E
I_c	arbitrary moment of inertia for comparison
i_m	ratio of moment of inertia of pier (layer) m to sum of moments of inertia of all piers (layers)
a	story height
H	shear wall height
l_m	span of connecting beams
a_m	distance of center lines of pier (layer) m to pier (layer) m+1
b_m	distance of center line of pier (layer) m to midspan of connecting beams of interface m
c_m	distance of center line of pier (layer) m+1 to midspan of connecting beams of interface m
r	number of piers (layers)
y	coordinate of deflection
x, η, λ	coordinate of pier axis (layer axis)
ξ	= x/H
$p(x)$	external loading

$p_m(x)$	external loading of pier (layer) m
$q_m(x)$	shear intensity in connecting medium
$n_m(x)$	normal force intensity in connecting medium
N_m^*	singular normal force in connecting medium
$M_o(x)$	total bending moment
$M_{o,m}(x)$	bending moment in pier (lamina) m due to $p_m(x)$ in statically determinate system
$M_{q,m}(x)$	bending moment in pier (lamina) m due to $q_m(x)$ in statically determinate system
$M_{n,m}(x)$	bending moment in pier (lamina) m due to $n_m(x)$ in statically determinate system
$M_m(x)$	bending moment in pier (lamina) m in statically indeterminate system
$\bar{M}(x)$	$= M_m(x) \frac{I_c}{I_m}$
$N_m(x)$	Normal force in pier (layer)
x_b	Location of connecting beam
$Q_m(x_b)$	shear force in connecting beam
$N_m^c(x_b)$	normal force in connecting beam

CHAPTER I

Introduction

1.1 Introduction

In the last few years research of composite structures was of increasing importance. This was partially due to demands for more efficient design and partially due to the interest of engineers and scientists in investigating how an actual structure as a whole responds to actual conditions.

Shear walls can be considered as composite structures. In this case the walls of arbitrary shape correspond to the layers of the composite structure and the connecting beams correspond to the flexible connection of the composite structure.

This report investigates a special problem of composite and shear wall structures, namely the multiplier shear wall under arbitrary horizontal loading and the multilayer sandwich beam under symmetrical loading. The mathematical problem for both structures is the same.

1.2 Research on multiplier shear walls

The first investigation and solution of a shear wall problem was given by Beck ⁽¹⁾ in 1956. In this paper Beck gave the solution for a symmetrical two-pier shear wall, neglecting the effect of normal deformation of the piers and using the so called continuous method. This method is based on the assumption, that a large number

of discrete connectors can be considered as a continuous connection 2
consisting of very small laminas. The advantage is, that the large
number of redundants is replaced by one function of the unknown shear
intensity in the connecting laminas.

The idea of the continuous method turned out to be very efficient
and was used in many other research projects, as it will be used in
this thesis as well.

A later contribution to the shear wall topic by Beck ⁽²⁾ was to take
the effect of normal deformation of the piers into account and he
developed the $\bar{\alpha}$ -parameter, which showed that if the stiffness of the
connecting beams is very small, the effect of normal deformation of the
piers can be neglected, or if the stiffness of the connecting beams is
very large, full interaction can be assumed. Full interaction means that
the unknown shear intensity as well as all other reactions and
deformations can be determined with the well-known beam theory.

In 1958 Beck ⁽³⁾ published a paper investigating a multilayer problem,
however neglecting the normal deformation of the layers. This simpli-
fication again leads to one differential equation of the unknown shear
intensity and is only agreeable, if the stiffness of the connection
(connecting beams) is very small. For a reasonably stiff connection the
normal deformation of the layers (walls) cannot be neglected and a multi-
layer, or a multiplier problem leads to a system of inhomogeneous
differential equations of the second order with constant coefficients.

Based on the publication of Beck, Eriksson ⁽⁴⁾ solved the multiplier shear wall

problem including the effect of normal deformation of the piers. Eriksson solved the set of $(n - 1)$ differential equations for a shear wall system of n piers by stepwise substituting one unknown shear intensity after the other, and finally obtained one differential equation of $(2n-2)$ order. This standard method of solution is very tedious and not practical for a large number of piers.

Another approach to this problem was made by Eisert⁽⁵⁾ in 1967 using matrix methods. The solution type of Sinh and Cosh or e-function respectively for the unknown shear intensities eliminates the second derivatives. The remaining matrix of coefficients can be solved with eigenvalues and eigenvectors. However Eisert chose a special type of solution which only gives a solution for the load cases: single load on top of the piers and uniformly distributed load. Obviously this is a limited case, and a more complete solution is desirable. This solution, based on the same theory as⁽⁵⁾, was presented by Despeyroux⁽⁶⁾ in 1969. Despeyroux did not choose a special type of solution as did Eisert⁽⁵⁾. Instead he developed the eigenvectors and the proper functions. This is mathematically more consistent, and leads to a more powerful and complete solution.

1.3 Object and Scope

It should be mentioned that the author came to know the publications (4), (6) after having finished his own development of theory. The findings of Eisert⁽⁵⁾ were used

- (a) to develop a complete solution of the multiplier shear wall problem
- (b) to investigate if, similar to the $\bar{\alpha}$ -parameters of Beck⁽²⁾, certain

ρ_i -parameters for each interface i could be found

4

(c) to analyse the multilayer sandwich beam under symmetrical loading

A new type of solution was found by means of Fourier series which seems to be more comprehensible and gives a better insight into the nature of the structure.

The corresponding programs are simpler than for the other methods since the calculation of the eigenvalues and eigenvectors can be avoided.

CHAPTER II

Development of the basic differential equations for the multiplier shear wall problem and the multilayer sandwich beam problem

2.1 Real and continuous system

The real discontinuous system is assumed to have the following properties, (Fig. 2.1.1):

- a) The cross-section of the piers is constant over the shear wall height but may differ from pier to pier.
- b) The story height a is constant. In each story the piers are connected by connecting beams. The connecting beams of each interface have the same properties: the same length, moment of inertia and effective shear area. The last connecting beam on shear wall top however only has half of the moment of inertia and effective shear area of the other connecting beams of the same interface.

These properties of the connecting beams can be different for different interfaces.

- c) The piers are cantilevers with fixed ends.

For the continuous system (Fig. 2.1.2) the connecting beams are assumed to be replaced by a continuous row of laminas of thickness dx . The moment of inertia of these laminas is $I B_m \frac{dx}{a}$ and the effective shear area is $A B_m \frac{dx}{a}$.

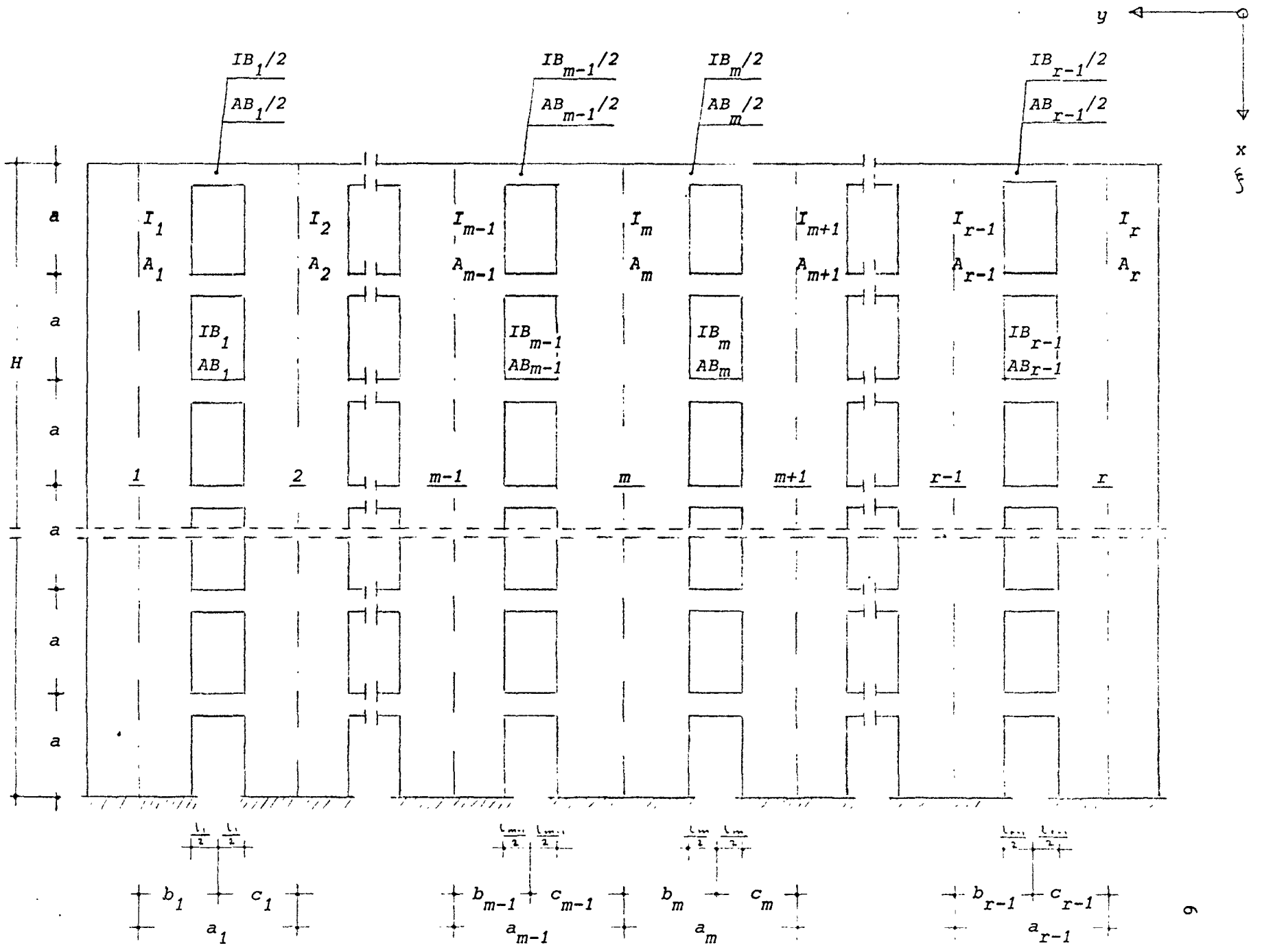


Fig. 2.1.1. Real System

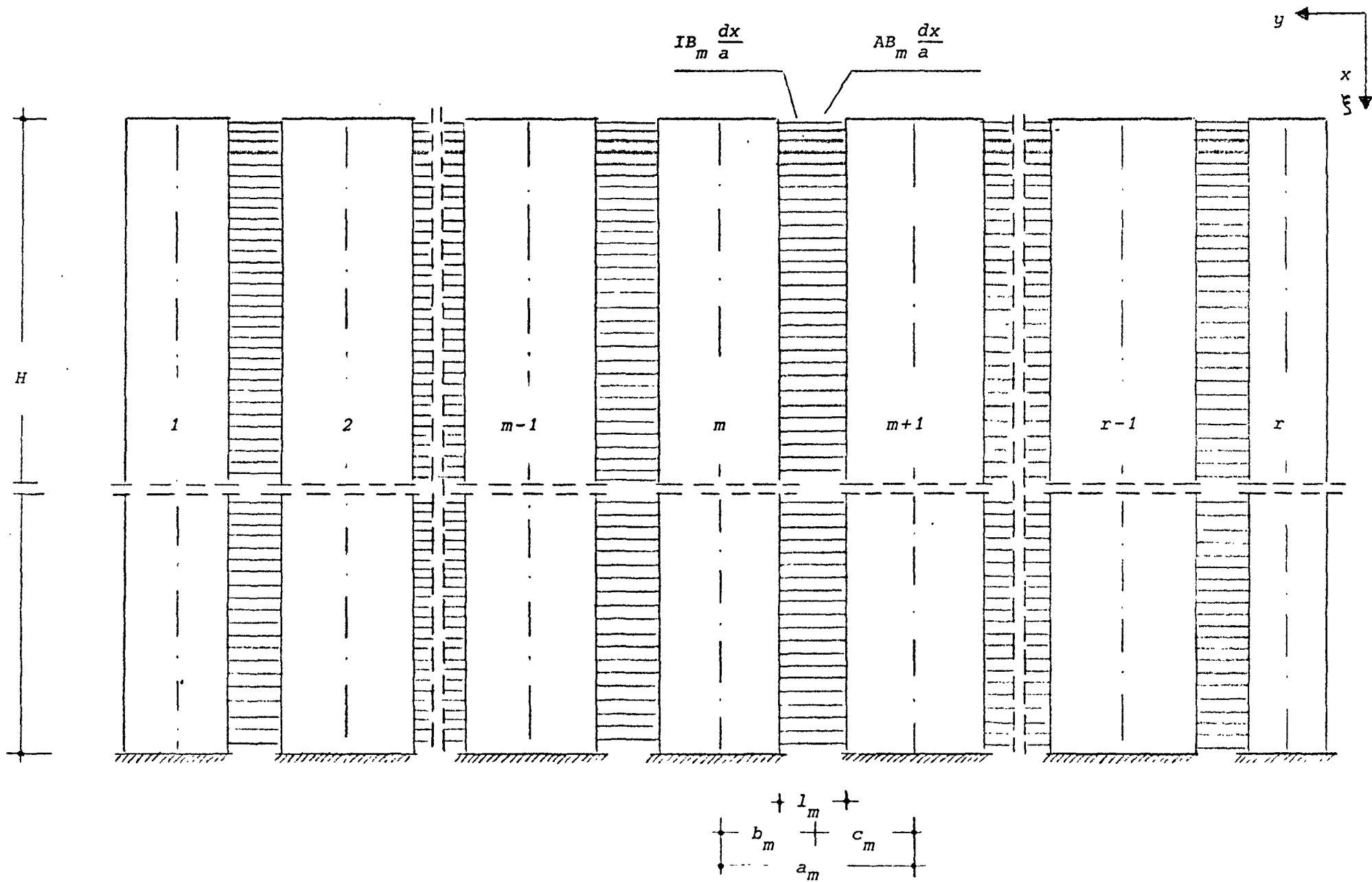


Fig. 2.1.2. Continuous System

2.2 Assumptions

For the development of the multiplier problem the following assumptions are made:

- a) The validity of the beam theory
- b) Shear deformation of the piers is negligible
- c) The connecting beams and laminas respectively are rigid in direction y but flexible in direction x (i.e. the normal deformation of the laminas is assumed to be negligible)
- d) The stiffness of the connecting beams is small compared with the stiffness of the piers such that the joint rotation of the pier-connecting beam joints can be neglected.
- e) From (a), (b) and (c) it follows that the center lines of all piers deflect equally. The differential equation for deflection is the same for all piers, namely $E I_c y''(x) = - M_m(x) \frac{I_c}{I_m} = - \bar{M}(x)$.
- f) From (d) and (e) follows that the point of contraflexure of the laminas is in the middle of the laminas.
- g) From (e) it also follows that the external loads $p(x)$ can be assumed distributed in such manner, that each pier is loaded according to the ratio of its own moment of inertia to the sum of moments of inertia of all piers:

$$P_m(x) = p(x) \frac{I_m}{\sum_{v=1}^r I_v} = p(x) \frac{I_m}{\sum I} \quad (2.2.1)$$

In order to obtain a statically determinate system all piers are assumed to be cut off in the middle of the laminas (Fig. 2.3.1). The only unknown forces in the middle of the laminas are:

- a) the shear intensity (i. e. the function of shear forces per unit length) $q_m(x)$, which is assumed positive in direction $+x$ at a positive interface (i. e. an interface with the axis $+y$ perpendicular to it)
- b) the normal forces per unit length $n_m(x)$, which are assumed positive as tension.
- c) the singular normal forces N_m^* at the top of the shear wall, are assumed positive when in tension.

As the points of contraflexure of the laminas are postulated to be at midspan, the bending moments vanish at the midspan.

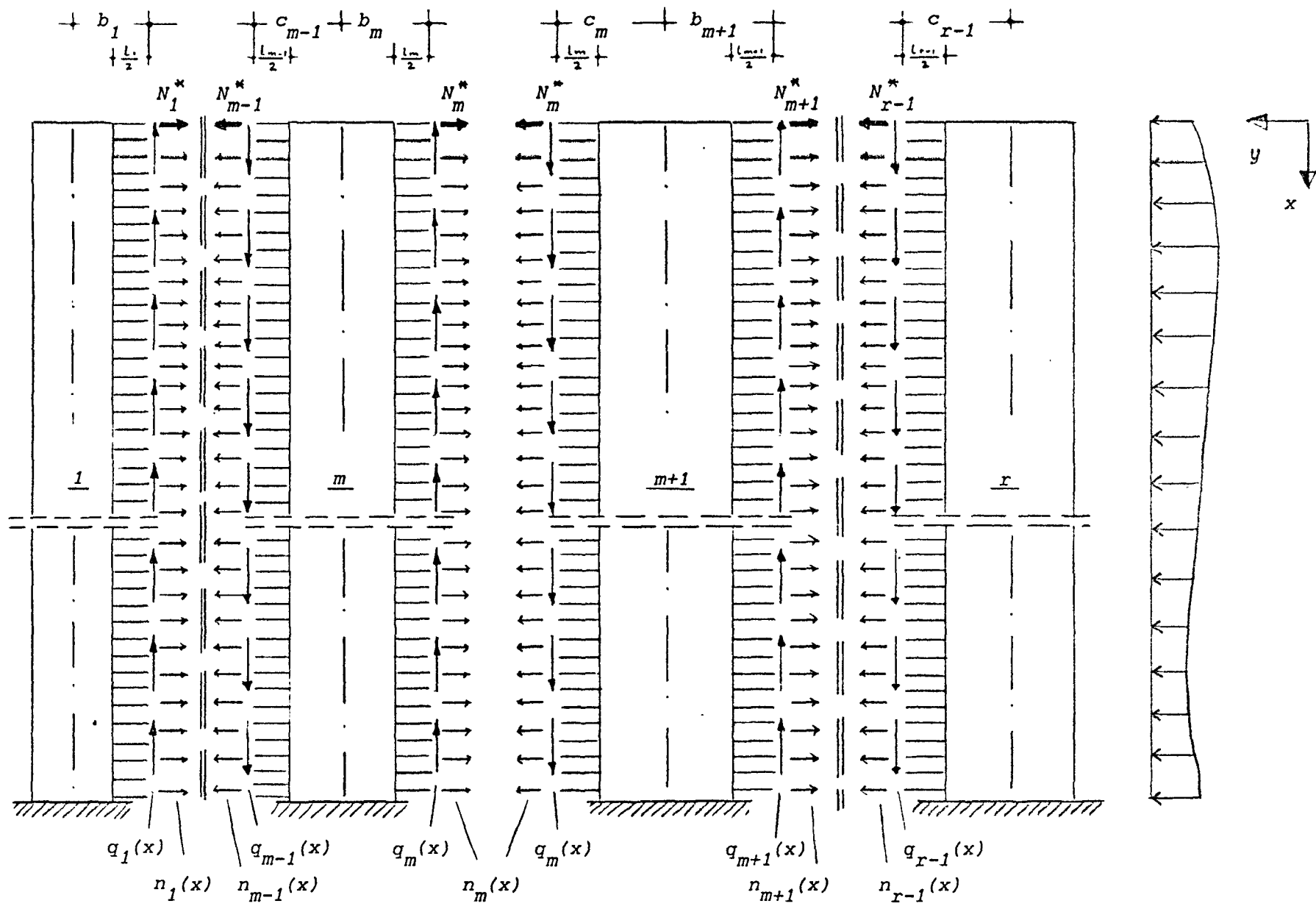


Fig. 2.3.1. Reactions

The bending moments $M_m(x)$ in the piers shall be positive, if the outer fibres of a positive interface are in tension. The bending moments caused by the loading $p_m(x)$ are called $M_{o,m}(x)$. The normal forces $N_m(x)$ in the piers are positive when in tension.

The bending moments in pier (m) can be determined as follows:

Bending moments due to shear intensities $q_{m-1}(\eta)$ and $q_m(\eta)$:

$$M_{q,m}(x) = \int_0^x [-b_m q_m(\eta) - c_{m-1} q_{m-1}(\eta)] d\eta \quad (2.3.1)$$

Bending moments due to normal forces $n_{m-1}(\eta)$ and $n_m(\eta)$

$$M_{n,m}(x) = \int_0^x [n_m(\eta) - n_{m-1}(\eta)] (x-\eta) d\eta + [N_m^* - N_{m-1}^*] \cdot x \quad (2.3.2)$$

(note: $1 \leq m \leq r$; $q_0(\eta) = q_r(\eta) = n_0(\eta) = n_r(\eta) = 0$;
 $N_0^* = N_r^* = 0$)

The total bending moment $M_m(x)$ can be written as

$$M_m(x) = M_{o,m}(x) + M_{q,m}(x) + M_{n,m}(x) \quad (2.3.3)$$

From (2.3.2) it is obvious that

$$\sum_{v=1}^r M_{n,v}(x) = 0$$

such that the sum of all bending moments of the piers gives

$$\sum_{v=1}^r M_v(x) = \sum_{v=1}^r M_{o,v}(x) + \sum_{v=1}^r M_{q,v}(x) \quad (2.3.4)$$

Eq. (2.3.4) provides the possibility to express $M_v(x)$ only as a function of $q_v(x)$.

According to the load distribution Eq. (2.2.1) we can write

$$M_{o,m}(x) = \frac{I_m}{\sum I} \sum_{v=1}^r M_{o,v}(x). \quad (2.3.5)$$

since from Eq. (2.2.1) we observe the relation

$$\frac{p_m(x)}{p(x)} = \frac{M_{o,m}(x)}{\sum_{v=1}^r M_{o,v}(x)} = \frac{I_m}{\sum I}$$

From the assumption that all piers have the same deflection we obtain

$$\frac{M_m(x)}{I_m} = \frac{M_v(x)}{I_v} = \frac{\sum_{v=1}^r M_v(x)}{\sum I} \quad (2.3.6)$$

With the abbreviation

$$i_m = \frac{I_m}{\sum_{v=1}^r I_v} \quad (2.3.7)$$

Eq. (2.3.5) and Eq. (2.3.6) can be written

$$M_{o,m}(x) = i_m \sum_{v=1}^r M_{o,v}(x) \quad (2.3.8)$$

$$M_m(x) = i_m \sum_{v=1}^r M_v(x) \quad (2.3.9)$$

Multiplying Eq. (2.3.4) by i_m and substituting Eq. (2.3.8) and Eq. (2.3.9) into Eq. (2.3.4) we obtain

$$M_m(x) = M_{0,m}(x) + i_m \sum_{v=1}^r M_{q,v}(x) \quad (2.3.10)$$

The differential equation for deflection is the same for all piers:

$$E I_m y'' = - M_m(x) \quad (2.3.11)$$

2.4 Compatibility

The relative displacements of the laminas in the statically determinate system have to vanish in the original statical indeterminate system by means of the unknown shear intensities $q_m(x)$

- a) The relative displacements of the tips of the laminas (Fig. 2.4.1) due to the pier deflection $y(x)$ are

$$\begin{aligned} \delta_{1,m}(x) &= \delta_{1,m}^{(1)}(x) + \delta_{1,m}^{(2)}(x) \\ &= b_m y'(x) + c_m y'(x) = a_m y'(x) \end{aligned} \quad (2.4.1)$$

- b) The relative displacements of the laminatips due to shear intensity $q_m(x)$ (Fig. 2.4.2) in consequence of bending deformation are

$$\begin{aligned} \delta_{2,m}(x) &= \delta_{2,m}^{(1)}(x) + \delta_{2,m}^{(2)}(x) \\ &= -\frac{1}{24} L_m^3 \frac{a}{E I B_m} q_m(x) - \frac{1}{24} L_m^3 \frac{a}{E I B_m} q_m(x) \\ &= -\frac{1}{12} L_m^3 \frac{a}{E I B_m} q_m(x) \end{aligned} \quad (2.4.2)$$

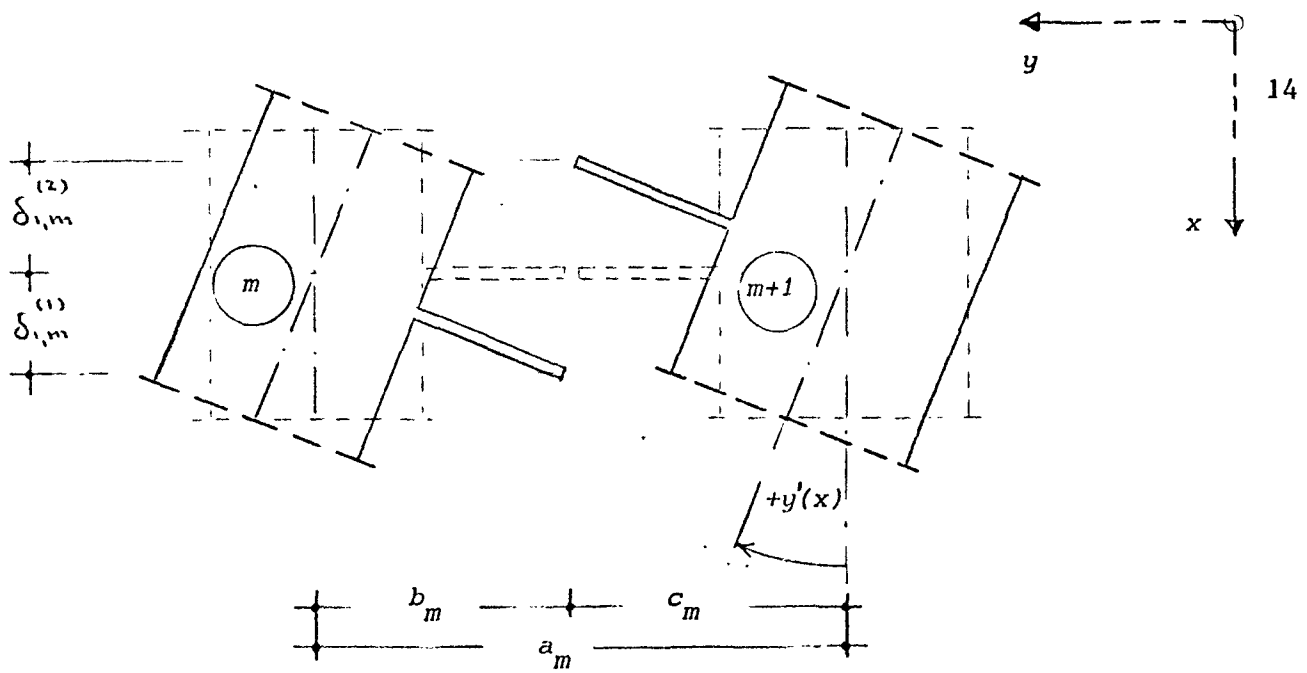
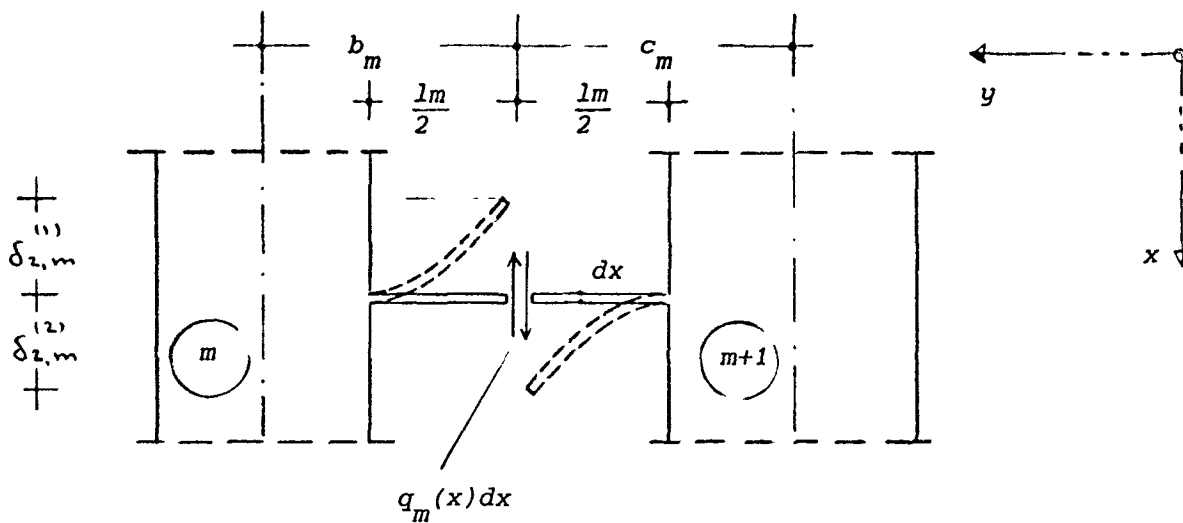


Fig. 2.4.1 Lamina displacements due to $y(x)$



Moment of inertia of lamina: $\frac{I B_m}{a} dx$

shear force in lamina: $q_m(x) dx$

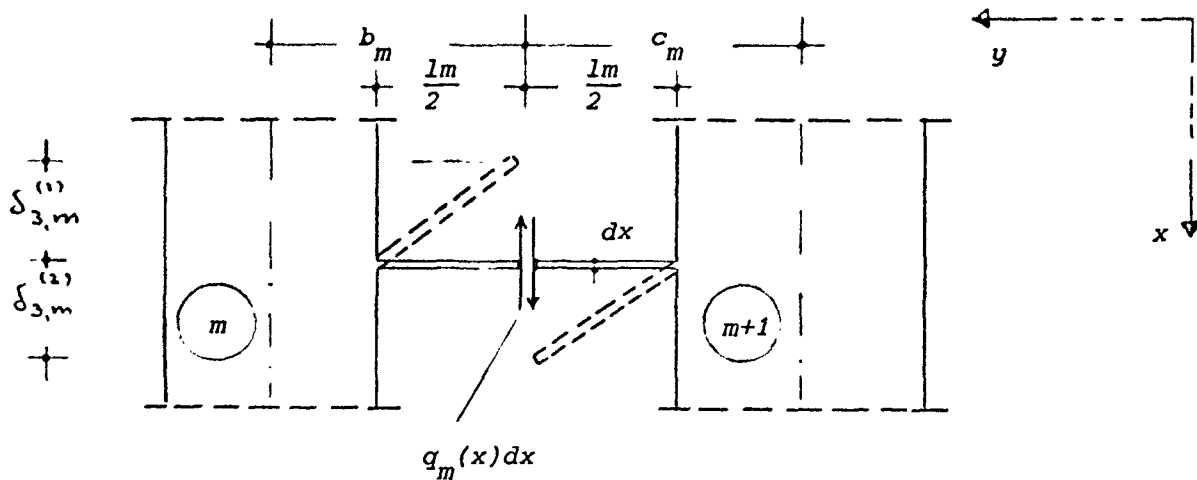
displacement $\delta_{2,m}^{(1)} = \delta_{2,m}^{(2)} = -\frac{q_m(x) dx}{3E \frac{I B_m}{a} dx} \left(\frac{L_m}{2}\right)^3$

Fig. 2.4.2 Bending deformation of laminas

c) The relative displacements of the lamina tips due to shear intensity $q_m(x)$ as a consequence of shear deformation (Fig. 2.4.3) are

15

$$\begin{aligned} \delta_{3,m} &= \delta_{3,m}^{(1)} + \delta_{3,m}^{(2)} \\ &= - \frac{q_m(x) \cdot a}{G \cdot AB_m} \frac{lm}{2} - \frac{q_m(x) \cdot a}{G \cdot AB_m} \frac{lm}{2} \\ &= - \frac{q_m(x) \cdot a}{G \cdot AB_m} lm \end{aligned} \quad (2.4.3)$$



effective shear area of a lamina: $\frac{AB_m}{a} dx$

shear forces in lamina: $q_m(x) dx$

displacement: $\delta_{3,m}^{(1)} = \delta_{3,m}^{(2)} = - \frac{q_m(x) dx}{G \frac{AB_m}{a} dx} \frac{lm}{2}$

Fig. 2.4.3 Shear deformation of laminas

d) The relative displacements of the lamina tips due to normal deformation of the piers (Fig. 2.4.4) are

16

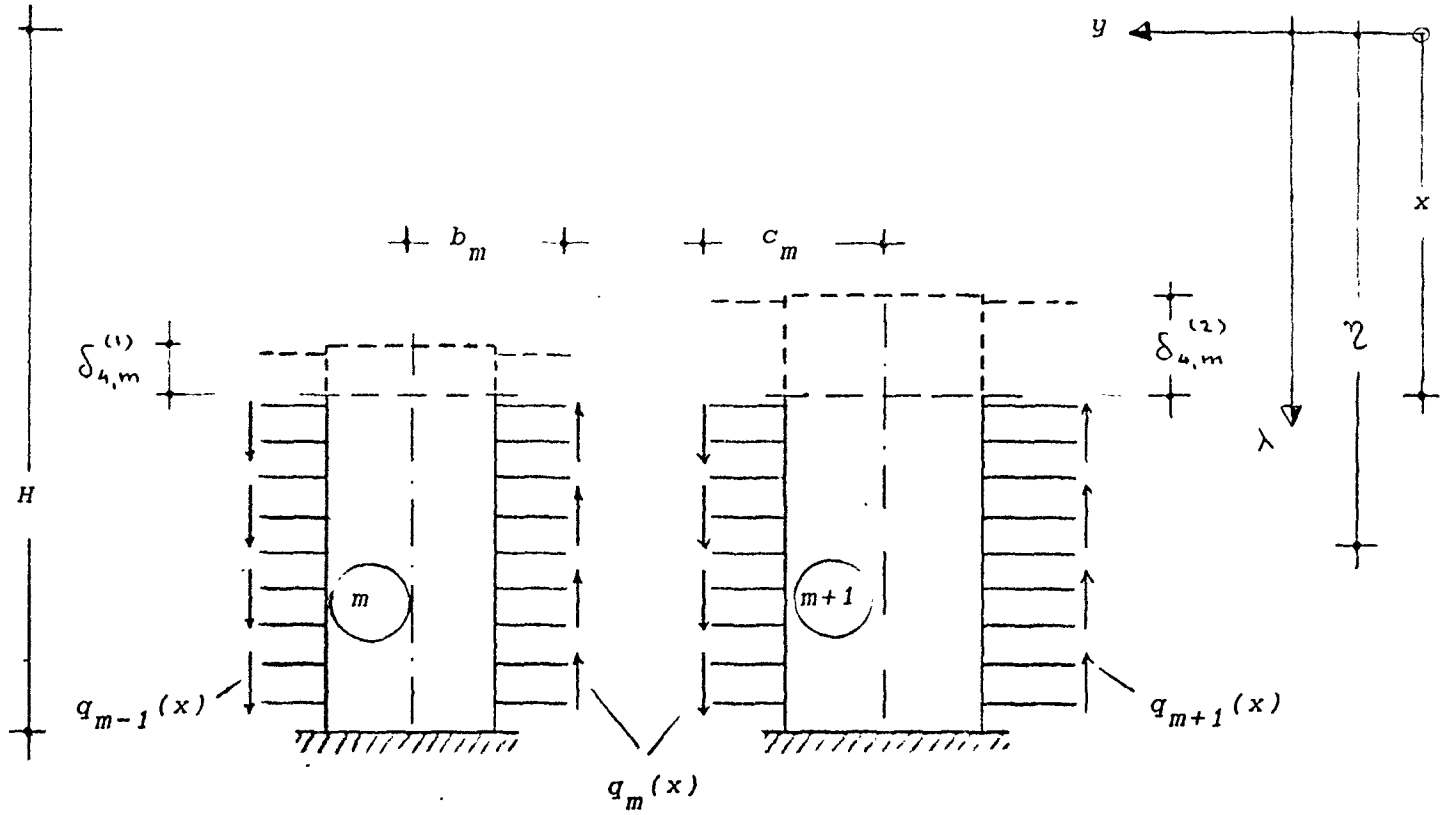
$$\begin{aligned}
 \delta_{4,m} &= \delta_{4,m}^{(2)} - \delta_{4,m}^{(1)} \\
 &= \frac{1}{EA_m} \int_x^H \left\{ \int_0^{\eta} q_{m-1}(\lambda) d\lambda \right\} d\eta \\
 &\quad - \left(\frac{1}{EA_m} + \frac{1}{EA_{m+1}} \right) \int_x^H \left\{ \int_0^{\eta} q_m(\lambda) d\lambda \right\} d\eta \\
 &\quad + \frac{1}{EA_{m+1}} \int_x^H \left\{ \int_0^{\eta} q_{m+1}(\lambda) d\lambda \right\} d\eta
 \end{aligned} \tag{2.4.4}$$

Now the compatibility condition can be defined as

$$\delta_{1,m} + \delta_{2,m} + \delta_{3,m} + \delta_{4,m} = 0 \tag{2.4.5}$$

Substituting (2.4.1), (2.4.2), (2.4.3) and (2.4.4) into (2.4.5) we obtain

$$\begin{aligned}
 a_m \gamma'(x) &- \left(\frac{L_m \cdot a^3}{12 EIB_m} + \frac{L_m \cdot a}{GAB_m} \right) q_m(x) \\
 &+ \frac{1}{EA_m} \int_x^H \left\{ \int_0^{\eta} q_{m-1}(\lambda) d\lambda \right\} d\eta \\
 &- \left(\frac{1}{EA_m} + \frac{1}{EA_{m+1}} \right) \int_x^H \left\{ \int_0^{\eta} q_m(\lambda) d\lambda \right\} d\eta \\
 &+ \frac{1}{EA_{m+1}} \int_x^H \left\{ \int_0^{\eta} q_{m+1}(\lambda) d\lambda \right\} d\eta = 0
 \end{aligned} \tag{2.4.6}$$



$$N_m(\eta) = \int_0^{2\zeta} [q_m(\lambda) - q_{m-1}(\lambda)] d\lambda$$

$$N_{m+1}(\eta) = \int_0^{2\zeta} [q_{m+1}(\lambda) - q_m(\lambda)] d\lambda$$

$$\delta_{4,m}^{(1)} = + \int_x^H \frac{N_m(\eta)}{EA_m} d\eta = + \frac{1}{EA_m} \int_x^H \left\{ \int_0^{2\zeta} [q_m(\lambda) - q_{m-1}(\lambda)] d\lambda \right\} d\eta$$

$$\delta_{4,m}^{(2)} = + \int_x^H \frac{N_{m+1}(\eta)}{EA_{m+1}} d\eta = + \frac{1}{EA_{m+1}} \int_x^H \left\{ \int_0^{2\zeta} [q_{m+1}(\lambda) - q_m(\lambda)] d\lambda \right\} d\eta$$

Fig. 2.4.4 Lamina displacement due to normal deformation of piers

Defining

18

$$k_m = \frac{1}{\frac{l_m^3 a}{12 E I B_m} + \frac{l_m a}{G A B_m}} \quad (2.4.7)$$

and differentiating (2.4.6) twice and observing that

$$\frac{d}{dx} \left(+ \int_x^H \left\{ \int_0^{\eta} q_{m-1}(\lambda) d\lambda \right\} d\eta \right) = - \int_0^x q_{m-1}(\lambda) d\lambda$$

and

$$\frac{d}{dx} \left(- \int_0^x q_{m-1}(\lambda) d\lambda \right) = - q_{m-1}(x)$$

and substituting (2.4.7) into the second derivative of Eq. (2.4.6)

gives

$$\begin{aligned} a_m y'''(x) - \frac{1}{k_m} q_m''(x) - \frac{1}{EA_m} q_{m-1}(x) \\ + \left(\frac{1}{EA_m} + \frac{1}{EA_{m+1}} \right) q_m(x) \\ - \frac{1}{EA_{m+1}} q_{m+1}(x) = 0 \end{aligned} \quad (2.4.8)$$

Substituting Eq. (2.3.1) into Eq. (2.3.10) we obtain

$$M_m(x) = M_{0,m}(x) + i_m \sum_{v=1}^{r-1} [-a_v \int_0^x q_v(\eta) d\eta] \quad (2.5.1)$$

The first derivative of Eq. (2.5.1) is

$$M'_m(x) = M'_{0,m}(x) - i_m \sum_{v=1}^{r-1} a_v q_v(x) \quad (2.5.2)$$

Differentiating Eq. (2.3.11) and with Eq. (2.5.2) we obtain from Eq. (2.4.8)

$$\begin{aligned} & -\frac{1}{k_m} q''_m(x) - \frac{1}{EA_m} q_{m-1}(x) \\ & + \left(\frac{1}{EA_m} + \frac{1}{EA_{m+1}} \right) q_m(x) - \frac{1}{EA_{m+1}} q_{m+1}(x) \\ & + \frac{a_m i_m}{EI_m} \sum_{v=1}^{r-1} a_v q_v(x) = \frac{a_m}{EI_m} M'_{0,m}(x) \end{aligned} \quad (2.5.3)$$

Multiplying Eq. (2.5.3) by $(-\Sigma EI)$ and observing that

$$\frac{\Sigma EI}{EI_m} a_m M'_{0,m}(x) = a_m \frac{M'_{0,m}(x)}{i_m} = a_m M'_0(x)$$

then Eq. (2.5.3) can be written

$$\begin{aligned} & \frac{\Sigma EI}{k_m} q''_m(x) + \frac{\Sigma EI}{EA_m} q_{m-1}(x) - \left(\frac{\Sigma EI}{EA_m} + \frac{\Sigma EI}{EA_{m+1}} \right) q_m(x) \\ & + \frac{\Sigma EI}{EA_{m+1}} q_{m+1}(x) - \sum_{v=1}^{r-1} a_m a_v q_v(x) \\ & = -a_m M'_0(x) \end{aligned} \quad (2.5.4)$$

Eq. (2.5.4) represents a system of $(r-1)$ linear, nonhomogeneous differential equations of second order with constant coefficients. To show this clearly, certain constants may be rewritten

$$\gamma_m = + \frac{\sum EI}{k_m} \quad \text{for } 1 \leq m \leq r-1 \quad (2.5.5)$$

$$\delta_{m,v} = a_m a_v \quad \text{for } 1 \leq v \leq m-2 \\ m+2 \leq v \leq r-1$$

$$\delta_{m,m-1} = a_m a_{m-1} - \frac{\sum EI}{EA_m} \quad \text{for } v = m-1$$

$$\delta_{m,m} = a_m^2 + \frac{\sum EI}{EA_m} + \frac{\sum EI}{EA_{m+1}} \quad \text{for } v = m \quad (2.5.6)$$

$$\delta_{m,m+1} = a_m a_{m+1} - \frac{\sum EI}{EA_{m+1}} \quad \text{for } v = m+1$$

With the abbreviations (2.5.5) and (2.5.6) the system of differential equations Eq. (2.5.4) now can be written

$$\gamma_m q_m''(x) - \sum_{v=1}^{r-1} \delta_{m,v} q_v''(x) = -a_m M_0'(x) \quad (2.5.7)$$

$$\text{for } 1 \leq m \leq r-1$$

The matrix notation for (2.5.7) is

$$[\gamma] \{q''\} - [\delta] \{q\} = -\{a\} M_0'(x) \quad (2.5.8)$$

where the diagonal matrix $[\gamma]$ is

$$[\gamma] = \begin{bmatrix} \gamma_1 & 0 & 0 & \dots & 0 \\ 0 & \gamma_2 & 0 & \dots & 0 \\ 0 & 0 & \gamma_3 & \dots & 0 \\ \vdots & \vdots & \vdots & \ddots & \vdots \\ 0 & 0 & 0 & \dots & \gamma_{r-1} \end{bmatrix}$$

and the vector $\{q''\}$ is

$$\{q''\} = \begin{bmatrix} q_1''(x) \\ q_2''(x) \\ \vdots \\ q_{r-1}''(x) \end{bmatrix}$$

and the matrix $[\delta]$ is

$$[\delta] = \begin{bmatrix} \delta_{1,1} & \delta_{1,2} & \delta_{1,3} & \dots & \delta_{1,r-1} \\ \delta_{2,1} & \delta_{2,2} & \delta_{2,3} & \dots & \delta_{2,r-1} \\ \delta_{3,1} & \delta_{3,2} & \delta_{3,3} & \dots & \delta_{3,r-1} \\ \vdots & \vdots & \vdots & \ddots & \vdots \\ \delta_{r-1,1} & \delta_{r-1,2} & \delta_{r-1,3} & \dots & \delta_{r-1,r-1} \end{bmatrix}$$

and the vector $\{q\}$ is

22

$$\{q\} = \begin{bmatrix} q_1(x) \\ q_2(x) \\ q_3(x) \\ \vdots \\ q_{r-1}(x) \end{bmatrix}$$

and the vector $\{a\}$ is

$$\{a\} = \begin{bmatrix} a_1 \\ a_2 \\ a_3 \\ \vdots \\ a_{r-1} \end{bmatrix}$$

CHAPTER III

Solution of the system of differential equations for the multiplier shear wall problem

3.1 Boundary conditions

From Eq. (2.4.6) it can be observed that at location $x = H$

$$q_m(H) = 0 \quad (3.1.1)$$

since at $x = H$ the slope $y'(H) = 0$

and the integrals $\int_H^H () d\eta = 0$

Eq. (3.1.1) states that all shear intensities $q_m(x)$ in the laminas are zero at the built-in ends of the shear walls. This is obvious from the fact that at $x = H$ there is no relative displacement and rotation of the adjacent interface.

Differentiating Eq. (2.4.6) and with abbreviation (2.4.7) we get

$$\begin{aligned} a_m y''(x) - \frac{1}{k_m} q_m'(x) - \frac{1}{EA_m} \int_0^x q_{m+1}(\lambda) d\lambda \\ + \left(\frac{1}{EA_m} + \frac{1}{EA_{m+1}} \right) \int_0^x q_m(\lambda) d\lambda \\ - \frac{1}{EA_{m+1}} \int_0^x q_{m+1}(\lambda) d\lambda = 0 \end{aligned} \quad (3.1.2)$$

At $x = 0$ the bending moments in the shear walls $M_m(0) = 0$. Therefore from Eq. (2.3.11) we observe $y''(0) = 0$. Also the integrals $\int_0^0 () d\lambda = 0$

and with Eq. (3.1.2) we obtain the second boundary condition

24

$$q'_m(x=0) = 0 \quad (3.1.3)$$

3.2 Solution of the system of differential equations by means of Fourier series

Using the theory of Fourier series and assuming the periodical shape as in Fig. 3.2.1 the total shear force $M'_0(\xi)$ can be developed as a series.

Since certain properties of symmetry are assumed (Fig. 3.2.1) the general series can be specified as follows:

a) $f(\xi)$ is symmetrical about the axis

$$\xi = k \cdot T \quad \text{with } k = 0, 1, 2, 3, \dots$$

therefore all $B_n = 0$

b) $f(\xi)$ is symmetrical about the axis

$$\xi = \frac{T}{2} + k \cdot T \quad \text{with } k = 0, 1, 2, 3, \dots$$

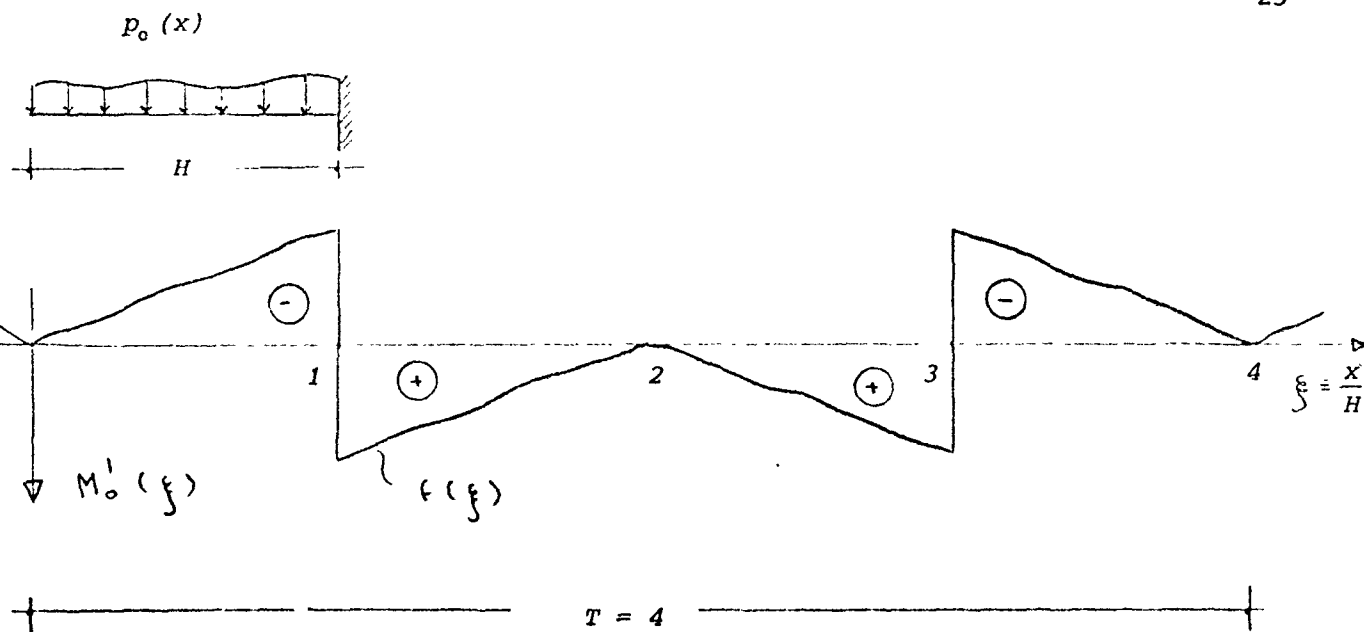
and $f(\xi)$ is antisymmetrical about the axis

$$\xi = \frac{T}{4} + k \cdot \frac{T}{2} \quad \text{with } k = 0, 1, 2, 3, \dots$$

therefore

$$A_n = 0 \quad \text{for } n = 2, 4, 6, \dots$$

$$A_n \neq 0 \quad \text{for } n = 1, 3, 5, \dots$$



Fourier series for $M'_0(\xi)$ in general:

$$M'_0(\xi) = \sum_{n=1}^{\infty} \left(A_n \cos \frac{n2\pi\xi}{T} + B_n \sin \frac{n2\pi\xi}{T} \right)$$

$$A_n = \frac{2}{T} \int_0^T f(\xi) \cos \frac{n2\pi\xi}{T} d\xi$$

$$B_n = \frac{2}{T} \int_0^T f(\xi) \sin \frac{n2\pi\xi}{T} d\xi$$

Fig. 3.2.1 Total shear force $M'_0(\xi)$ developed as Fourier series

With these specifications the Fourier series for $M_0'(\xi)$ can be written as

26

$$M_0'(\xi) = \sum_{n=1}^{\infty} A_n \cos \frac{(2n-1) 2\pi \xi}{T} \quad (3.2.1)$$

and with $\xi = \frac{x}{H}$ and $T = \frac{4H}{H} = 4$

we obtain

$$M_0'(\xi) = \sum_{n=1}^{\infty} A_n \cos \frac{(2n-1)\pi \xi}{2} \quad (3.2.2)$$

The coefficients A_n are:

$$A_n = 4 \frac{2}{T} \int_0^{T/4} f(\xi) \cos \frac{(2n-1) 2\pi \xi}{T} d\xi$$

and with $T=4$ we can write

$$A_n = 2 \int_0^1 f(\xi) \cos \frac{(2n-1)\pi \xi}{2} d\xi \quad (3.2.3)$$

As for any inhomogeneous differential equation of second order and with constant coefficients the particular solution is chosen of the type of the right hand side, i.e. the shear intensities are

$$q_m(\xi) = \sum_{n=1}^{\infty} C_{m,n} A_n \cos \frac{(2n-1)\pi \xi}{2} \quad (3.2.4)$$

The first and second derivatives of $q_m(\xi)$

with respect to x are

$$q_m'(\xi) = - \sum_{n=1}^{\infty} C_{m,n} A_n \frac{(2n-1)\pi}{2H} \sin \frac{(2n-1)\pi \xi}{2} \quad (3.2.5)$$

$$q_m''(\xi) = - \sum_{n=1}^{\infty} C_{m,n} A_n \frac{(2n-1)^2 \pi^2}{4H^2} \cos \frac{(2n-1)\pi\xi}{2} \quad (3.2.6)$$

From Eqs. (3.2.4) and (3.2.5) we can see that the boundary conditions (3.1.1) and (3.1.3) are already satisfied since

$$q_m(\xi=1) = \sum_{n=1}^{\infty} C_{m,n} A_n \cos \frac{(2n-1)\pi}{2} = 0 \quad (3.2.7)$$

and

$$q_m'(\xi=0) = - \sum_{n=1}^{\infty} C_{m,n} A_n \frac{(2n-1)\pi}{2H} \sin 0 = 0 \quad (3.2.8)$$

Now the advantage of the Fourier solution is obvious: The particular solution is already the complete solution.

For each term n of the Fourier series for $M_0'(\xi)$ there corresponds a term n of the Fourier series for $q_m(\xi)$. Thus in order to determine the coefficients $C_{m,n}$ in $q_m(\xi)$ we drop the summation symbol in Eqs. (3.2.4) and (3.2.6) and substitute into Eq. (2.5.7)

For each $n = 1, 2, 3, \dots$ we obtain

$$\begin{aligned} & - \gamma_m C_{m,n} A_n \frac{(2n-1)^2 \pi^2}{4H^2} \cos \frac{(2n-1)\pi\xi}{2} \\ & - \sum_{v=1}^{r-1} \delta_{m,v} C_{v,n} A_n \cos \frac{(2n-1)\pi\xi}{2} \\ & = - a_m A_n \cos \frac{(2n-1)\pi\xi}{2} \end{aligned} \quad (3.2.9)$$

Dividing Eq. (3.2.9) by $(-a_m A_n \cos \frac{(2n-1)\pi f}{2})$ and defining

28

$$\bar{\delta}_{m,v} = \frac{\delta_{m,v}}{a_m} \quad \text{for } \begin{matrix} 1 \leq v \leq m-1 \\ m+1 \leq v \leq r-1 \end{matrix} \quad (3.2.10)$$

$$\bar{\delta}_{m,m} = \frac{\delta_{m,m}}{a_m} + \frac{\gamma_m}{a_m} \frac{(2n-1)^2 \pi^2}{4 H^2} \quad \text{for } v=m$$

we can write for Eq. (3.2.9)

$$\sum_{v=1}^{r-1} \{ \bar{\delta}_{m,v} C_{v,n} \} = 1 \quad (3.2.11)$$

for $\begin{matrix} 1 \leq v \leq r-1 \\ 1 \leq m \leq r-1 \end{matrix}$

Eq. (3.2.11) represents the m -th row of a system of $(r-1)$ linear equations of $(r-1)$ unknown coefficients $C_{v,n}$. In matrix notation Eq. (3.2.11) can be written as

$$[\bar{\delta}] \{ c_n \} = \{ 1 \} \quad (3.2.12)$$

where the matrix $[\bar{\delta}]$ is

$$[\bar{\delta}] = \begin{bmatrix} \bar{\delta}_{1,1} & \bar{\delta}_{1,2} & \bar{\delta}_{1,3} & \dots & \bar{\delta}_{1,r-1} \\ \bar{\delta}_{2,1} & \bar{\delta}_{2,2} & \bar{\delta}_{2,3} & \dots & \bar{\delta}_{2,r-1} \\ \vdots & \vdots & \vdots & \ddots & \vdots \\ \bar{\delta}_{m,1} & \bar{\delta}_{m,2} & \bar{\delta}_{m,3} & \dots & \bar{\delta}_{m,r-1} \\ \vdots & \vdots & \vdots & \ddots & \vdots \\ \bar{\delta}_{r-1,1} & \bar{\delta}_{r-1,2} & \bar{\delta}_{r-1,3} & \dots & \bar{\delta}_{r-1,r-1} \end{bmatrix}$$

and the vector $\{c_n\}$ is

29

$$\{c_n\} = \begin{bmatrix} c_{1,n} \\ c_{2,n} \\ c_{3,n} \\ \vdots \\ c_{m,n} \\ \vdots \\ c_{r-1,n} \end{bmatrix}$$

and the vector $\{1\}$ is

$$\{1\} = \begin{bmatrix} 1 \\ 1 \\ \vdots \\ \vdots \\ \vdots \\ 1 \end{bmatrix}$$

The terms $\bar{\delta}_{m,v}$ are in detail (compare Eq. (2.5.6))

$$\bar{\delta}_{m,v} = a_v \quad \text{for } 1 \leq v \leq m-2 \\ m+2 \leq v \leq r-1$$

$$\bar{\delta}_{m,m-1} = a_{m-1} - \frac{\sum EI}{a_m EA_m} \quad (3.2.13)$$

$$\bar{\delta}_{m,m} = a_m + \frac{\sum EI}{a_m EA_m} + \frac{\sum EI}{a_m EA_{m+1}} + \frac{f_m (2n-1)^2 \pi^2}{a_m 4H^2}$$

$$\bar{\delta}_{m,m+1} = a_{m+1} - \frac{\sum EI}{a_m EA_{m+1}}$$

The solution of Eq. (3.2.12) is

30

$$\{c_n\} = [\bar{\delta}]^{-1} \{1\} \quad (3.2.14)$$

As may be seen from Eq. (3.2.14), it is a necessary condition for the existence of a solution for the coefficients $C_{v,n}$ that the matrix $[\bar{\delta}]$ is regular and non-singular, i.e. that the inverse matrix $[\bar{\delta}]^{-1}$ exists. This is true if the determinant $|\bar{\delta}| \neq 0$, i.e. if the matrix row or column vectors are linearly independent. Since from Eq. (3.2.13) in each row or column the terms $\bar{\delta}_{m,m-1}$, $\bar{\delta}_{m,m}$ and $\bar{\delta}_{m,m+1}$ are different from the corresponding terms in the other rows or columns, the linear independence is proven for a general case.

3.3 Reactions and deflection

3.3.1 Normal force intensities $n_m(\xi)$ in laminas

Substituting (2.3.1) and (2.3.2) into (2.3.3) and dividing by I_m we obtain

$$\begin{aligned} \frac{M_m(x)}{I_m} &= \frac{M_{0,m}(x)}{I_m} + \frac{1}{I_m} \int_0^x [-b_m q_m(\eta) - c_{m-1} q_{m-1}(\eta)] d\eta \\ &+ \frac{1}{I_m} \int_0^x [n_m(\eta) - n_{m-1}(\eta)] (x-\eta) d\eta \\ &+ \frac{1}{I_m} [N_m^* - N_{m-1}^*] \cdot x \end{aligned} \quad (3.3.1.1)$$

Similarly for interface $m+1$ we can write

$$\begin{aligned} \frac{M_{m+1}(x)}{I_{m+1}} &= \frac{M_{0,m+1}(x)}{I_{m+1}} + \frac{1}{I_{m+1}} \int_0^x [-b_{m+1} q_{m+1}(\eta) \\ &- c_m q_m(\eta)] d\eta + \frac{1}{I_{m+1}} \int_0^x [n_{m+1}(\eta) \\ &- n_m(\eta)] (x-\eta) d\eta + \frac{1}{I_{m+1}} [N_{m+1}^* - N_m^*] x \end{aligned} \quad (3.3.1.2)$$

Since from Eq. (2.3.6) we observe, that

31

$$\frac{M_m(x)}{I_m} = \frac{M_{m+1}(x)}{I_{m+1}} \quad \text{and} \quad \frac{M_{0,m}(x)}{I_m} = \frac{M_{0,m+1}(x)}{I_{m+1}}$$

we equate Eqs. (3.3.1.1) and (3.3.1.2) and obtain

$$\begin{aligned} & \frac{b_{m+1}}{I_{m+1}} \int_0^x q_{m+1}(\eta) d\eta + \left(\frac{c_m}{I_{m+1}} - \frac{b_m}{I_m} \right) \int_0^x q_m(\eta) d\eta \\ & - \frac{c_{m+1}}{I_m} \int_0^x q_{m+1}(\eta) d\eta = \frac{1}{I_{m+1}} \int_0^x n_{m+1}(\eta) (x-\eta) d\eta \\ & - \left(\frac{1}{I_{m+1}} + \frac{1}{I_m} \right) \int_0^x n_m(\eta) (x-\eta) d\eta \\ & + \frac{1}{I_m} \int_0^x n_{m+1}(\eta) (x-\eta) d\eta + \frac{N_{m+1}^* - N_m^*}{I_{m+1}} x - \frac{N_m^* - N_{m+1}^*}{I_m} x \end{aligned} \quad (3.3.1.3)$$

Differentiating Eq. (3.3.1.3) twice with respect to x gives

$$\begin{aligned} & \frac{b_{m+1}}{I_{m+1}} q'_{m+1}(x) + \left(\frac{c_m}{I_{m+1}} - \frac{b_m}{I_m} \right) q'_m(x) \\ & - \frac{c_{m+1}}{I_m} q'_{m+1}(x) = \frac{1}{I_{m+1}} n_{m+1}(x) \\ & - \left(\frac{1}{I_{m+1}} + \frac{1}{I_m} \right) n_m(x) + \frac{1}{I_m} n_{m+1}(x) \end{aligned} \quad (3.3.1.4)$$

Defining

$$\begin{aligned} \beta_{m,m-1} &= \frac{1}{I_m} \\ \beta_{m,m} &= - \left(\frac{1}{I_{m+1}} + \frac{1}{I_m} \right) \\ \beta_{m,m+1} &= \frac{1}{I_{m+1}} \\ R_m(x) &= \frac{b_{m+1}}{I_{m+1}} q'_{m+1}(x) + \left(\frac{c_m}{I_{m+1}} - \frac{b_m}{I_m} \right) q'_m(x) \\ & - \frac{c_{m+1}}{I_m} q'_{m+1}(x) \end{aligned} \quad (3.3.1.5)$$

Now Eq. (3.3.1.4) can be written as

$$\beta_{m,m-1} n_{m-1}(x) + \beta_{m,m} n_m(x) + \beta_{m,m+1} n_{m+1}(x) = R_m(x) \quad (3.3.1.6)$$

Eq. (3.3.1.6) is the m^{th} row of a system of linear equations for the unknown normal force intensities $n_j(x)$. In matrix notation this system of linear equations is

$$[\beta] \{n\} = \{R\} \quad (3.3.1.7)$$

where the diagonal band matrix $[\beta]$ is

$$[\beta] = \begin{bmatrix} \beta_{11} & \beta_{12} & 0 & 0 & \dots & 0 & 0 \\ \beta_{21} & \beta_{22} & \beta_{23} & 0 & \dots & 0 & 0 \\ 0 & \beta_{32} & \beta_{33} & \beta_{34} & \dots & 0 & 0 \\ \vdots & \vdots & \vdots & \vdots & \ddots & \vdots & \vdots \\ 0 & 0 & 0 & 0 & \dots & \beta_{r-1,r-2} & \beta_{r-1,r-1} \end{bmatrix}$$

and the vector $\{n\}$ is

$$\{n\} = \begin{bmatrix} n_1(x) \\ n_2(x) \\ n_3(x) \\ \vdots \\ n_{r-1}(x) \end{bmatrix}$$

and the vector $\{R\}$ is

$$\{R\} = \begin{bmatrix} R_1(x) \\ R_2(x) \\ R_3(x) \\ \vdots \\ R_{r-1}(x) \end{bmatrix}$$

Calling the inverse $[\beta]^{-1} = [\bar{\beta}]$; i.e.

$$[\beta]^{-1} = [\bar{\beta}] = \begin{bmatrix} \bar{\beta}_{1,1} & \bar{\beta}_{1,2} & \bar{\beta}_{1,3} & \cdots & \bar{\beta}_{1,r-1} \\ \bar{\beta}_{2,1} & \bar{\beta}_{2,2} & \bar{\beta}_{2,3} & \cdots & \bar{\beta}_{2,r-1} \\ \vdots & \vdots & \vdots & \ddots & \vdots \\ \bar{\beta}_{r-1,1} & \bar{\beta}_{r-1,2} & \bar{\beta}_{r-1,3} & \cdots & \bar{\beta}_{r-1,r-1} \end{bmatrix}$$

and premultiplying Eq. (3.3.1.7) by $[\bar{\beta}]$ we get

$$\{n\} = [\bar{\beta}] \{R\} \quad (3.3.1.8)$$

The m^{th} row of Eq. (3.3.1.8) is the solution for $n_m(x)$, namely

$$n_m(x) = \sum_{v=1}^{r-1} (\bar{\beta}_{m,v} R_v(x)) \quad (3.3.1.9)$$

With definition Eq. (3.3.1.5) of $R_v(x)$ Eq. (3.3.1.9) can be transformed to

$$n_m(x) = \sum_{v=1}^{r-1} \left[(\bar{\beta}_{m,v-1} - \bar{\beta}_{m,v}) \frac{b_v}{I_v} + (\bar{\beta}_{m,v} - \bar{\beta}_{m,v+1}) \frac{c_v}{I_{v+1}} \right] q_v'(x) \quad (3.3.1.10)$$

Defining

$$(\bar{\beta}_{m,v-1} - \bar{\beta}_{m,v}) \frac{b_v}{I_v} + (\bar{\beta}_{m,v} - \bar{\beta}_{m,v+1}) \frac{c_v}{I_{v+1}} = \varepsilon_{m,v} \quad (3.3.1.11)$$

we finally can write for Eq. (3.3.1.10)

$$n_m(x) = \sum_{v=1}^{r-1} \varepsilon_{m,v} q_v'(x) \quad (3.3.1.12)$$

with $q_v'(x)$ from Eq. (3.2.5)

3.3.2 Singular normal forces N_m^* in laminas at shear wall top

Differentiating Eq. (3.3.1.3) once with respect to x we get

$$\begin{aligned} & \frac{b_{m+1}}{I_{m+1}} q_{m+1}'(x) + \left(\frac{c_m}{I_{m+1}} - \frac{b_m}{I_m} \right) q_m'(x) \\ & - \frac{c_{m-1}}{I_m} q_{m-1}'(x) = \frac{1}{I_{m+1}} \int_0^x n_{m+1}(\eta) d\eta \\ & - \left(\frac{1}{I_{m+1}} + \frac{1}{I_m} \right) \int_0^x n_m(\eta) d\eta \quad (3.3.2.1) \\ & + \frac{1}{I_m} \int_0^x n_{m-1}(\eta) d\eta + \frac{1}{I_{m+1}} N_{m+1}^* \\ & - \left(\frac{1}{I_{m+1}} + \frac{1}{I_m} \right) N_m^* + \frac{1}{I_m} N_{m-1}^* \end{aligned}$$

At shear wall top, i.e. for $x=0$ Eq. (3.3.2.1) reduces to

$$\begin{aligned} & \frac{b_{m+1}}{I_{m+1}} q_{m+1}(0) - \left(\frac{c_m}{I_{m+1}} - \frac{b_m}{I_m} \right) q_m(0) - \frac{c_{m-1}}{I_m} q_{m-1}(0) \\ & = + \frac{1}{I_{m+1}} N_{m+1}^* - \left(\frac{1}{I_{m+1}} + \frac{1}{I_m} \right) N_m^* + \frac{1}{I_m} N_{m-1}^* \quad (3.3.2.2) \\ & = - + \beta_{m,m-1} N_{m-1}^* + \beta_{m,m} N_m^* + \beta_{m,m+1} N_{m+1}^* \end{aligned}$$

with β -definition Eq. (3.3.1.5)

Observing the similarity of Eq. (3.3.1.4) and Eq. (3.3.2.2)

immediately yields

$$N_m^*(x) = \sum_{v=1}^{r-1} \epsilon_{m,v} q_v(0) \quad (3.3.2.3)$$

3.3.3 Normal forces $N_m(x)$ in piers

From Fig. 2.4.4

$$N_m(x) = \int_0^x [q_m(\lambda) - q_{m-1}(\lambda)] d\lambda \quad (3.3.3.1)$$

Substituting $q_m(\lambda)$ from Eq. (3.2.4) yields

$$\begin{aligned} N_m(x) &= \int_0^x \sum_{n=1}^{\infty} (C_{m,n} - C_{m-1,n}) A_n \cos \frac{(2n-1)\pi\lambda}{2H} d\lambda \\ &= \sum_{n=1}^{\infty} [(C_{m,n} - C_{m-1,n}) A_n \int_0^x \cos \frac{(2n-1)\pi\lambda}{2H} d\lambda] \end{aligned}$$

$$N_m(x) = \sum_{n=1}^{\infty} [(C_{m,n} - C_{m-1,n}) A_n \frac{2H}{(2n-1)\pi} \sin \frac{(2n-1)\pi x}{2H}]$$

or

(3.3.3.2)

$$N_m(\xi) = \sum_{n=1}^{\infty} [(C_{m,n} - C_{m-1,n}) A_n \frac{2H}{(2n-1)\pi} \sin \frac{(2n-1)\pi \xi}{2}]$$

3.3.4 Bending moments $M_m(x)$ in piers

Substituting Eq. (3.2.4) into Eq. (2.5.1) results in

$$M_m(x) = M_{0,m}(x) - i_m \sum_{v=1}^{r-1} a_v \int_0^x \left[\sum_{n=1}^{\infty} C_{v,n} A_n \cos \frac{(2n-1)\pi \eta}{2H} \right] d\eta$$

$$M_m(x) = M_{0,m}(x) - i_m \sum_{v=1}^{r-1} a_v \sum_{n=1}^{\infty} C_{v,n} A_n \frac{2H}{(2n-1)\pi} \cdot \sin \frac{(2n-1)\pi x}{2H}$$

or

$$M_m(\xi) = M_{0,m}(\xi) - i_m \sum_{v=1}^{r-1} a_v \sum_{n=1}^{\infty} C_{v,n} A_n \frac{2H}{(2n-1)\pi} \cdot \sin \frac{(2n-1)\pi \xi}{2}$$

(3.3.4.1)

From Eq. (2.3.8), $M_{0,m}(x) = i_m M_0(x)$

and with Eq. (3.2.2), $M_0'(x) = \sum_{n=1}^{\infty} A_n \cos \frac{(2n-1)\pi x}{2H}$

we obtain after integration of Eq. (3.2.2)

$$M_{0,m}(x) = i_m \sum_{n=1}^{\infty} A_n \frac{2H}{(2n-1)\pi} \sin \frac{(2n-1)\pi x}{2H} \quad (3.3.4.2)$$

Substituting Eq. (3.3.4.2) into Eq. (3.3.4.1) and transforming yields

$$M_m(x) = i_m \left[\sum_{n=1}^{\infty} A_n \frac{2H}{(2n-1)\pi} \left(1 - \sum_{v=1}^{r-1} a_v C_{v,n} \right) \cdot \sin \frac{(2n-1)\pi x}{2H} \right] \quad (3.3.4.3)$$

Eq. (2.3.11) and Eq. (3.3.4.3) result in the second derivative of the deflection by means of Fourier series:

$$y''(x) = - \frac{1}{E \Sigma I} \left[\sum_{n=1}^{\infty} A_n \frac{2H}{(2n-1)\pi} \left(1 - \sum_{\nu=1}^{r-1} a_{\nu} C_{\nu,n} \right) \cdot \sin \frac{(2n-1)\pi x}{2H} \right] \quad (3.3.5.1)$$

Also from integration

$$y'(x) = + \frac{1}{E \Sigma I} \left[\sum_{n=1}^{\infty} A_n \frac{4H^2}{(2n-1)^2 \pi^2} \left(1 - \sum_{\nu=1}^{r-1} a_{\nu} C_{\nu,n} \right) \cos \frac{(2n-1)\pi x}{2H} \right] + K_1$$

and

$$y(x) = + \frac{1}{E \Sigma I} \left[\sum_{n=1}^{\infty} A_n \frac{8H^3}{(2n-1)^3 \pi^3} \left(1 - \sum_{\nu=1}^{r-1} a_{\nu} C_{\nu,n} \right) \sin \frac{(2n-1)\pi x}{2H} \right] + K_1 x + K_2 \quad (3.3.5.2)$$

The boundary conditions are

(a) $y'(H) = 0$

(b) $y(H) = 0$

(a) yields with $\cos \frac{(2n-1)\pi}{2} = 0 \rightarrow K_1 = 0$

(b) yields with $\sin \frac{(2n-1)\pi}{2} = (-1)^{n+1}$

$$K_2 = \frac{1}{E \Sigma I} \left[\sum_{n=1}^{\infty} A_n \frac{8H^3}{(2n-1)^3 \pi^3} \left(1 - \sum_{\nu=1}^{r-1} a_{\nu} C_{\nu,n} \right) (-1)^n \right] \quad (3.3.5.3)$$

Substituting Eq. (3.3.5.3) into Eq. (3.3.5.2) and defining

$$\bar{A}_n = A_n \frac{8H^3}{(2n-1)^3 \pi^3} \quad (3.3.5.4)$$

we finally get

$$y(x) = \frac{1}{E \Sigma I} \left[\sum_{n=1}^{\infty} \bar{A}_n \left(1 - \sum_{\nu=1}^{r-1} a_{\nu} C_{\nu,n} \right) \cdot \left(\sin \frac{(2n-1)\pi x}{2H} + (-1)^n \right) \right] \quad (3.3.5.5)$$

The lamina forces in the continuous system (Fig. 2.3.1) can be integrated over the influence area of each discrete connecting beam.

If x_b is the location of any connecting beam and $a =$ story height, then the connector forces can be determined by integration $\int_{x_b - \frac{a}{2}}^{x_b + \frac{a}{2}}$ and if $x_b = 0$, i. e. on shear wall top, then the integration is $\int_0^{a/2}$

(a) Shear force in connecting beams

With Eq. (3.2.4) we get

$$Q_m(x_b) = \int_{x_b - \frac{a}{2}}^{x_b + \frac{a}{2}} \left(\sum_{n=1}^{\infty} C_{m,n} A_n \cos \frac{(2n-1)\pi x}{2H} \right) dx$$

$$Q_m(x_b) = \sum_{n=1}^{\infty} C_{m,n} A_n \frac{2H}{(2n-1)\pi} \left(\sin \frac{(2n-1)\pi (x_b + \frac{a}{2})}{2H} - \sin \frac{(2n-1)\pi (x_b - \frac{a}{2})}{2H} \right) \quad (3.4.1)$$

or

$$Q_m(x_b) = \sum_{n=1}^{\infty} C_{m,n} A_n \frac{4H}{(2n-1)\pi} \cos \frac{(2n-1)\pi x_b}{2H} \cdot \sin \frac{(2n-1)\pi a}{4H} \quad (3.4.2)$$

and on shear wall top $x_b = 0$ the integration results in

$$Q_m(0) = \sum_{n=1}^{\infty} C_{m,n} A_n \frac{2H}{(2n-1)\pi} \sin \frac{(2n-1)\pi a}{4H} \quad (3.4.3)$$

(b) Normal forces in connecting beams

$$N_m^c(x_b) = \int_{x_b - \frac{a}{2}}^{x_b + \frac{a}{2}} n_m(x) dx$$

With Eqs. (3.3.1.12) and (3.2.5) we obtain

$$N_m^c(x_b) = \int_{x_b - \frac{a}{2}}^{x_b + \frac{a}{2}} \left(\sum_{v=1}^{r-1} \varepsilon_{m,v} \sum_{n=1}^{\infty} C_{m,n} A_n \frac{(2n-1)\pi}{2H} \sin \frac{(2n-1)\pi x}{2H} \right) dx$$

$$N_m^c(x_b) = \sum_{v=1}^{r-1} \varepsilon_{m,v} \sum_{n=1}^{\infty} C_{m,n} A_n \left(\cos \frac{(2n-1)\pi(x_b + \frac{a}{2})}{2H} - \cos \frac{(2n-1)\pi(x_b - \frac{a}{2})}{2H} \right) \quad (3.4.4)$$

or

$$N_m^c(x_b) = \sum_{v=1}^{r-1} \varepsilon_{m,v} \sum_{n=1}^{\infty} \left(-2 C_{m,n} A_n \sin \frac{(2n-1)\pi x_b}{2H} \cdot \sin \frac{(2n-1)\pi a}{4H} \right) \quad (3.4.5)$$

and on shear wall top $x_b = 0$ the integration yields

$$N_m^c(0) = \sum_{v=1}^{r-1} \left\{ \varepsilon_{m,v} \sum_{n=1}^{\infty} C_{m,n} A_n \cos \frac{(2n-1)\pi a}{4H} \right\} + N_m^* \quad (3.4.6)$$

with N_m^* from Eq. (3.3.2.3)

If the forces $Q_m(x_b)$ and $N_m^c(x_b)$ in the connecting beams are determined, then it is possible to calculate the bending moments and normal forces of the piers from equilibrium considerations. The advantage of this method would be, that the more time consuming equations (3.3.4.3) for bending moments and (3.3.3.2) for normal forces would be avoided and

the real discrete system is taken into account immediately. This method was used in the computation programs.

3.5 Some special loading cases

While the coefficients $C_{v,n}$ only depend on the properties of the shear wall system (Eq. 3.2.14), the coefficients A_n depend on the special loading cases.

Three kinds of loading will be examined, single load at any distance from shear wall top, UDL, and piecewise trapezoidal load.

(a) Single load at arbitrary location

With $M'_0(x) = f(x)$ from Fig. 3.5.1 and with Eq. (3.2.3) the coefficients A_n can be determined as

$$\begin{aligned}
 A_n &= \frac{2}{H} \int_0^H f(x) \cos \frac{(2n-1)\pi x}{2H} dx \\
 &= -\frac{2}{H} \int_{x_0}^H P \cos \frac{(2n-1)\pi x}{2H} dx \\
 &= -\frac{4P}{(2n-1)\pi} \left[\sin \frac{(2n-1)\pi}{2} - \sin \frac{(2n-1)\pi x_0}{2H} \right] \\
 &= -\frac{4P}{(2n-1)\pi} \left[(-1)^{n+1} - \sin \frac{(2n-1)\pi x_0}{2H} \right]
 \end{aligned}$$

Finally we get

$$A_n = \frac{4P}{(2n-1)\pi} \left[(-1)^n + \sin \frac{(2n-1)\pi x_0}{2H} \right] \quad (3.5.1)$$

(b) Uniformly distributed load (UDL)

With $M'_0(x) = f(x) = -p_0 x$ from Fig. 3.5.2 and with Eq. (3.2.3)

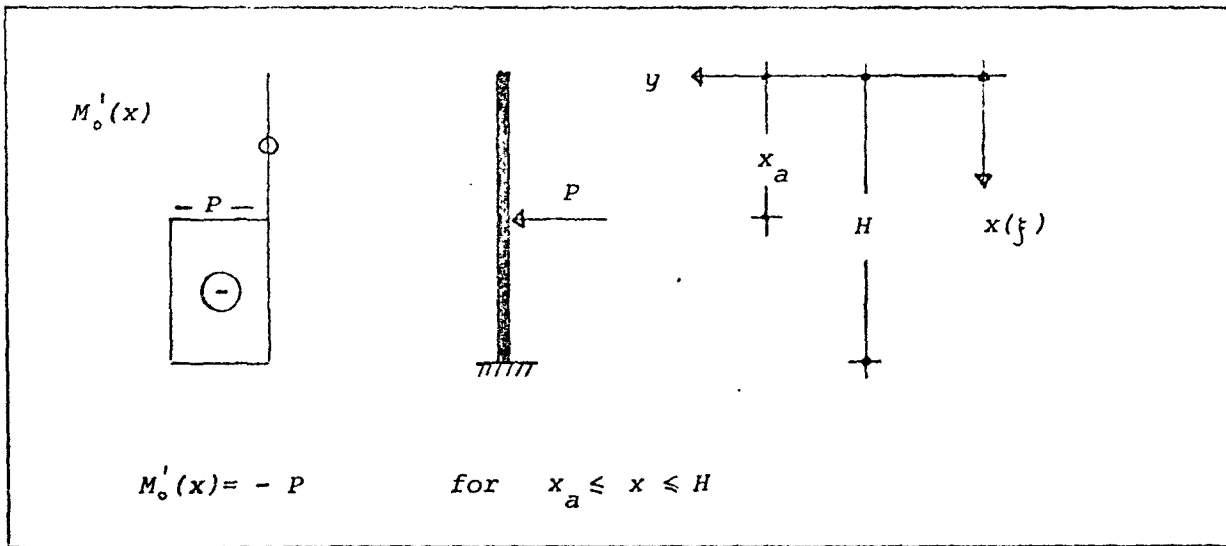
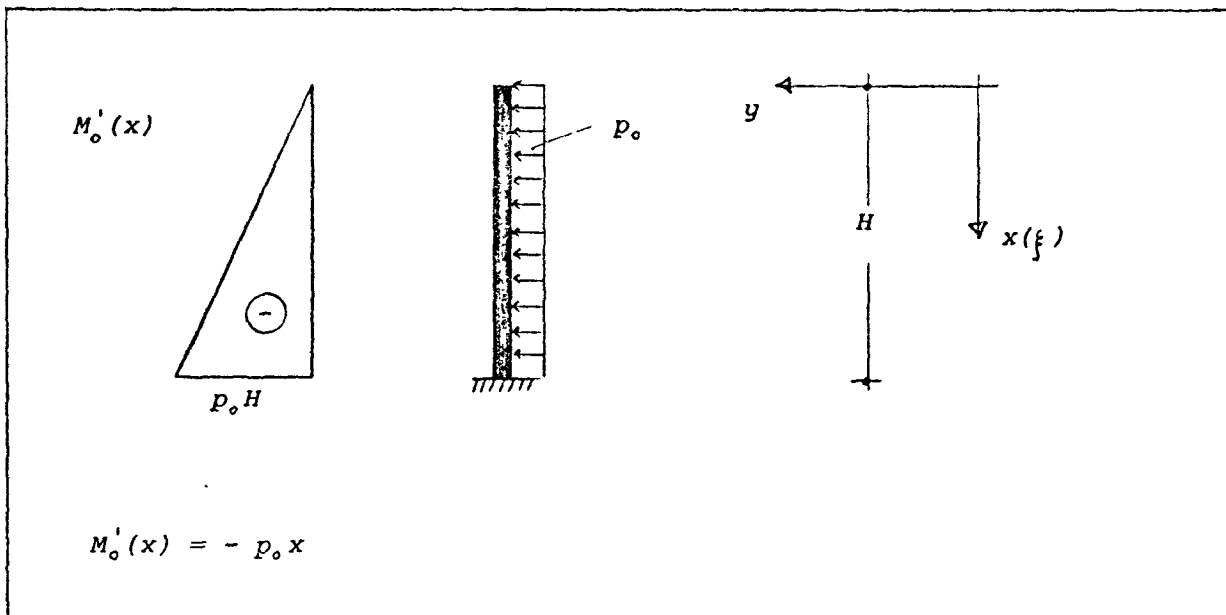
we obtain

$$\begin{aligned}
 A_n &= \frac{2}{H} \int_0^H -p_0 x \cos \frac{(2n-1)\pi x}{2H} dx \\
 &= -\frac{2p_0}{H} \left[\frac{4H^2}{(2n-1)^2\pi^2} \cos \frac{(2n-1)\pi x}{2H} + \frac{x \cdot 2H}{(2n-1)\pi} \sin \frac{(2n-1)\pi x}{2H} \right]_0^H \\
 &= -\frac{2p_0}{H} \left[\frac{2H^2}{(2n-1)\pi} (-1)^{n+1} - \frac{4H^2}{(2n-1)^2\pi^2} \right] \\
 &= \frac{4p_0 H}{(2n-1)\pi} \left[(-1)^n + \frac{2}{(2n-1)\pi} \right]
 \end{aligned}$$

$$A_n = \frac{4p_0 H}{\pi^2} \left[\frac{2 + (-1)^n (2n-1)\pi}{(2n-1)^2} \right] \quad (3.5.2)$$

(c) Piecewise trapezoidal load

A more complicated but very useful kind of loading is the piecewise trapezoidal load. This load case includes many other load cases, as for example UDL, triangular load, piecewise UDL, and it provides for the possibility to approximate all arbitrary shapes of loading to a high degree of accuracy by dividing the given

Fig. 3.5.1. $M'_o(x)$ for single loadFig. 3.5.2. $M'_o(x)$ for U D L

shape of loading (from wind tunnel experiments or actual measurements) into appropriate sections of piecewise trapezoidal loading. Even single loads, which normally do not actually exist but always have a certain influence area, can be simulated by piecewise trapezoidal loading.

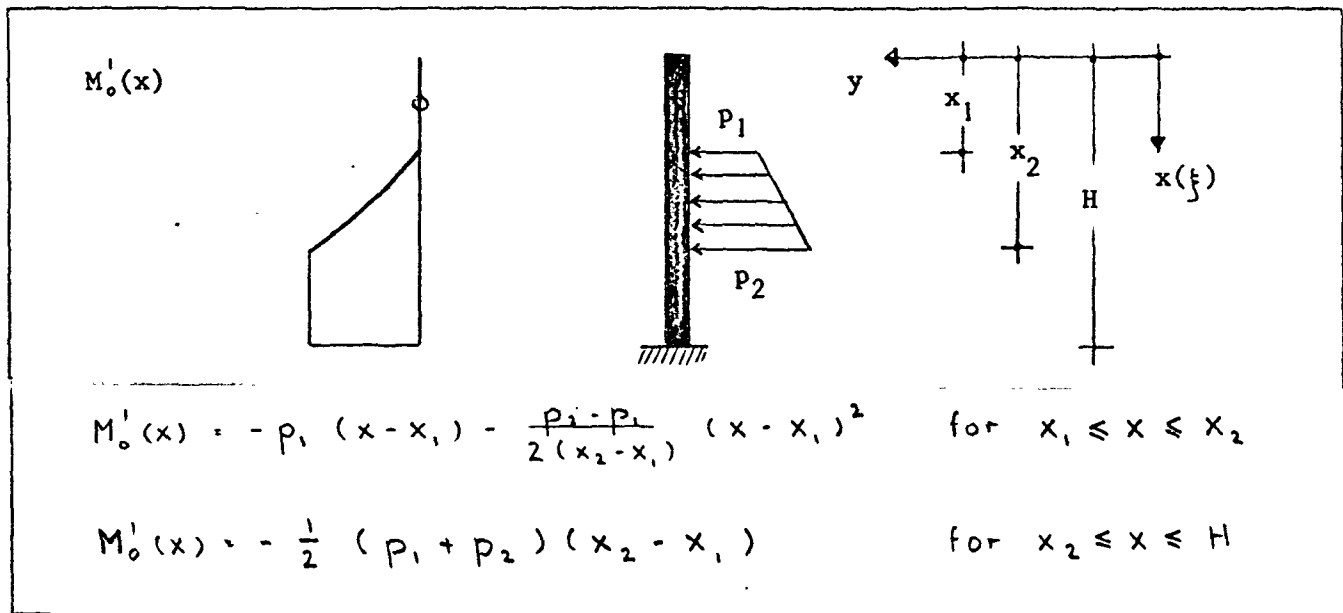


Fig. 3.5.3 $M'_0(x)$ for piecewise trapezoidal load

With $M'_0(x)$ from Fig. 3.5.3 we obtain

$$\begin{aligned} M_0(x) &= p_1 x + p_1 x_1 - \frac{p_2-p_1}{2(x_2-x_1)}(x^2 - 2x_1 x + x_1^2) \\ &= p_1 x_1 - \frac{p_2-p_1}{2(x_2-x_1)} x^2 + \left[\frac{(p_2-p_1)}{(x_2-x_1)} x_1 - p_1 \right] x \\ &\quad - \frac{p_2-p_1}{2(x_2-x_1)} x_1^2 \quad \text{for } x_1 \leq x \leq x_2 \end{aligned}$$

$$M_0(x) = -\frac{1}{2}(p_1-p_2)(x_2-x_1) \quad \text{for } x_2 \leq x \leq H$$

Defining

$$\begin{aligned}
 M_{03} &= p_1 x_1 - \frac{p_2 - p_1}{2(x_2 - x_1)} x_1^2 \\
 M_{02} &= \frac{(p_2 - p_1)}{(x_2 - x_1)} x_1 - p_1 \\
 M_{01} &= -\frac{(p_2 - p_1)}{2(x_2 - x_1)} \\
 M_{04} &= -\frac{1}{2} (p_1 - p_2) (x_2 - x_1)
 \end{aligned} \tag{3.5.3}$$

With Eq. (3.5.3) $M_0'(x)$ can be written as

$$\begin{aligned}
 M_0'(x) &= M_{01} x^2 + M_{02} x + M_{03} \quad \text{for } x_1 \leq x \leq x_2 \\
 M_0'(x) &= M_{04} \quad \text{for } x_2 \leq x \leq H
 \end{aligned} \tag{3.5.4}$$

With Eq. (3.5.4) and Eq. (3.2.3) we can write

$$\begin{aligned}
 A_n &= \frac{2}{H} \int_{x_1}^{x_2} (M_{01} x^2 + M_{02} x + M_{03}) \cos \frac{(2n-1)\pi x}{2H} dx \\
 &\quad + \frac{2}{H} \int_{x_2}^H M_{04} \cos \frac{(2n-1)\pi x}{2H} dx \\
 &= \frac{2}{H} M_{01} \int_{x_1}^{x_2} x^2 \cos \frac{(2n-1)\pi x}{2H} dx \\
 &\quad + \frac{2}{H} M_{02} \int_{x_1}^{x_2} x \cos \frac{(2n-1)\pi x}{2H} dx \\
 &\quad + \frac{2}{H} M_{03} \int_{x_1}^{x_2} \cos \frac{(2n-1)\pi x}{2H} dx \\
 &\quad + \frac{2}{H} M_{04} \int_{x_2}^H \cos \frac{(2n-1)\pi x}{2H} dx
 \end{aligned}$$

$$\begin{aligned}
A_n &= \frac{2}{H} M_{01} \left[\left(\frac{x_2^2 2H}{(2n-1)\pi} - \frac{16H^3}{(2n-1)^3 \pi^3} \right) \sin \frac{(2n-1)\pi x}{2H} \right. \\
&\quad \left. + \frac{x_1 \cdot 8H^2}{(2n-1)^2 \pi^2} \cos \frac{(2n-1)\pi x}{2H} \right] x_2 \\
&+ \frac{2}{H} M_{02} \left[\frac{4H^2}{(2n-1)^2 \pi^2} \cos \frac{(2n-1)\pi x}{2H} + \frac{x_2 \cdot 2H}{(2n-1)\pi} \sin \frac{(2n-1)\pi x}{2H} \right] x_1 \\
&+ \frac{2}{H} M_{03} \left[\frac{2H}{(2n-1)\pi} \sin \frac{(2n-1)\pi x}{2H} \right] x_2 \\
&+ \frac{2}{H} M_{04} \left[\frac{2H}{(2n-1)\pi} \sin \frac{(2n-1)\pi x}{2H} \right] x_1
\end{aligned}$$

Finally we get

$$\begin{aligned}
A_n &= \frac{4M_{01}}{(2n-1)\pi} \left[\left(x_2^2 - \frac{3H^2}{(2n-1)^2 \pi^2} \right) \sin \frac{(2n-1)\pi x_2}{2H} \right. \\
&\quad \left. - \left(x_1^2 - \frac{3H^2}{(2n-1)^2 \pi^2} \right) \sin \frac{(2n-1)\pi x_1}{2H} \right. \\
&\quad \left. + \frac{x_2 \cdot 4H}{(2n-1)\pi} \cos \frac{(2n-1)\pi x_2}{2H} \right. \\
&\quad \left. - \frac{x_1 \cdot 4H}{(2n-1)\pi} \cos \frac{(2n-1)\pi x_1}{2H} \right] \\
&+ \frac{4M_{02}}{(2n-1)\pi} \left[\frac{2H}{(2n-1)\pi} \left(\cos \frac{(2n-1)\pi x_2}{2H} - \cos \frac{(2n-1)\pi x_1}{2H} \right) \right. \\
&\quad \left. + x_2 \sin \frac{(2n-1)\pi x_2}{2H} - x_1 \sin \frac{(2n-1)\pi x_1}{2H} \right] \\
&+ \frac{4M_{03}}{(2n-1)\pi} \left[\sin \frac{(2n-1)\pi x_2}{2H} - \sin \frac{(2n-1)\pi x_1}{2H} \right] \\
&- \frac{4M_{04}}{(2n-1)\pi} \left[(-1)^n + \sin \frac{(2n-1)\pi x_2}{2H} \right] \tag{3.5.5}
\end{aligned}$$

or

$$\begin{aligned}
A_n &= \frac{4}{(2n-1)\pi} \left[\left(M_{01} x_2^2 - \frac{3M_{01} H^2}{(2n-1)^2 \pi^2} + M_{02} x_2 + M_{03} \right. \right. \\
&\quad \left. \left. - M_{04} \right) \sin \frac{(2n-1)\pi x_2}{2H} - \left(M_{01} x_1^2 - \frac{3M_{01} H^2}{(2n-1)^2 \pi^2} \right. \right. \\
&\quad \left. \left. + M_{02} x_1 + M_{03} \right) \sin \frac{(2n-1)\pi x_1}{2H} \right. \\
&\quad \left. + \frac{2H}{(2n-1)\pi} (2M_{01} x_2 + M_{02}) \cos \frac{(2n-1)\pi x_2}{2H} \right. \\
&\quad \left. - \frac{2H}{(2n-1)\pi} (2M_{01} x_1 + M_{02}) \cos \frac{(2n-1)\pi x_1}{2H} \right. \\
&\quad \left. - M_{04} (-1)^n \right] \tag{3.5.6}
\end{aligned}$$

3.6 Examples

3.6.1 Symmetrical two-pier shear wall

(a) Solution given by Beck ⁽²⁾ for load case UDL (Fig. 3.6.1.1)

$$q(\xi) = \frac{p_0 H}{\alpha_1 \gamma^2} \xi + C_1 \cosh \bar{\alpha} \xi + C_2 \sinh \bar{\alpha} \xi$$

$$C_1 = \frac{p_0 H}{\alpha_1 \gamma^2} \left[\frac{\bar{\alpha} - \sinh \bar{\alpha} \xi}{\bar{\alpha} \cosh \bar{\alpha} \xi} \right]$$

$$C_2 = \frac{p_0 H}{\bar{\alpha} \alpha_1 \gamma^2}$$

$$\alpha^2 = \frac{6 \alpha_1^2 H^2 I B_1}{\alpha L^3 I_1}$$

(3.6.1.1)

$$\beta^2 = 1 + \frac{12 I B_1}{L^2 G \cdot A B_1}$$

$$\gamma^2 = 1 + \frac{4 I_1}{\alpha_1^2 A_1}$$

$$\bar{\alpha} = \frac{\alpha \gamma}{\beta}$$

$$\xi = \frac{x}{H}$$

(b) Fourier solution for load case UDL (Fig. 3.6.1.1)

From Eq. (3.2.13)

$$\bar{\delta}_{11} = a_1 + \frac{4EI_1}{a_1 EA_1} + \frac{\gamma_1 (2n-1)^2 \pi^2}{a_1 4H^2}$$

and with Eq. (3.2.11) we obtain

$$C_{1,n} = \frac{1}{\bar{\delta}_{11}} = \frac{1}{a_1 + \frac{4EI_1}{a_1 EA_1} + \frac{\gamma_1 (2n-1)^2 \pi^2}{a_1 4H^2}} \quad (3.6.1.2)$$

Also with A_n for UDL from Eq. (3.5.2) and with Eq. (3.2.4) we obtain

$$q\left(\frac{x}{H}\right) = \frac{4p_2 H}{\pi^2} \sum_{n=1}^{\infty} \left[\frac{2 + (-1)^2 (2n-1)\pi}{(2n-1)^2} \frac{1}{a_1 + \frac{4EI_1}{a_1 EA_1} + \frac{\gamma_1 (2n-1)^2 \pi^2}{a_1 4H^2}} \cos \frac{(2n-1)\pi x}{2} \right] \quad (3.6.1.3)$$

Numerically Eq. (3.6.1.1) and Eq. (3.6.1.3) coincide.

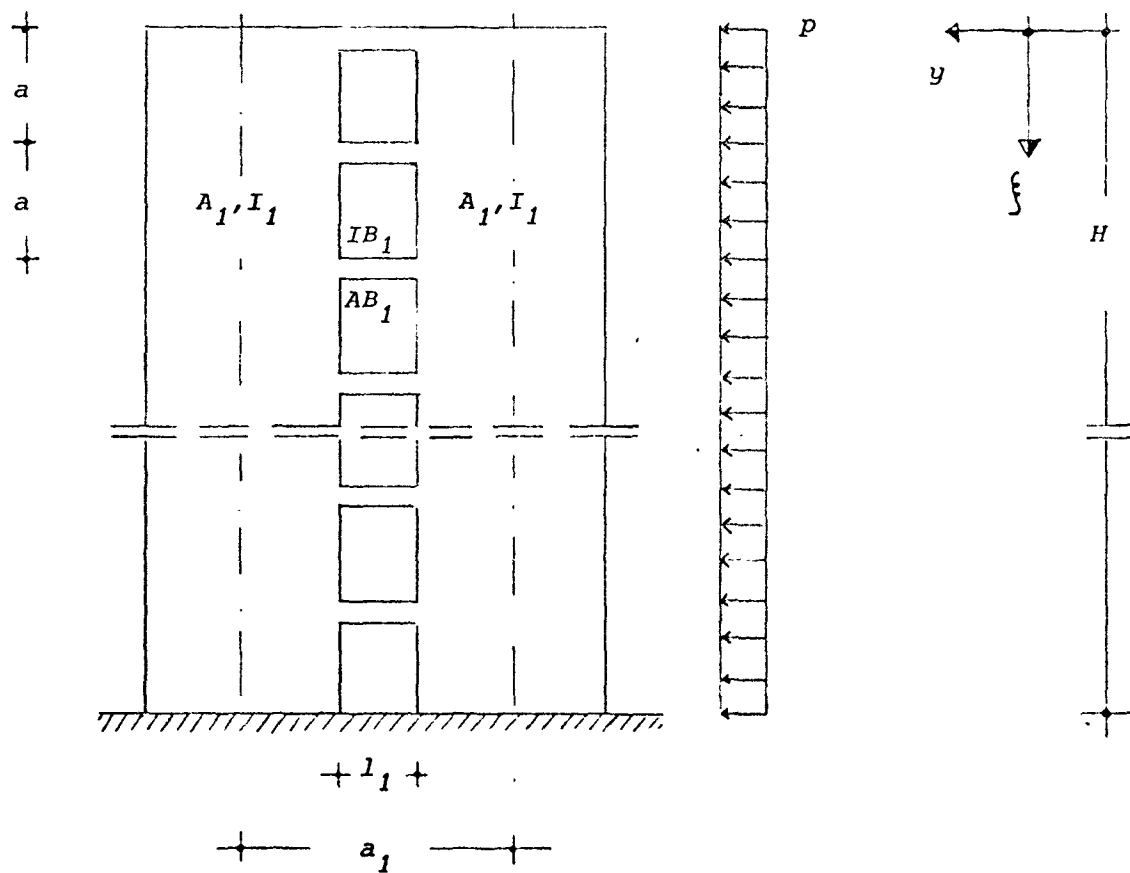


Fig. 3.6.1.1 Symmetrical two-pier shear wall with UDL

3.6.2 Symmetrical five-pier shear wall with arbitrary loading

49

This numerical example will demonstrate the flexibility of the Fourier series solution. An arbitrarily shaped loading can be approximated by piecewise stepped UDL, or by piecewise trapezoidal loading. In this special case the piecewise stepped UDL was chosen, because, in this program, the shear intensity can be compared with the shear intensities for complete interaction.

All dimensions can be assumed in Mp, m

where $1 \text{ Mp} = 1000 \text{ kp} = 10^6 \text{ grammes}$

$1 \text{ m} = 100 \text{ centimetre}$

All piers and all connecting beams are identical respectively. For loading and dimensions see Fig. 3.6.2.1

With

$$A_i = 1,0 \text{ m}^2$$

$$I_i = 2,1 \text{ m}^4$$

$$a_i = 6,0 \text{ m}$$

$$a = 3,5 \text{ m}$$

$$H = 70,0 \text{ m}$$

$$l_i = 1,0 \text{ m}$$

$$I B_i = 0,0036 \text{ m}^4$$

$$A B_i = 0,1 \text{ m}^2$$

$$E = 3 \cdot 10^6 \text{ Mp/m}^2$$

$$G/E = 0,43$$

and with loading from Fig. 3.6.2.1 the shear intensities and all other reactions can be calculated. A plot of the shear intensities for partial and complete interaction is given in Fig. 3.6.2.2.

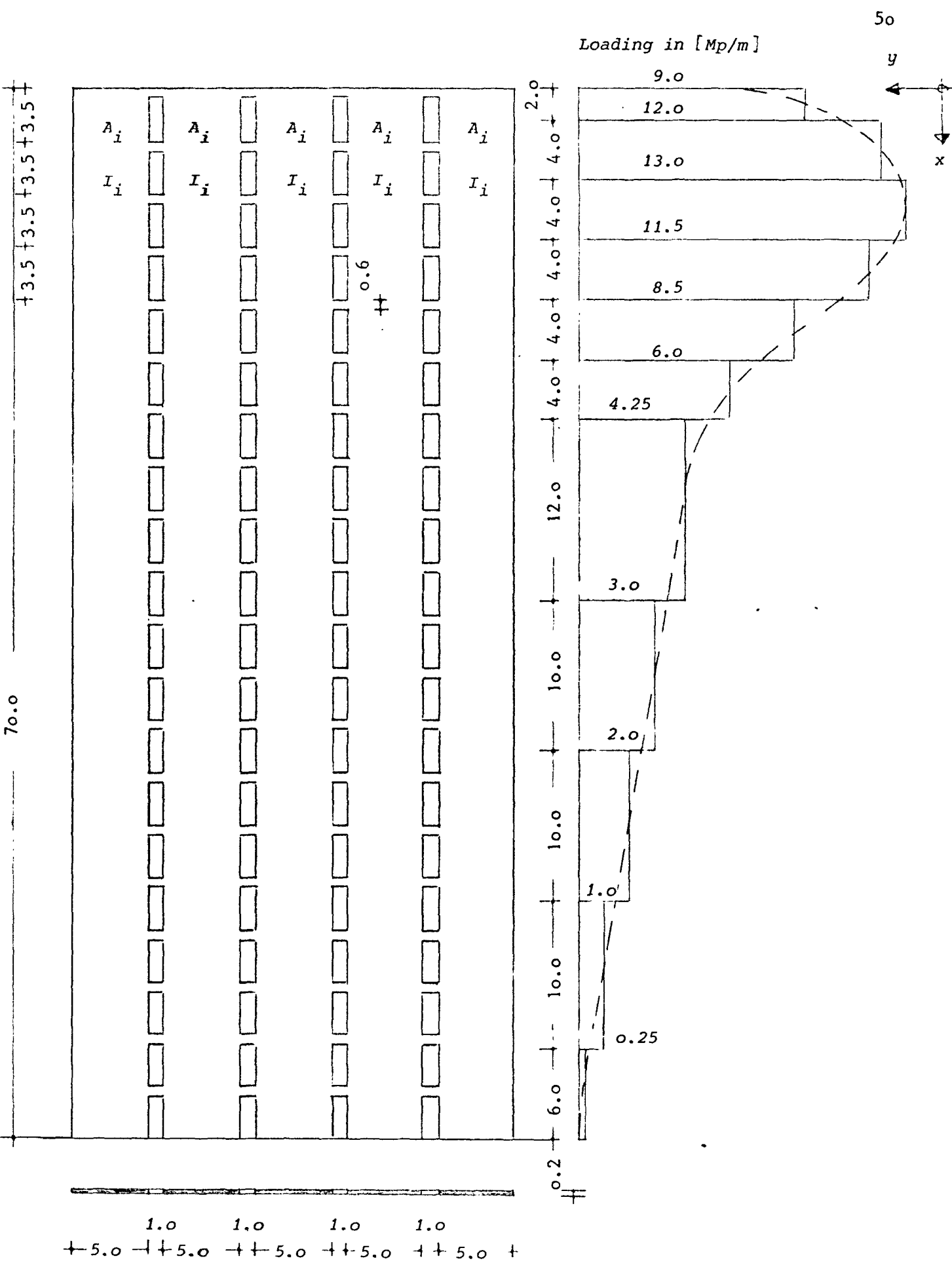


Fig. 3.6.2.1. System and loading for example 3.6.2.

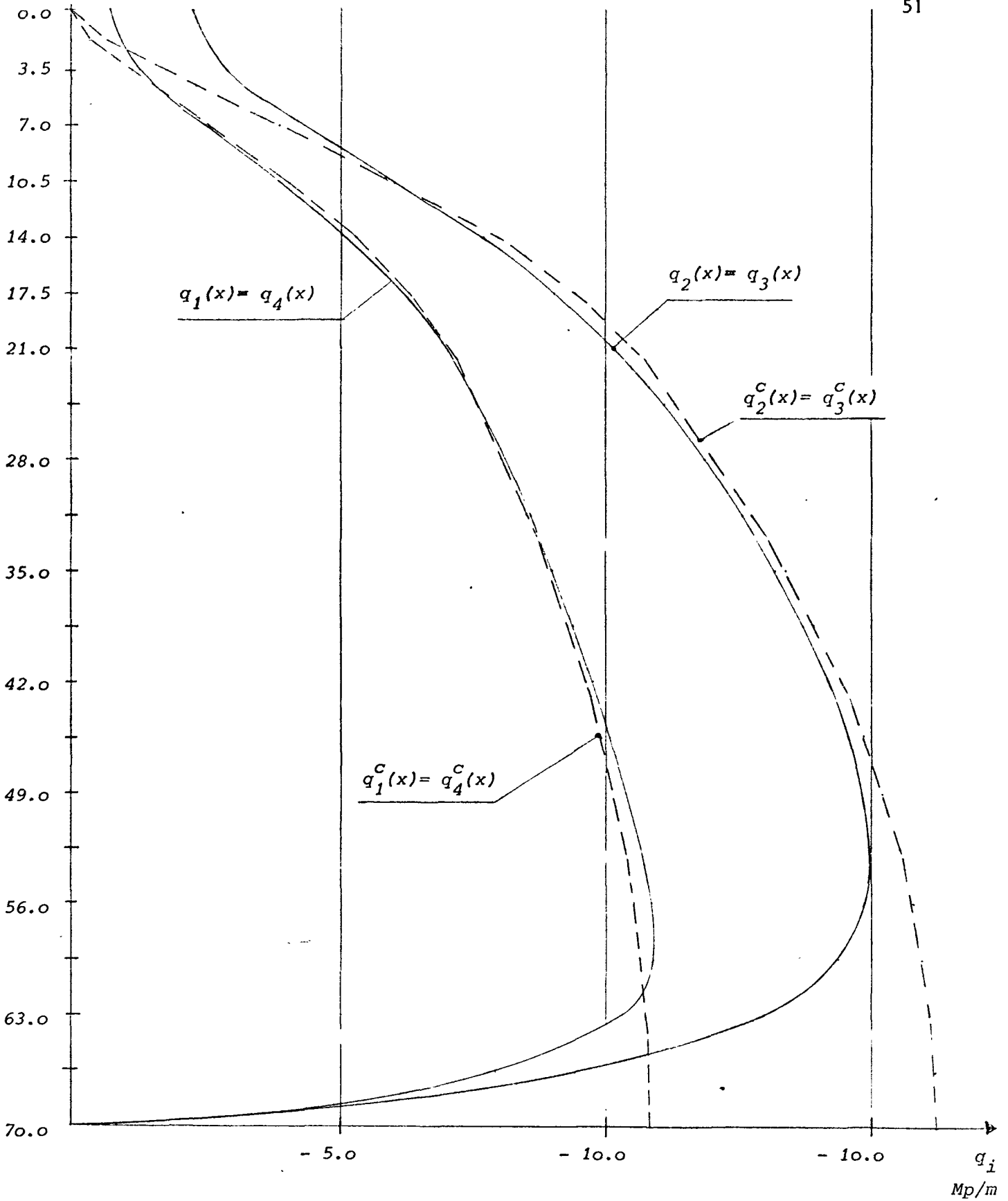


Fig. 3.6.2.2. Shear intensities for example 3.6.2.
dashed lines for complete interaction

CHAPTER IV

Stiffness parameter ξ_m

4.1 Derivation of the stiffness parameters ξ_m

The connecting beams establish the interaction between adjacent piers. The degree of interaction depends on the stiffness properties of the connecting beams and piers. This degree of interaction increases with the increasing stiffness of the connecting beams in comparison with the stiffness of the piers. The so-called complete interaction is reached when the shear forces in the connecting beams reach the same magnitude as those in rigid connection. As for complete interaction all reactions can be determined by means of ordinary beam theory, it is desirable to estimate this degree of interaction in advance and to determine the reactions by means of the beam theory, if the degree of interaction can be assumed to be close to that of the complete interaction. Also, in many practical cases it is possible to design a shear wall structure such that the dimensions can be chosen in order to obtain complete interaction. In his publication (2), Beck has developed a stiffness parameter $\bar{\alpha}$ for a symmetrical two-pier shear wall. For $\bar{\alpha} > 20$ complete interaction can be assumed and the time consuming calculations reduce to the simple determination of shear forces in the connecting beams by means of beam theory, i. e. by means of equation

$$q^c(x) = \frac{V_o(x) S}{I_{tot}} \quad (4.1.1)$$

where

$q^c(x)$ = shear intensity for complete interaction

53

$V_0(x)$ = total shear force at cross-section x

S = statical moment

I_{tot} = total moment of inertia for complete interaction

Similarly to the $\bar{\alpha}$ -parameter for symmetrical two-pier shear walls, g_i -parameters will be developed for shear walls of arbitrary number of piers.

Neglecting in Eq. (3.2.12) the part which is dependent on the connecting beam, i. e. setting $\frac{g_m (2n-1)^2 \pi^2}{a_m 4 H^2} = 0$ in the diagonal terms of Eqs. (3.2.12) and (3.2.13) respectively, the solution of Eq. (3.2.12) becomes the solution of the complete interaction.

In other words, the coefficients $C_{m,n}$ are unique and we obtain

$$C_{m,n} = C_m = \frac{S_m}{I_{tot}} \quad (4.1.2)$$

This will be demonstrated with an example of a symmetrical 3-pier shear wall with

$$a_1 = a_2 = a,$$

$$A_1 = A_2 = A_3 = A$$

$$I_1 = I_2 = I_3 = I$$

$$S_1 = a, A$$

$$I_{tot} = \sum I + 2 a_1^2 A = 3 I + 2 a_1^2 A$$

$$\bar{\delta}_{11} = \bar{\delta}_{22} = a_1 + \frac{6I}{a_1 A}$$

$$\bar{\delta}_{21} = \bar{\delta}_{12} = a_1 - \frac{3I}{a_1 A}$$

$$\begin{aligned} \det |\bar{\delta}| &= \bar{\delta}_{11}^2 - \bar{\delta}_{12}^2 = a_1^2 + \frac{12I}{A} + \frac{36I^2}{a_1^2 A^2} - a_1^2 + \frac{6I}{A} - \frac{9I^2}{a_1^2 A^2} \\ &= \frac{18I}{A} + \frac{27I^2}{a_1^2 A^2} \end{aligned}$$

With the inverse of $[\bar{\delta}]$

$$[\bar{\delta}]^{-1} = \frac{1}{\frac{18I}{A} + \frac{27I^2}{a_1^2 A^2}} \begin{bmatrix} \bar{\delta}_{22} & -\bar{\delta}_{21} \\ -\bar{\delta}_{12} & \bar{\delta}_{11} \end{bmatrix}$$

we get for

$$\begin{aligned} C_1 = C_2 &= \frac{\bar{\delta}_{22} - \bar{\delta}_{21}}{\frac{18I}{A} + \frac{27I^2}{a_1^2 A^2}} = \frac{\frac{9I}{a_1 A}}{\frac{18I}{A} + \frac{27I^2}{a_1^2 A^2}} \\ &= \frac{1}{2a_1 + \frac{3I}{a_1 A}} \end{aligned} \quad (4.1.3)$$

Also from Eq. (4.1.2) we obtain

$$C_1 = C_2 = \frac{S_1}{I_{tot}} = \frac{a_1 A}{2a_1^2 A + 3I} = \frac{1}{2a_1 + \frac{3I}{a_1 A}} \quad (4.1.4)$$

Eqs. (4.1.3) and (4.1.4) result in the same solution, i.e. the coefficients $C_{m,n}$ are the coefficients for complete interaction for the above stated assumptions.

For complete interaction at interface m the term $\frac{f_m (2n-1)^2 \pi^2}{a_m 4 H^2} = 0$ in $\bar{\delta}_{m,m}$

For no interaction $\frac{f_m (2n-1)^2 \pi^2}{a_m 4 H^2} = \infty$ in $\bar{\delta}_{m,m}$ at interface m

Therefore we can define with $n=1$

$$P_m = \frac{a_m + \frac{\sum I}{a_m} \left(\frac{1}{A_m} + \frac{1}{A_{m+1}} \right)}{\frac{f_m \pi^2}{a_m 4 H^2}} \quad (4.1.5)$$

Transforming with Eqs. (2.4.7) and (2.5.5) we finally obtain

$$p_m = \frac{4 H^2}{\pi^2 \left(\frac{l_m^3 a}{12 I B_m} + \frac{l_m a}{\mu A B_m} \right)} \left[\frac{a_m^2}{\Sigma I} + \frac{1}{A_m} + \frac{1}{A_{m+1}} \right] \quad (4.1.6)$$

From Eq. (4.1.5) we observe, that $p_m = \infty$ for complete interaction and $p_m = 0$ for no interaction.

The main problem now is, to find out for which numerical values of ρ an approximation to complete interaction can be assumed.

These numerical values can be determined by comparing the

ρ -parameters with the $\bar{\alpha}$ -parameters of Beck⁽²⁾ for symmetrical two-pier shear walls. They also can be determined by comparing the shear intensities for many examples with the corresponding shear intensities for complete interaction.

4.2 Comparison of ρ_m -parameters and $\bar{\alpha}$ -parameters for symmetrical two-pier shear walls

The $\bar{\alpha}$ -parameter is given in Eq. (3.6.1.1).

The ρ_1 -parameter specified for symmetrical two-pier shear wall is (s. Eq. 4.1.6)

$$p_1 = \frac{4 H^2}{\pi^2 \left(\frac{l_1^3 a}{12 I B_1} + \frac{l_1 a}{\mu A B_1} \right)} \left[\frac{a_1^2}{2 I_1} + \frac{2}{A_1} \right] \quad (4.2.1)$$

For a variety of examples the following results for $\bar{\alpha}$ and ρ_1 were calculated (s. table 4.2.1). The results of table 4.2.1 are also plotted in Fig. 4.2.1

$\bar{\alpha}$	q
8,7	31
13,4	73
20,1	164
25,5	263
40,2	657

Table 4.2.1

For a symmetrical two-pier shear wall with $H = 30$ [m] and varying dimensions of piers and connecting beams, three examples of the shear intensity q , for $\bar{\alpha} = 8.7, 13.4, 25.5$ and $q_i = 31, 73, 263$ respectively are plotted in Fig. 4.2.2. The applied load is UDL. The scales are changed such that the complete shear intensity appears to be the same for all three examples.

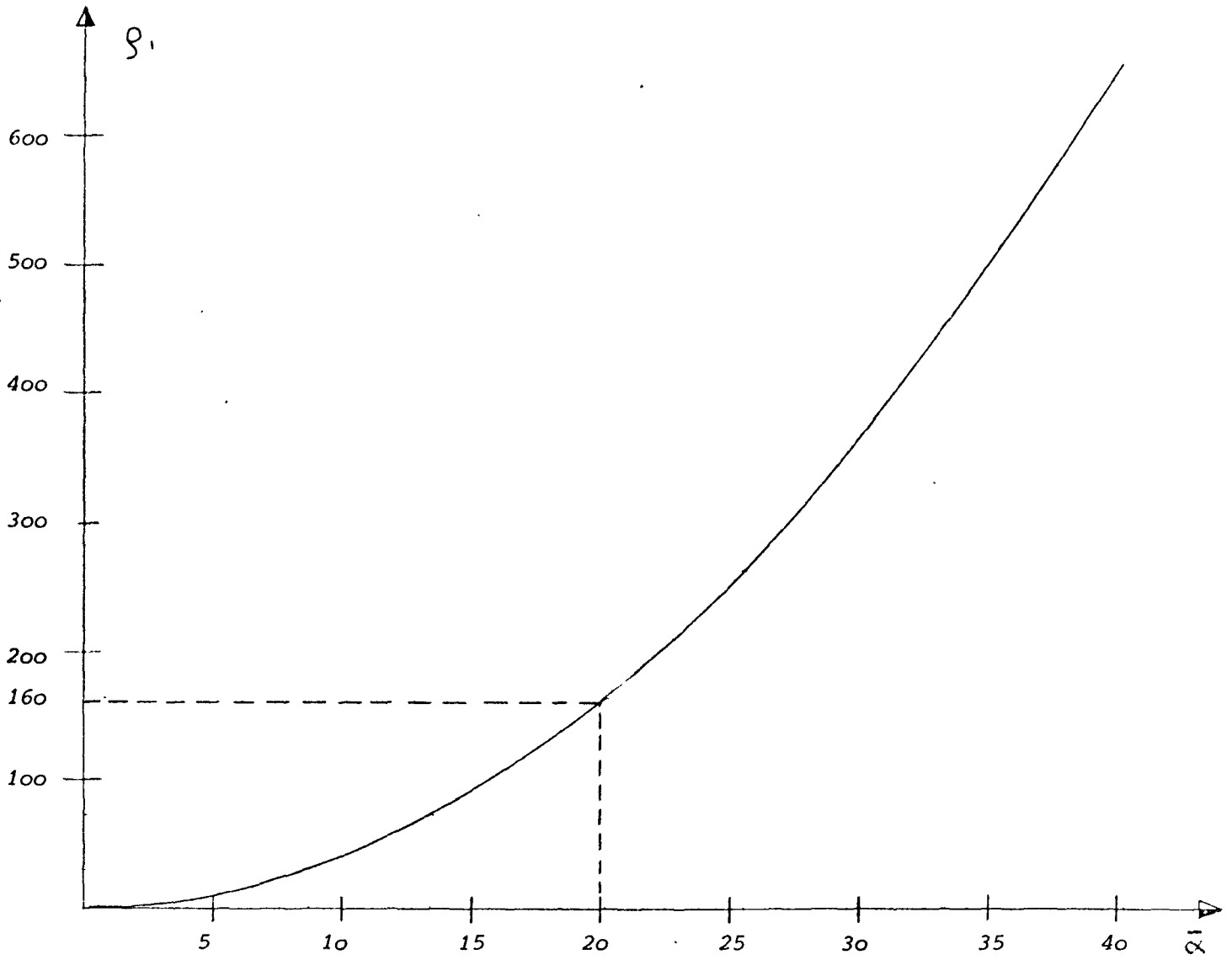


Fig. 4.2.1. Comparison of $\bar{\alpha}$ - parameters and q_1 - parameters for symmetrical two-pier shear walls

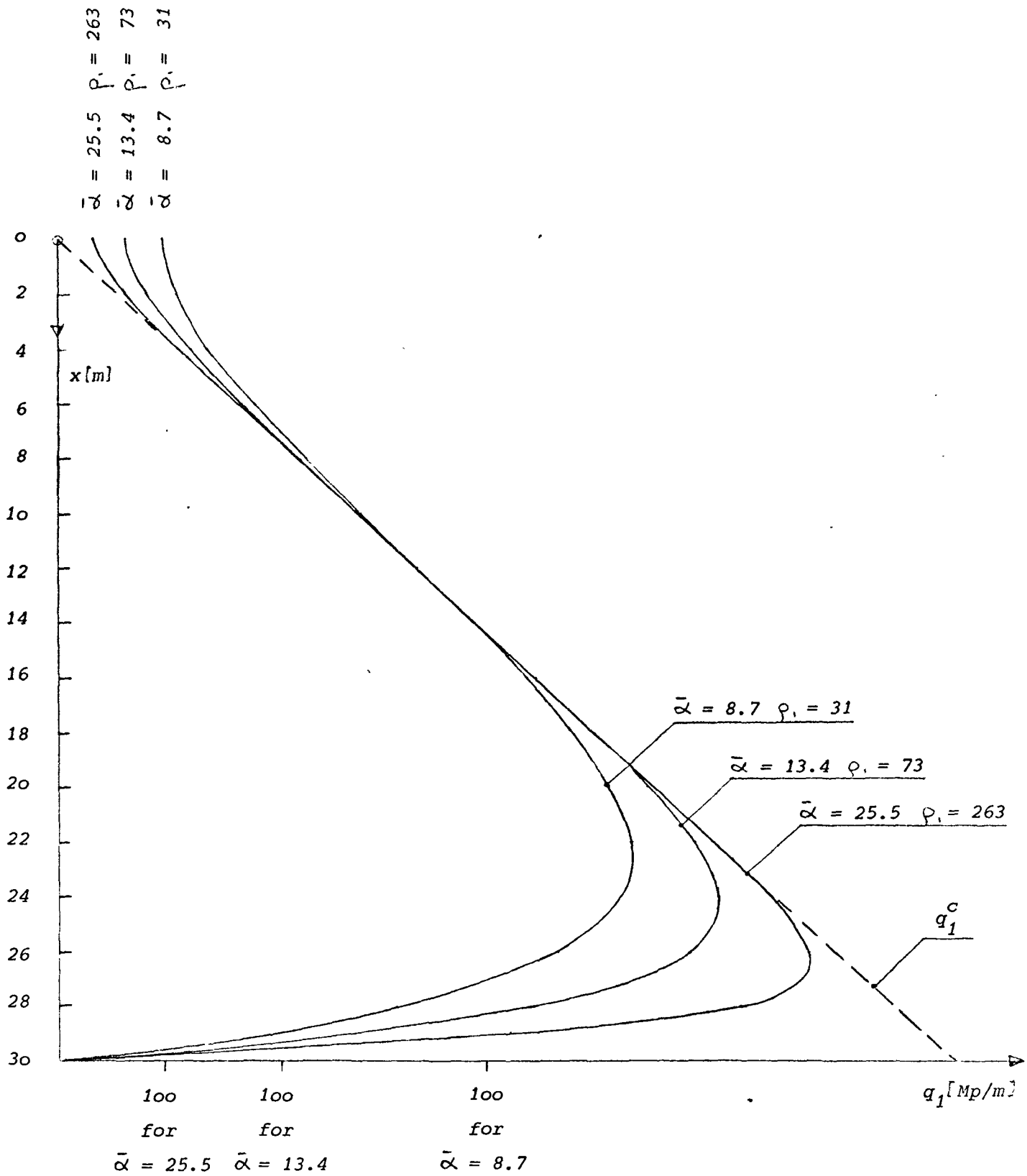


Fig. 4.2.2 Comparison of $\bar{\alpha}$ and ρ_1 for symmetrical two-pier shear walls

From the plot in Fig. 4.2.1 we observe that the parameter $\rho_1 = 160$ corresponds to the parameter $\bar{\alpha} = 20$.

Henceforth we will assume that nearly full interaction at any interface for multiplier shear walls can be assumed for $\rho_m = 160$

Hence

$$\boxed{\rho_m = 160 \quad \text{for nearly full interaction}} \quad (4.2.2)$$

Eq. (4.2.2) also was confirmed by a large variety of examples some of which are shown in the following chapter 4.3.

4.3 Examples for the significance of the ρ_m -parameters

The shear wall system for all examples is the same as in Fig. 3.6.2.1, i. e. the symmetrical five-pier shear wall. Only the stiffness properties of the connecting beams was varied. This can be done easily by varying the height of the connecting beams and by leaving the length and thickness unchanged.

For the shear wall system Fig. 3.6.2.1 the following stiffness parameters for all interfaces can be determined only by varying the height d of the connecting beams (s. table 4.3.1)

d [m]	ρ [%]
0.1	0.6
0.4	27.3
0.6	66.4
0.8	114.1
1.0	165.7
1.5	325.6

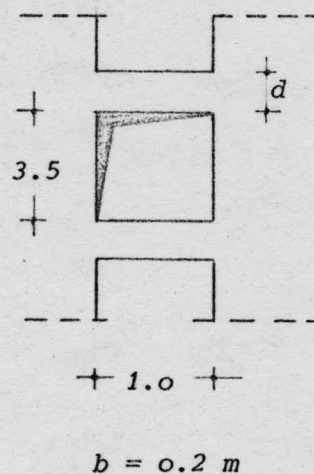


Table 4.3.1

In Fig. 4.3.1 - Fig. 4.3.6 for load cases UDL, single load at $x = 0.0$ (shear wall top), and single load at $x = 35.0$ the shear intensities and deflection are compared to the shear intensities and deflection for complete interaction. It can be observed, that for $\rho \approx 160$ the assumption of complete interaction is acceptable.

In Fig. 4.3.7 and Fig. 4.3.8 the normal force intensities for load case single load at $x = 35$ m are plotted in order to show a typical example of normal force intensities.

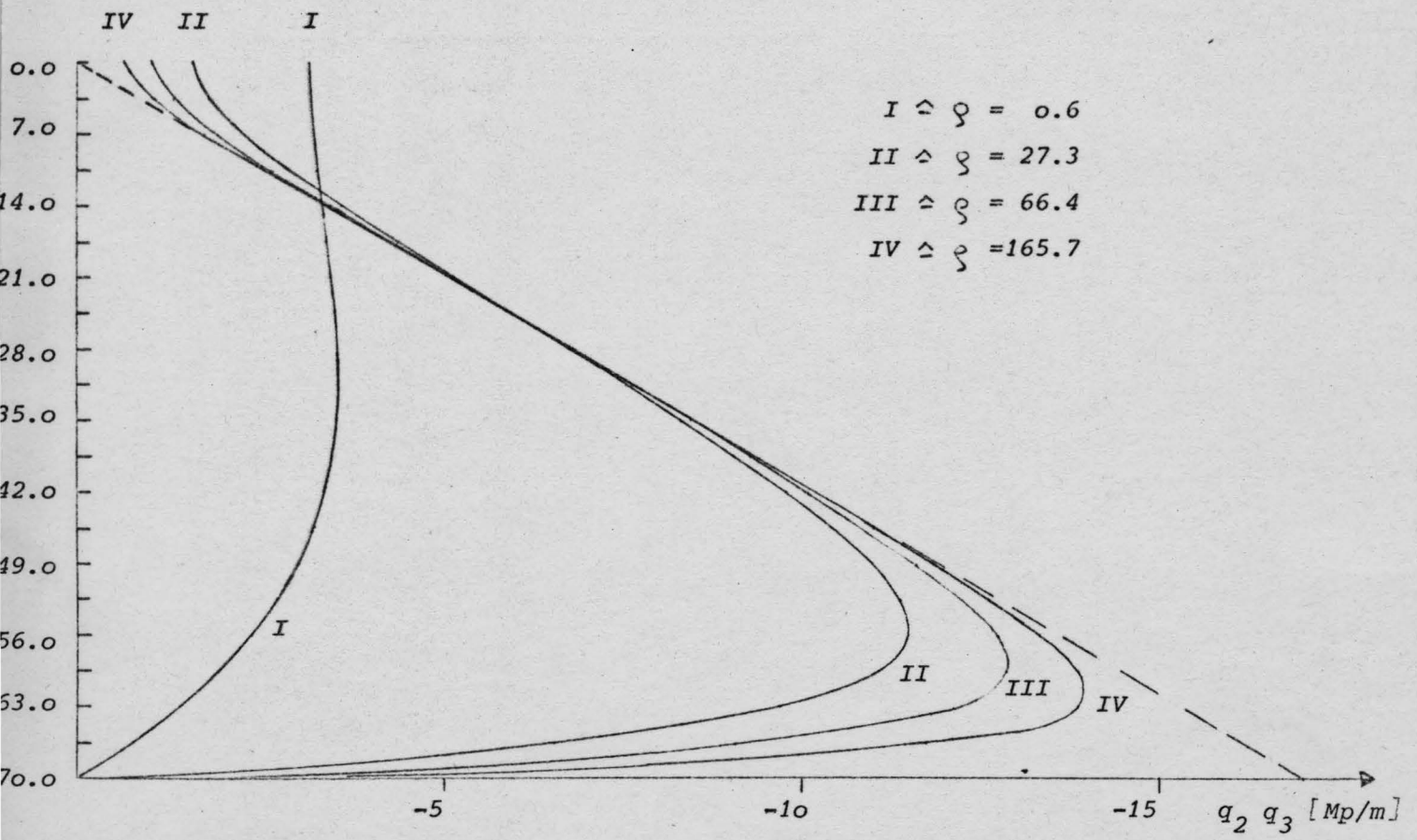
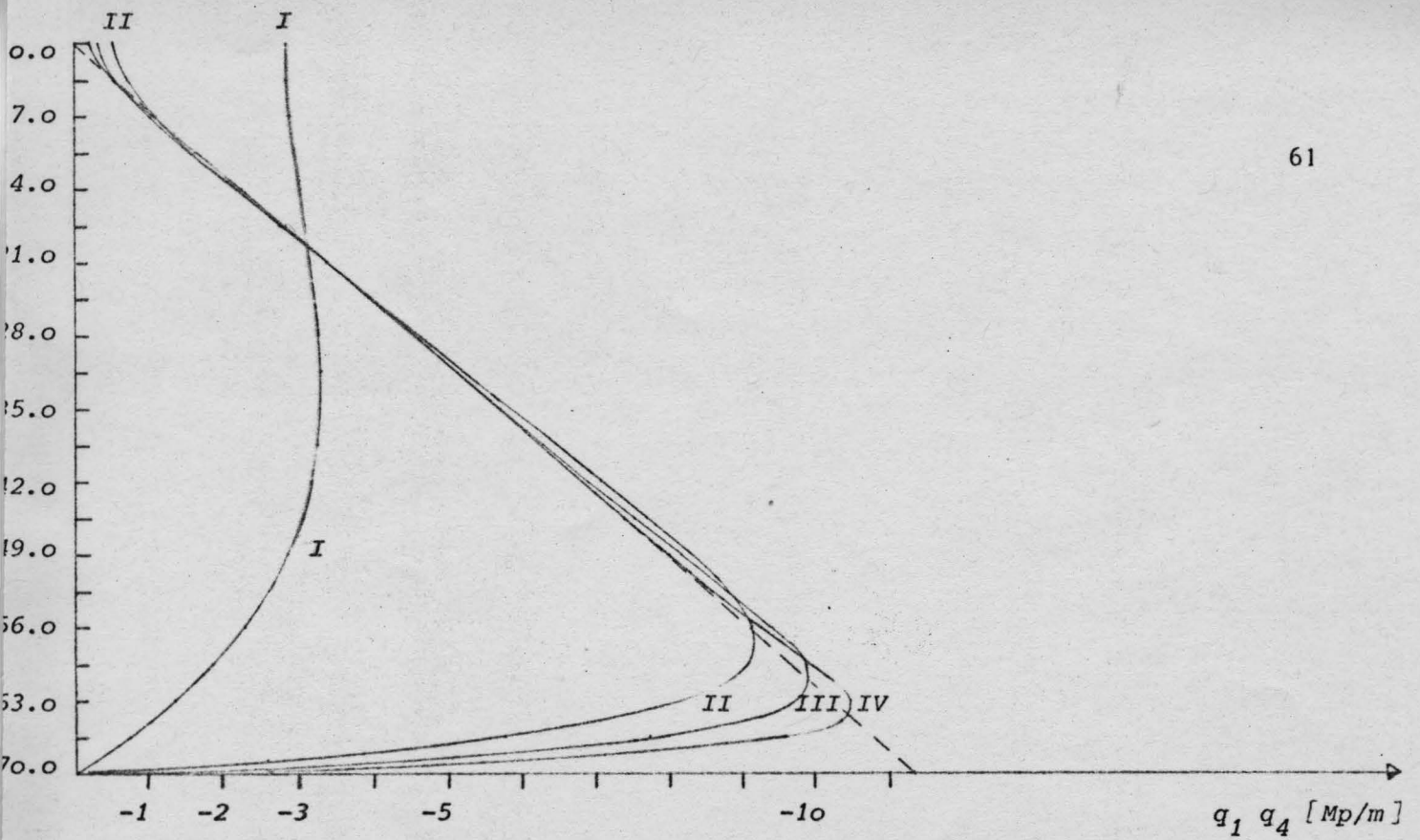


Fig. 4.3.1.- Shear intensities $q_1 \div q_4$ for symmetrical five-pier shear wall for $\zeta = 0.6, 27.3, 66.4, 165.7$ and for $UDL = 5.0$ [Mp/m]

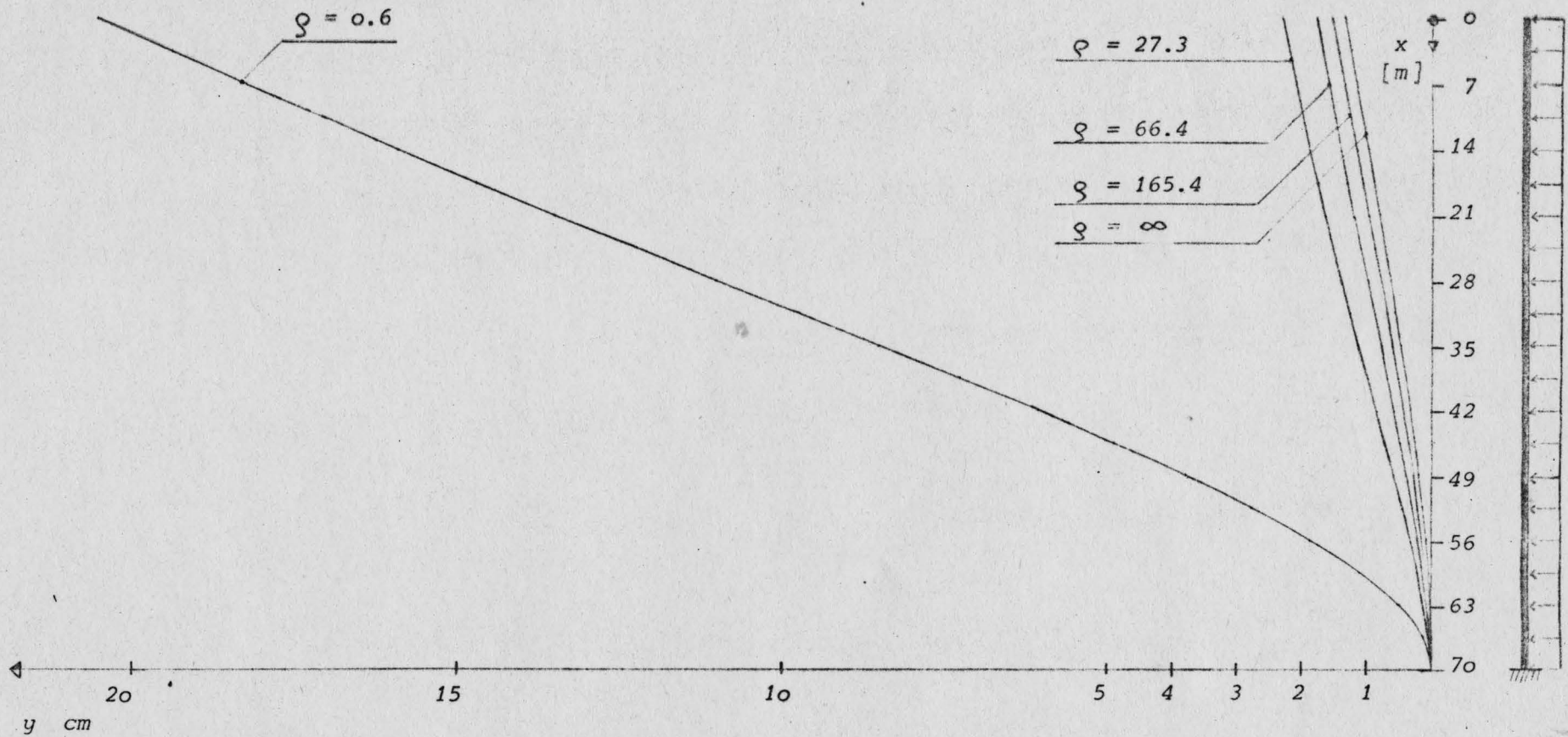


Fig. 4.3.2. Deflection y for symmetrical five-pier shear wall for UDL and $\zeta = 0.6, 27.3, 66.4, 165.7, \infty$

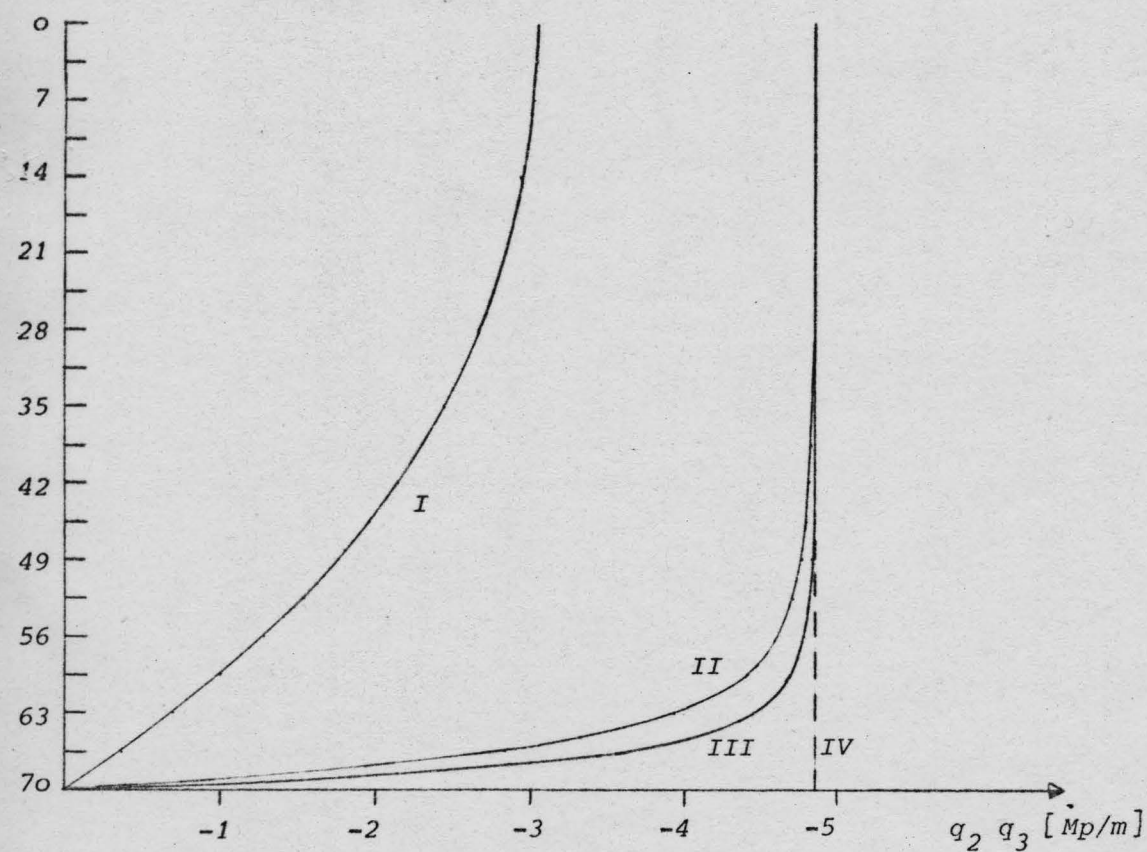
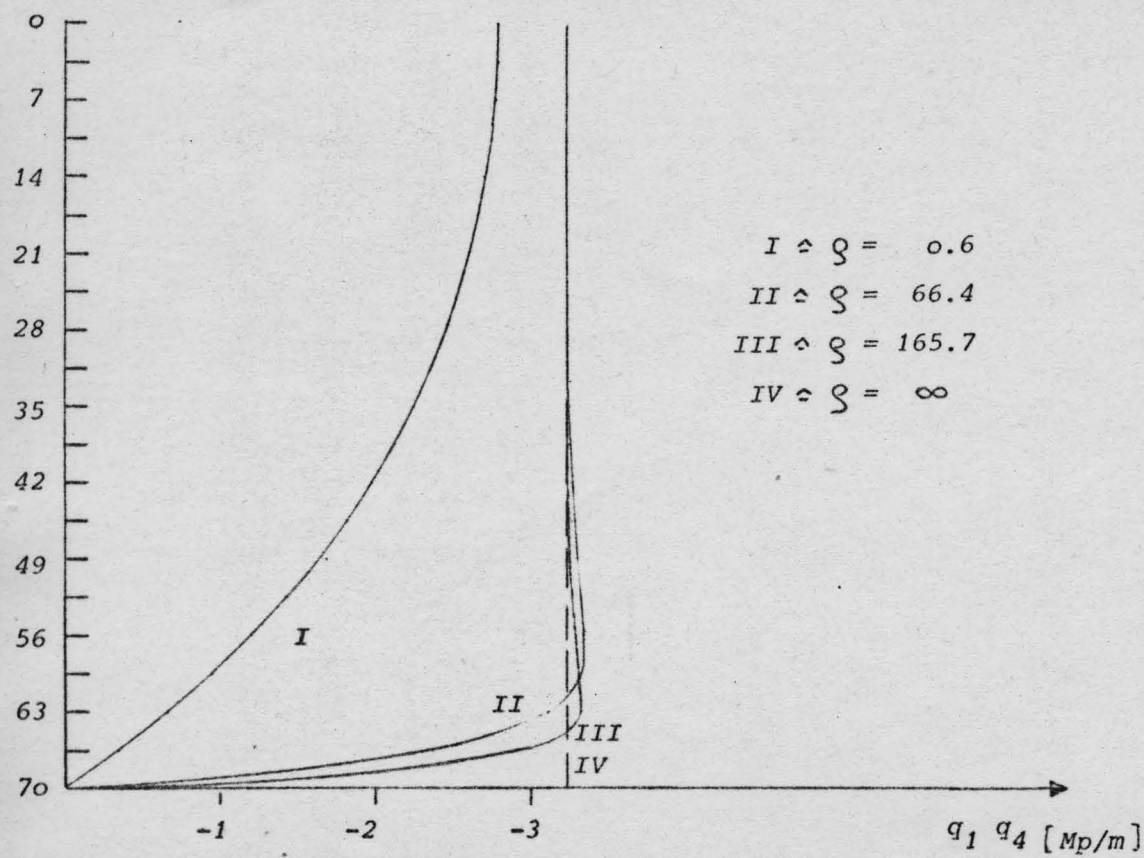


Fig. 4.3.3. Shear intensities q_1, q_2, q_3, q_4 for symmetrical five-pier shear wall for $P = 100$ Mp at $x = 0.0$ m and for $\zeta = 0.6, 66.4, 165.7, \infty$

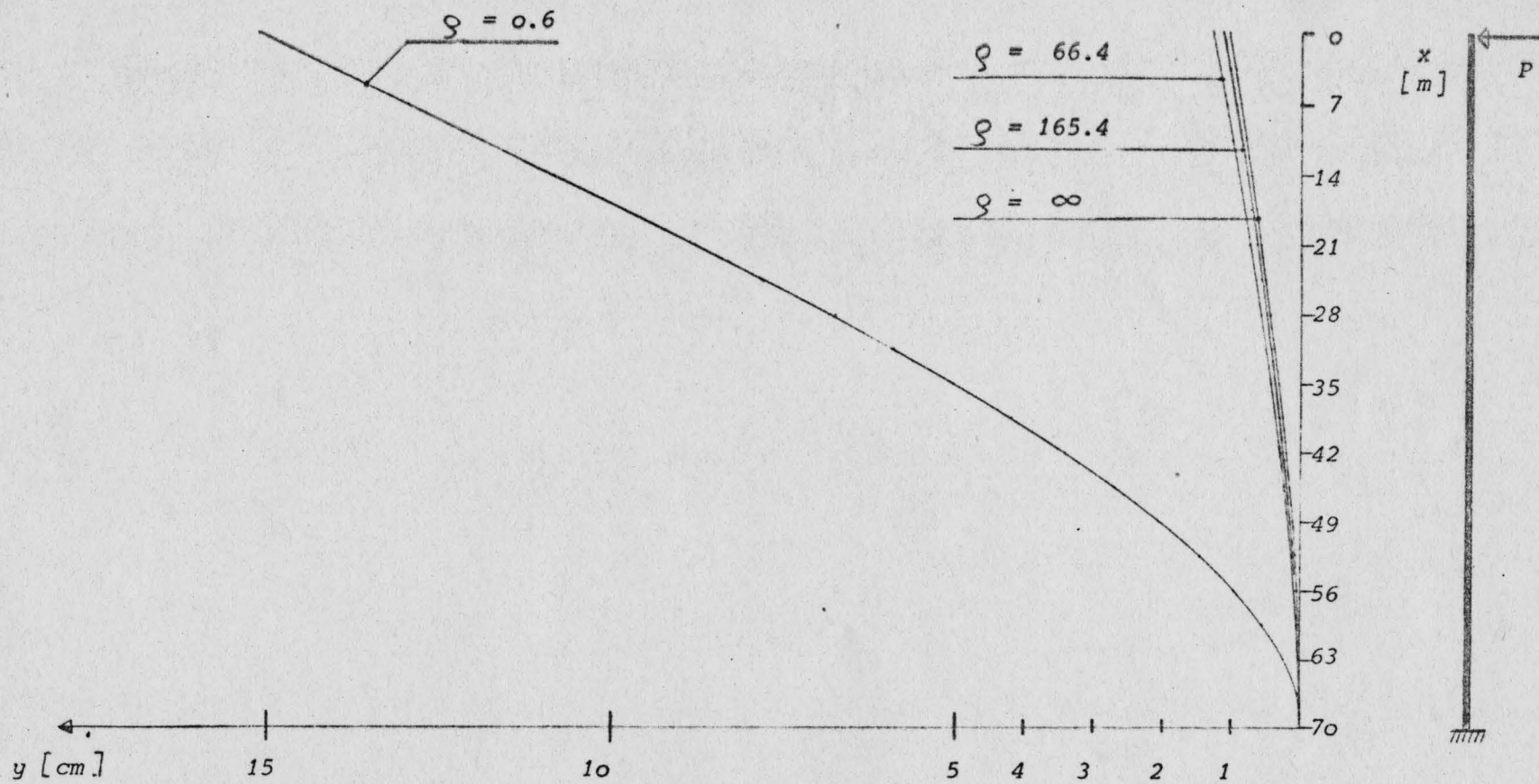


Fig. 4.3.4. Deflection y [cm] for symmetrical five-pier shear wall for $P = 100$ Mp at $x = 0.0$ m and for $\rho = 0.6, 66.4, 165.4, \infty$

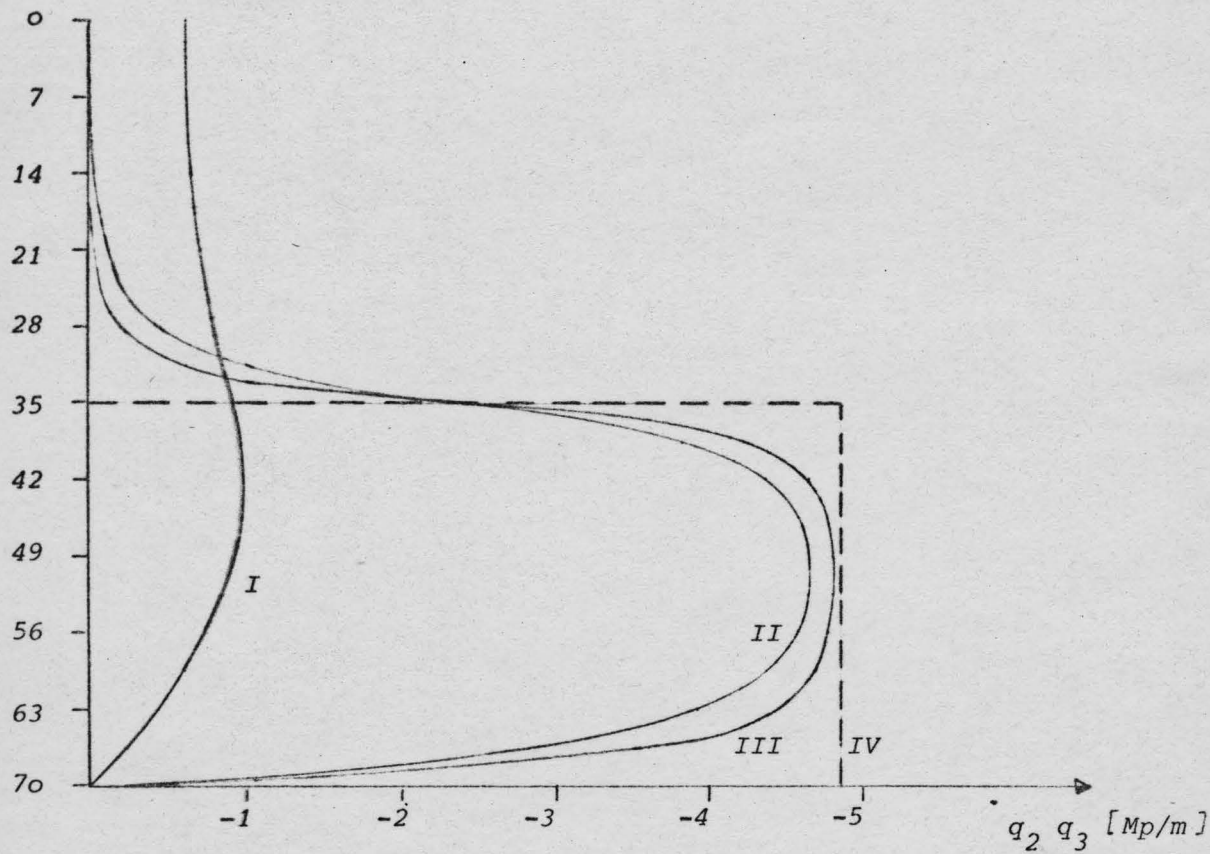
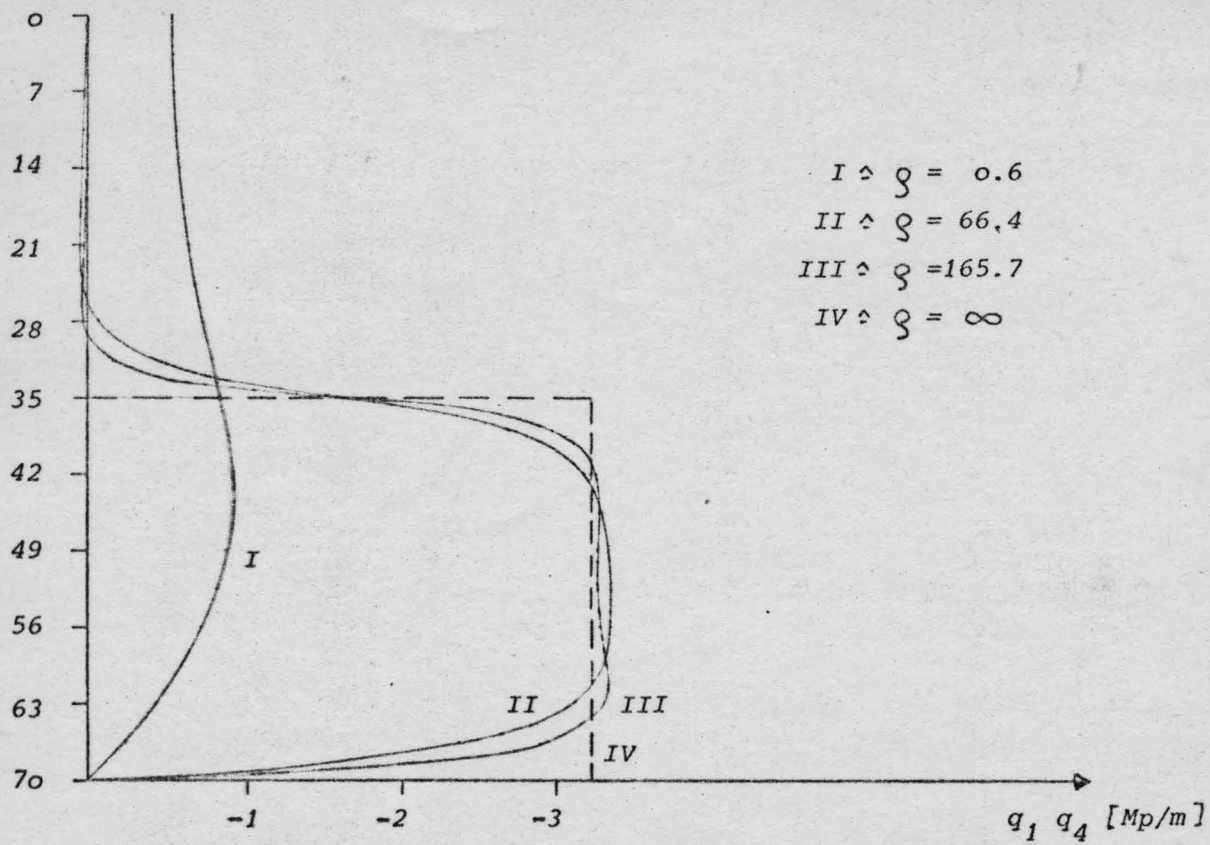


Fig. 4.3.5. Shear intensities q_1, q_2, q_3, q_4 for symmetrical five-pier shear wall for $P=100$ Mp at $x=35.0$ m and for $\zeta = 0.6, 66.4, 165.7, \infty$

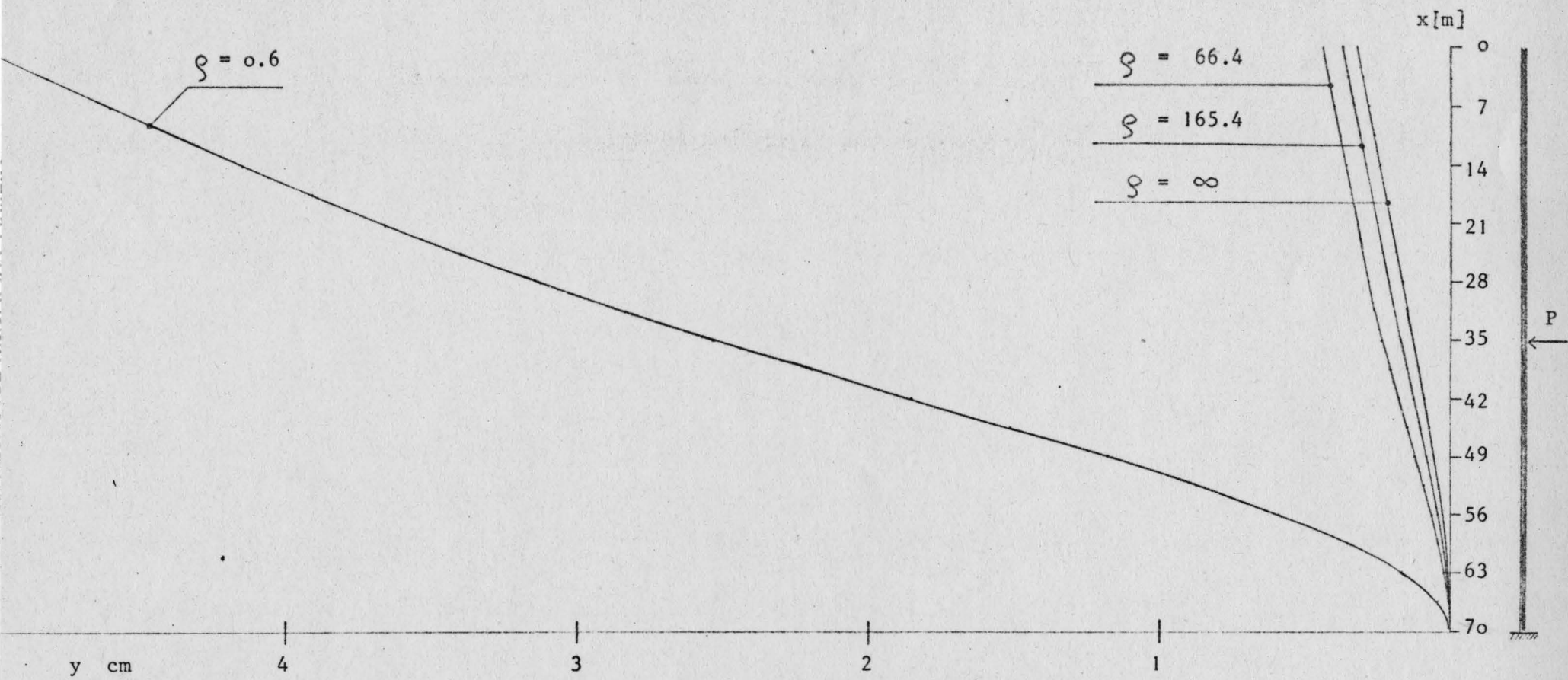


Fig. 4.3.6. Deflection y [cm] for symmetrical five-pier shear wall for $P = 100$ Mp at $x = 35.0$ m and for $\xi = 0.6, 66.4, 165.4, \infty$

$$N_1^* = -N_4^* \approx 0 \text{ for } \varrho \geq 66.4$$

- I $\triangle \varrho = 0.6$
- II $\triangle \varrho = 66.4$
- III $\triangle \varrho = 165.4$
- IV $\triangle \varrho = 325.6$

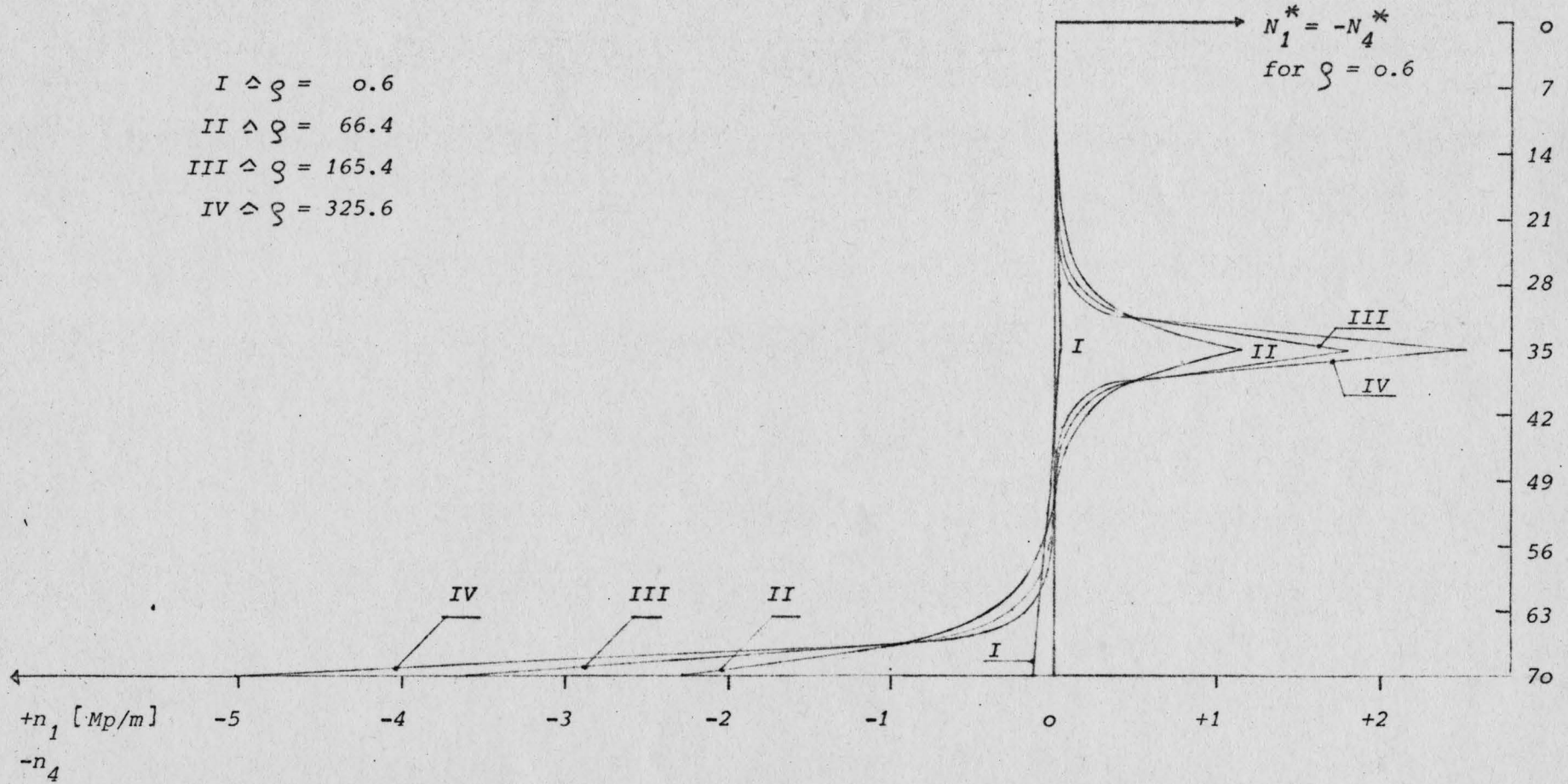


Fig. 4.3.7. Normal force intensities n_1, n_4 [Mp/m] for symmetrical five-pier shear wall for $P = 100 \text{ Mp}$ at $x = 35.0 \text{ m}$ and for $\varrho = 0.6, 66.4, 165.4, 325.6$

$$N_2^* = -N_3^* \approx 0 \text{ for } \varrho \geq 66.4$$

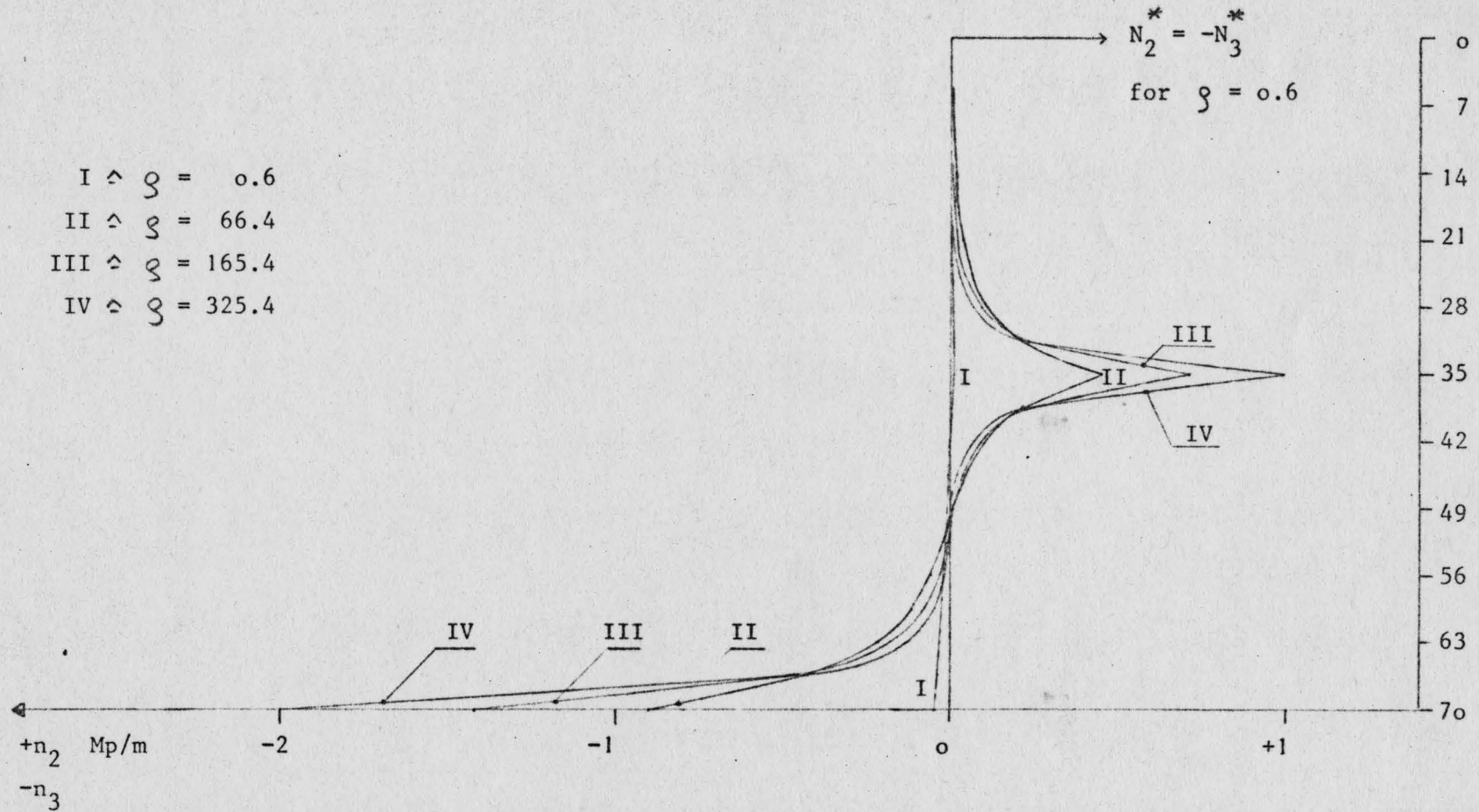


Fig. 4.3.8. Normal force intensities n_2 n_3 [Mp/m] for symmetrical five-pier shear wall for $P = 100$ Mp at $x = 35.0$ m and for $\varrho = 0.6, 66.4, 165.4, 325.6$

C H A P T E R V

The multilayer sandwich beam

5.1 Mathematical formulation of the multilayer sandwich beam

problem with simple supports and symmetrical loading

There is no basic difference between the multiplier shear wall problem and the multilayer sandwich beam problem, if the multilayer sandwich beam is simply supported and symmetrically loaded (Fig. 5.1.1).

The shear constant k_m for each interface must be known in the first place, since k_m is now a constant of the shear core (glue, studs, ...) between the layers. However the mathematical meaning of k_m remains the same.

For simple supports and symmetrical loading the slope of deflection $y(x)$ is zero at midpoint, i. e. at the axis of symmetry. We observe, that the boundary conditions for shear walls (Chapter 3.1) and for simply supported multilayer sandwich beams under symmetrical loading are the same. Therefore we can say, that the mathematical formulation of the simply supported multilayer sandwich beam under symmetrical loading and the multiplier shear wall problem is identical (Chapter II and III).

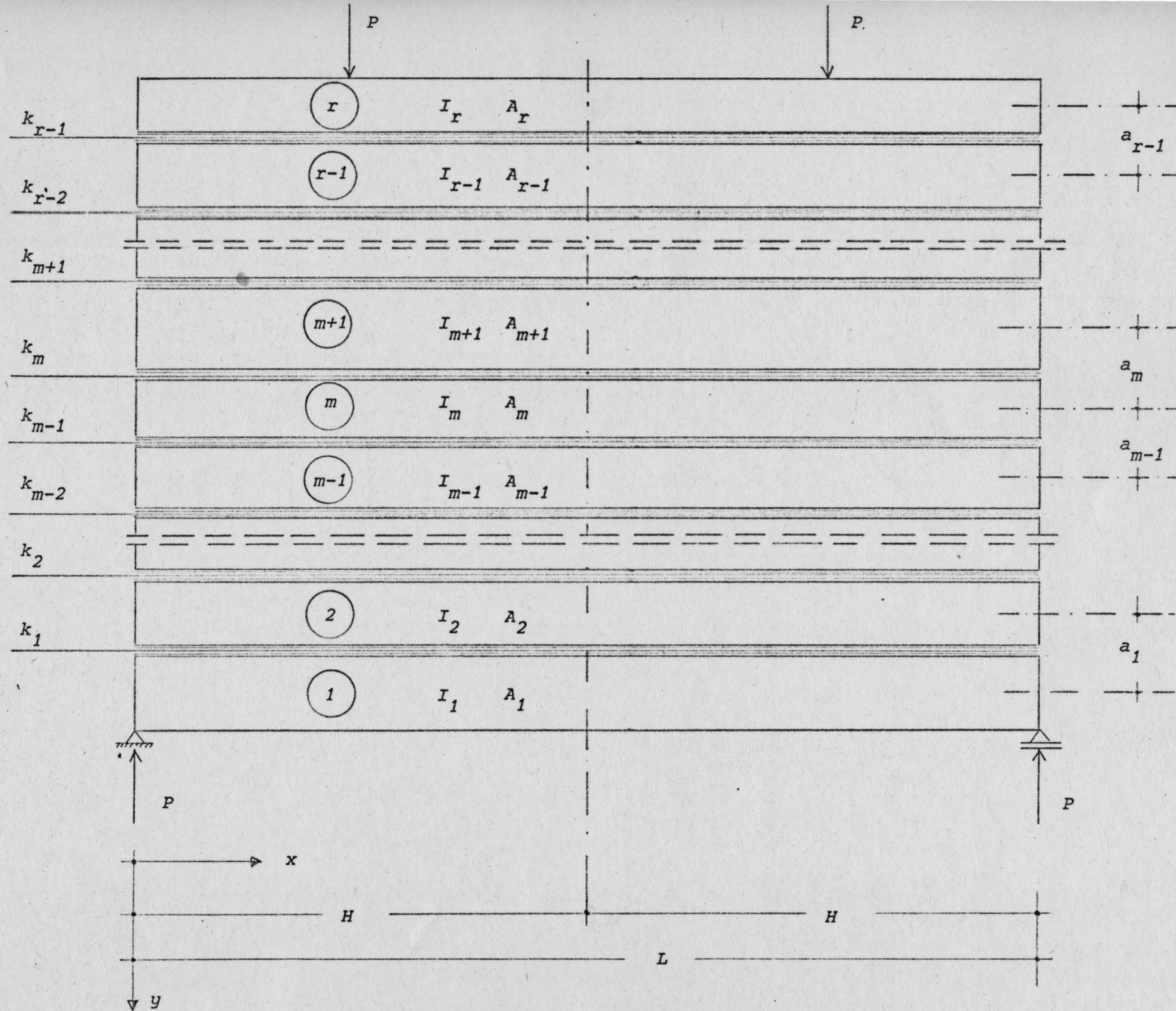


Fig. 5.1.1. Multilayer sandwich beam under symmetrical loading

5.2 Example

The example will demonstrate some characteristic properties of a multilayer sandwich beam. A large number of layers was chosen in order to show, how the strains in a cross-section deviate from the linear strain distribution for complete interaction or homogeneous material in a way, which is similar to the strain distribution of plates and obviously is due to the influence of shear deformation (Fig. 5.2.2).

In Fig. 5.2.3 the normal force intensities in the interfaces are plotted. Between the lower layers we obtain tension and between the upper layers we obtain compression.

In Fig. 5.2.4 the shear intensities in the interface are plotted.

Slip is defined as the relative displacement of originally adjacent points of opposite layer in the undeformed state. Therefore shear intensity and slip are proportional and slip can be calculated from the shear intensity by

$$\text{slip}_m(x) = \frac{q_m(x)}{k_m} \quad (5.2.1)$$

From Eq. (5.2.1) it follows that Fig. 5.2.4 also can be considered as the plot of $\text{slip}_m(x)$, if only the scales are changed.

In Fig. 5.2.5 the normal forces $N_m(x)$ in the layers are plotted and Fig. 5.2.6 shows the bending moments $M_m(x)$ which have to be equal for all layers.

The properties of the multilayer sandwich beam, which was chosen for this example, are specified as follows:

All layers and interfaces have the same properties.

The dimensions can be assumed as [kg, cm]

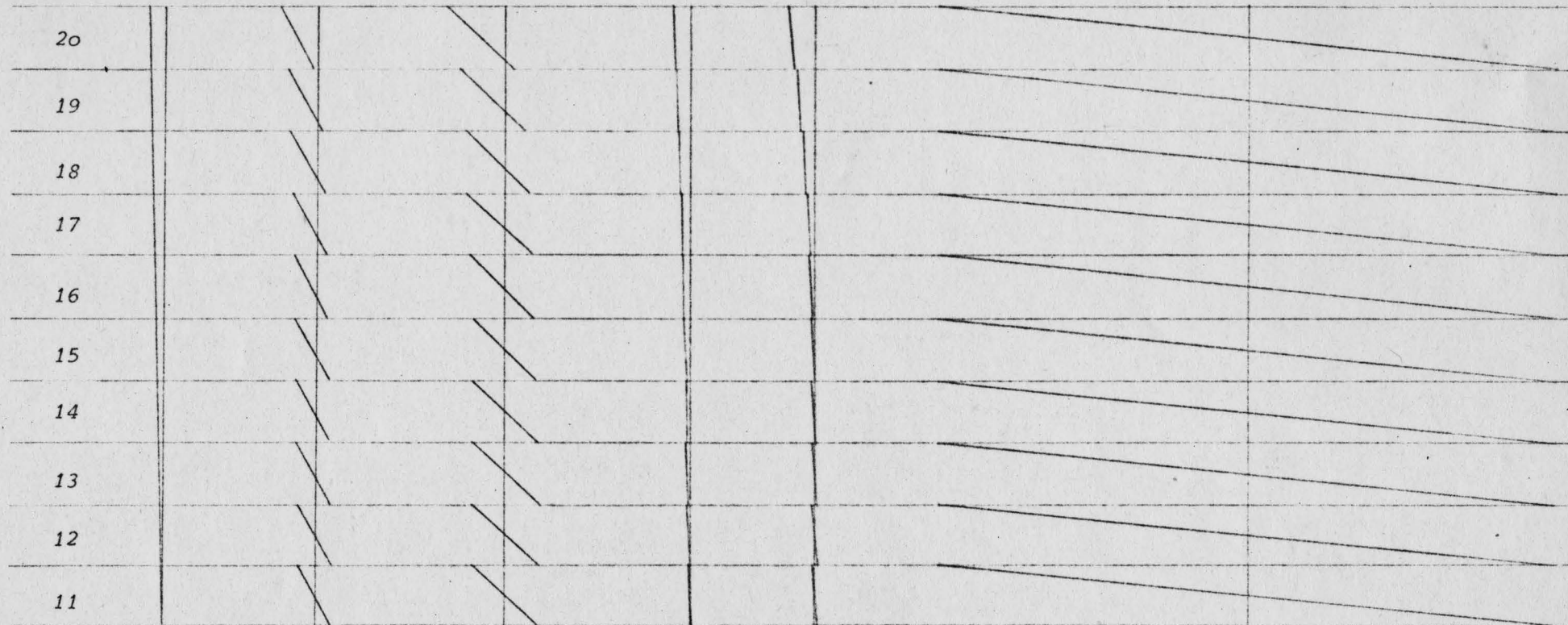
Note: 1 kg = 1000 grams = 2,20 lb
 1 cm = 0,394 inch

Further

E = $3 \cdot 10^6$ kg/cm²
 H = 100 cm
 P = 100 kp
 x_P = 50 cm
 A_m = 1,0 cm²
 I_m = 0,0834 cm⁴
 a_m = 1,0 cm
 r = 20 = number of layers
 K_{m1} = 10^4 kg/cm²

In order to compare the strain distribution for a lower degree of interaction a second example was computed with $k_{m2} = 0,25 \cdot 10^4$ kg/cm².

Number of
layer



$x_1:$	50	50	50			50
$x_2:$	100			100	100	100
$k_m:$		10^4	$0.25 \cdot 10^4$	10^4	$0.25 \cdot 10^4$	0

Fig. 5.2.2 Strain distribution under point of load application ($x = 50$) and at midspan ($x = 100$) in the upper left part of a multilayered beam

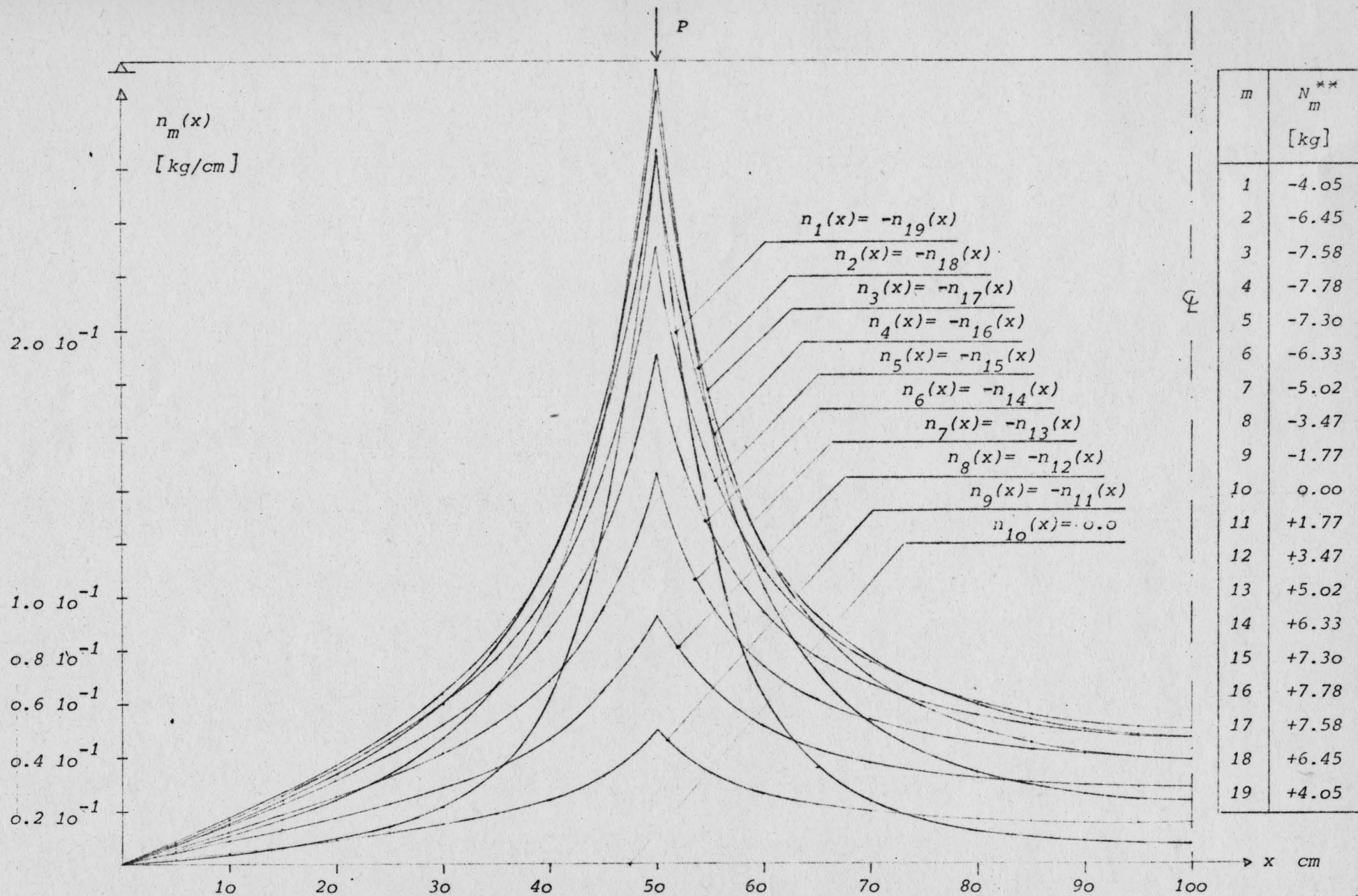


Fig. 5.2.3. Normal force intensities $n_1(x) \div n_{19}(x)$ for left hand side of a multilayered beam ($k_m = 10^4$). For singular normal forces $N_1^{**} \div N_{19}^{**}$ see table.

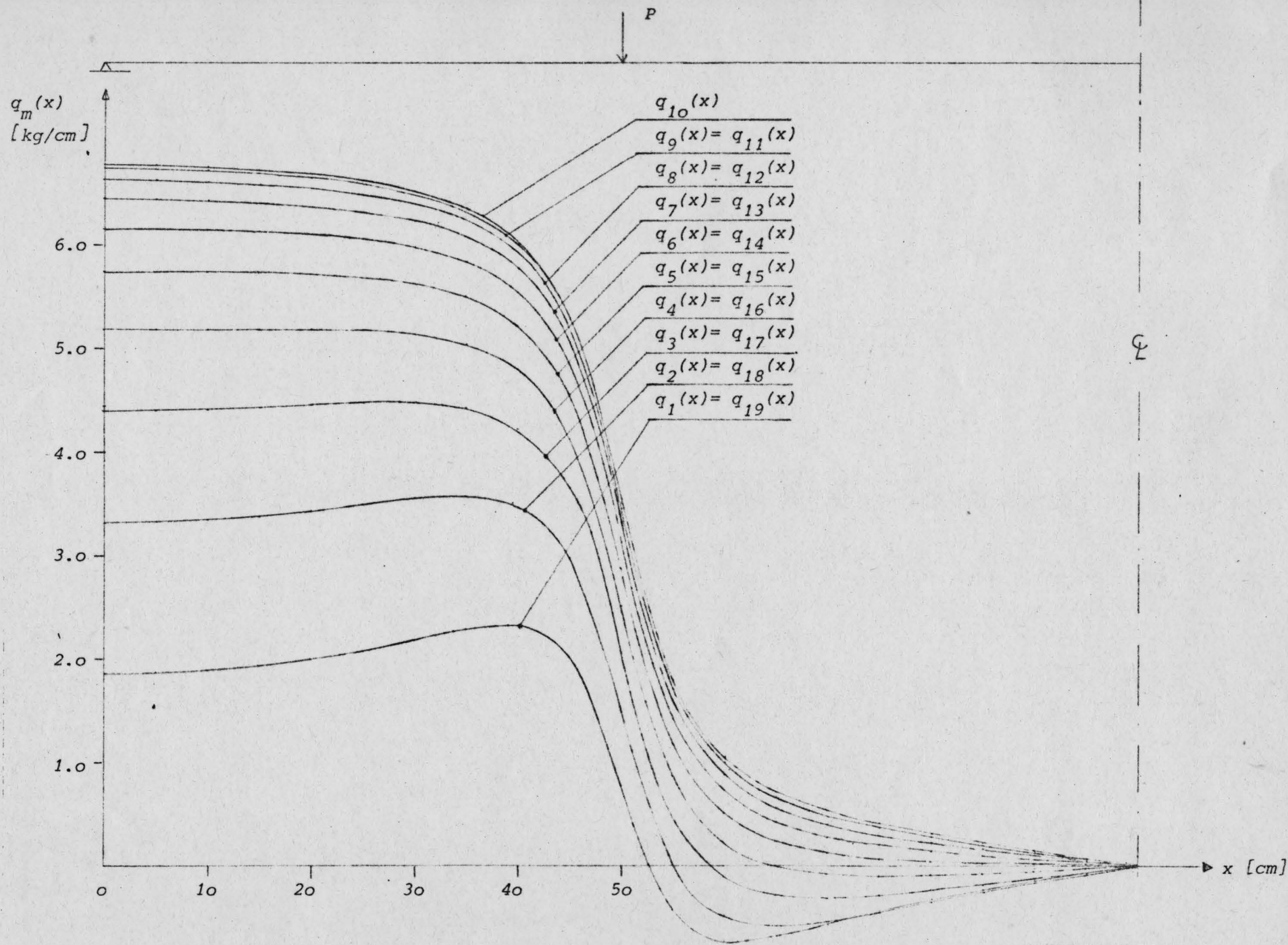


Fig. 5.2.4. Shear intensities $q_m(x)$ for left hand side of a multilayered beam ($k_m = 10^4$)

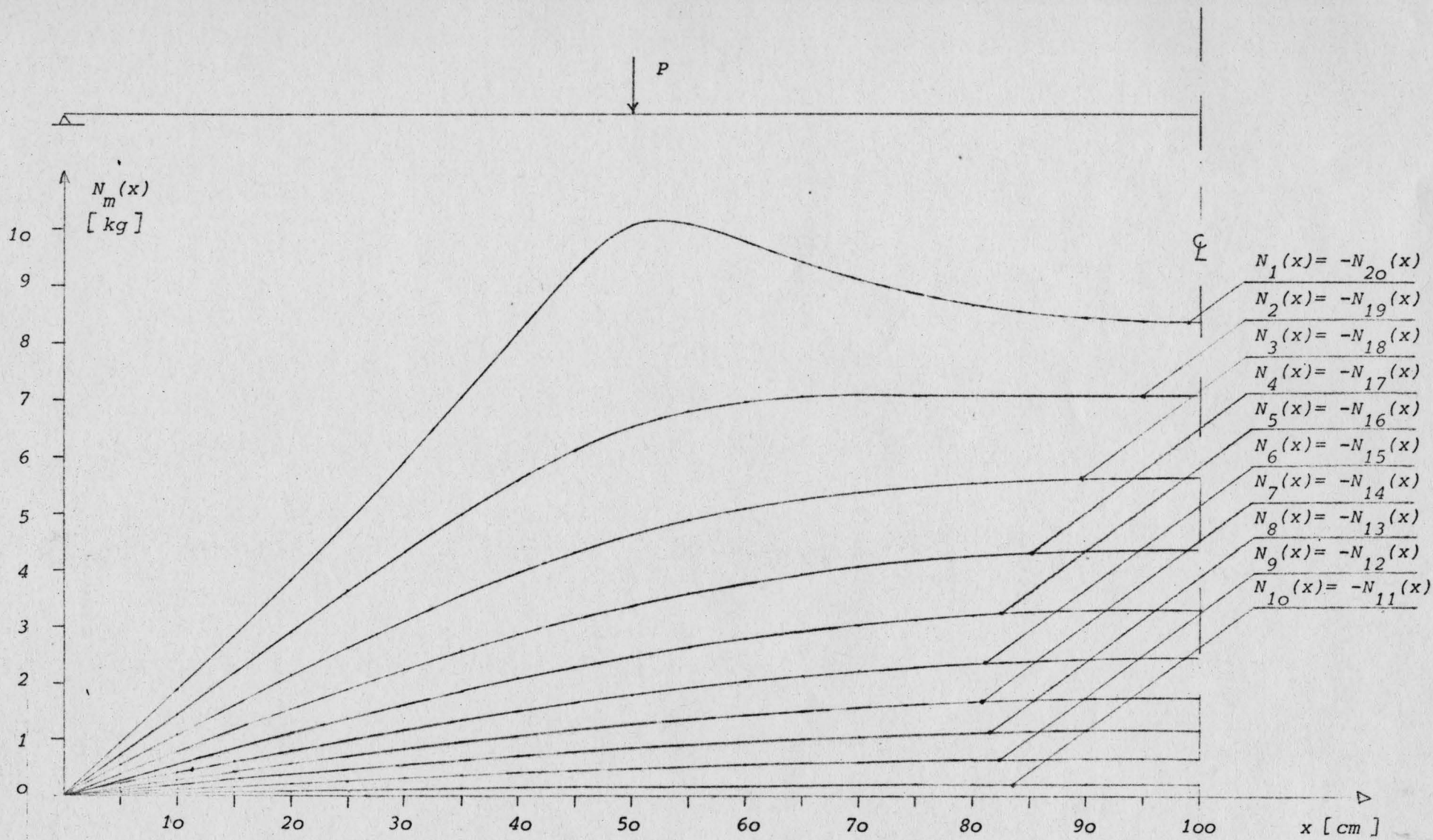


Fig. 5.2.5. Normal forces $N_m(x)$ for left hand side of a multilayered beam ($k_m = 10^4$)

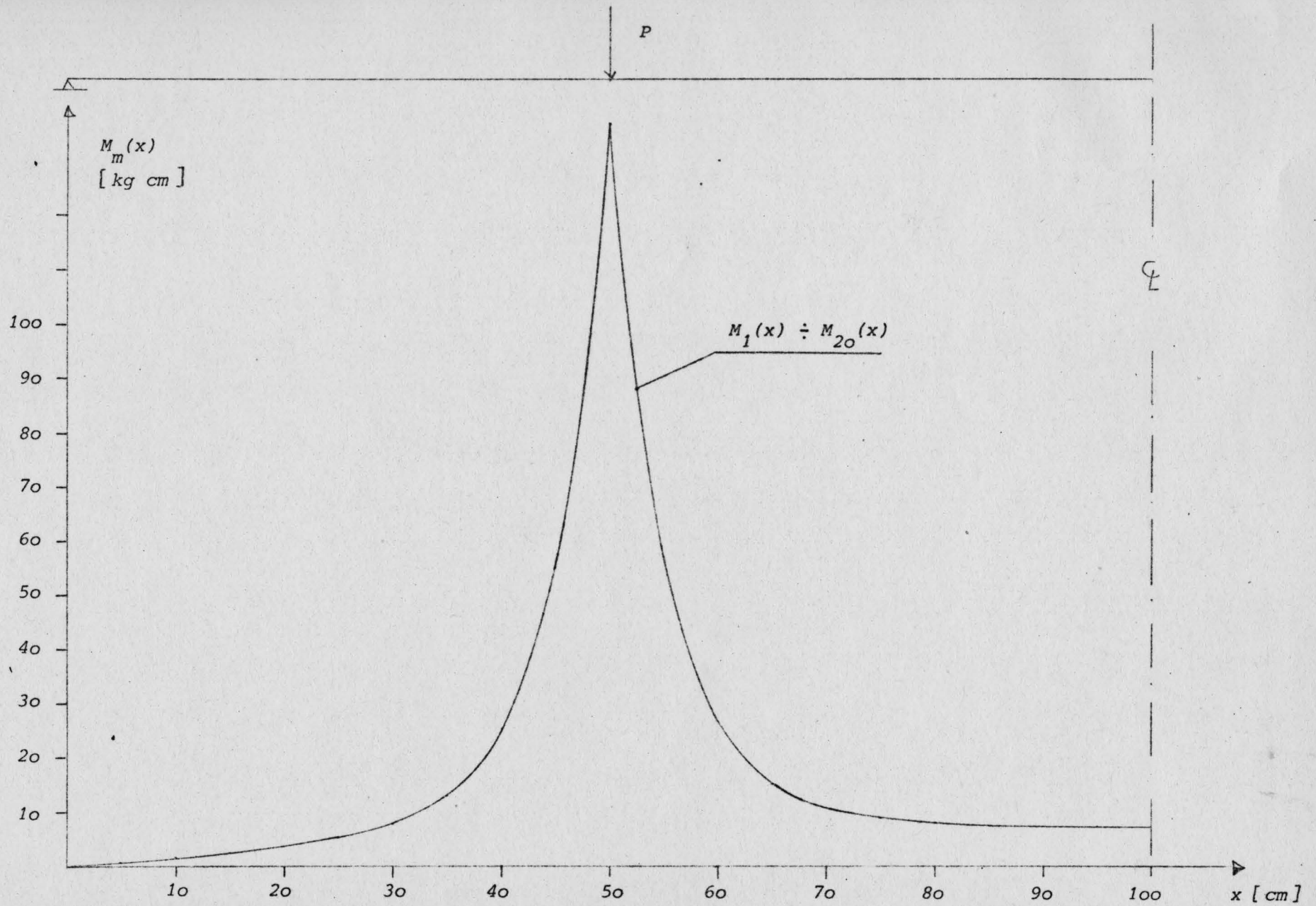


Fig. 5.2.6. Bending moments $M_m(x)$ for left hand side of a multilayered beam ($k_m = 10^4$)

5.3 Discussion of the results of chapter 5.2

a) The results of Fig. 5.2.2 show, that the strain distribution varies between linear strain distribution for a homogeneous beam or complete interaction respectively and the strain distribution for zero interaction, i. e. if the sandwich beam behaves as separate layers of beams.

We also may notice, that between $x = 100$ (midspan) and $x = 50$ (point of load application) an increase of strains takes place. This is due to the fact, that in this section contrary to the case of complete interaction already slip and shear intensities occur.

b) From experience we know, the upper layers tend to separate from each other and create small gaps. The lower layers tend to compress each other. According to this experience we would have expected positive normal force intensities in the interface of the upper part and negative normal force intensities (compression) in the interfaces of the lower part of the sandwich beam. However in this context we have to remember assumption (e) and Eq. (2.2.1). This assumption says, that we assume each layer loaded according to Eq. (2.2.1) in the first place. The lamina forces $q_m(x)$, $n_m(x)$ and N_m^* then are determined to "correct" this assumed statically determinate system. From there it is obvious that assumption (e) (Chapter 2.2) influences the normal force intensities $n_m(x)$ in a way, which can not be predicted. Adekola (7) has shown, how uplift forces can be determined without assumption (e).

For a two-layer sandwich beam this leads to differential equations, which only can be solved by finite difference methods.

- c) Let us consider the slip in the multilayer sandwich beam and the deformation due to shear in a homogeneous beam as being similar. Then from Fig. 5.2.5 and Fig. 5.2.6 we can see, that the bending moments $M_m(x)$ in the layers are concentrated under the points of load application and decrease rapidly up to the center line, while the normal forces $N_m(x)$ are nearly constant in the section between the points of load application. With respect to plasticity this would mean, that the plastic zones would be concentrated under the points of load application and would decrease up to the center lines. This shape of the plastic zones in a simply supported homogeneous beam under two point loads already has been observed in experiments. The theory, which says that the degree of plastification of a cross-section only depends on the magnitude of the applied moment, would mean for the simply supported homogeneous beam under two point loads, that the propagation of the plastic zones is constant in the section between the points of load application, because in this section the moments are constant. From there we assume, that shear deformation comes into play and gives rise to a loss of interaction similar to the multilayer sandwich beam.

C H A P T E R VI

Development of programs6.1 The multilayer sandwich beam program

Based on the results of chapter II and chapter III the multilayer sandwich beam program was developed. The program is restricted to the simply supported multilayer sandwich beam under two symmetrical point loads. The load dependent coefficients A_n for this special load case can be determined from Eq. (3.5.1) assuming a negative load $-P$ at $x = 0$ and a positive load $+P$ at $x = x_a$. Superimposing these two load cases we obtain from Eq. (3.5.1)

$$A_n = \frac{4P}{(2n-1)\pi} \sin \frac{(2n-1)\pi x_a}{2H} \quad (6.1.1)$$

The program consists of the following steps:

(a) The input

The input required for this program is

(i) Material properties -

E and the shear moduli K_m of the interfaces.

(ii) Geometrical properties - area, moment of inertia, thickness and distance of the center lines of the layers and the beam length.

(iii) Load data - load and point of load application.

(b) The B-matrix is built and inverted by subroutine MINV. The coefficients $\xi_{m,v}$ are calculated Eq. (3.3.1.11) .

(c) For each n of the Fourier series:

The $\bar{\delta}$ -matrix is built and solved by subroutine SOLVE [Eqs. (3.2.12) - (3.2.14)]. With the resultant coefficients $C_{v,n}$, with Eq. (6.1.1), and with Eqs. (3.3.1.12), (3.3.2.3), (3.3.3.2), (3.3.4.1) the reactions $q_m(x)$, $v_m(x)$, N_m^* , $N_m(x)$ and $M_m(x)$ and slip(x) are calculated. Each set of coefficients $C_{v,n}$ is checked with the initial set of coefficients $C_{v,1}$. If for all $\frac{C_{v,n}}{C_{v,1}} \leq \epsilon = 0.00001$ the accuracy is assumed to be satisfactory, otherwise the calculation is repeated for $n+1$. The resultant reactions and slip are the sum of reactions and slip for all n .

(d) From $M_m(x)$ and $N_m(x)$ the strains are determined.

(e) Output of reactions, strains and slip.

6.1.1 Limitation on the use of the program

(a) Load case -

The program was developed for a simply supported multilayer sandwich beam under two symmetrical point loads. Other symmetrical load cases could easily be incorporated.

(b) Structural properties -

For each layer area, moment of inertia and thickness have to be constant all over the length of the beam, but can vary from layer to layer. Also the shear moduli k_m have to be constant for each interface but may be different for different interfaces.

(c) Capacity of the program -

The actual capacity of the program is limited to $N1 = 30$ layers and to $N3 = 20$ steps subdividing x from 0 to H . However the capacity can be extended by extending the storage capacity

6.2 The shear wall program with piecewise trapezoidal load

For the shear wall program a very general type of loading was chosen i.e. the piecewise trapezoidal load. This type of loading includes uniformly distributed loading, triangular loading, piecewise uniformly distributed loading. Arbitrary shaped loading can be approximated as well.

The load-dependant coefficients A_n are given by Eqs. (3.5.5) or (3.5.6).

The program consists of the following steps:

(a) The input

The input required for this program is

(i) Material properties - E and ratio shear modulus to E

(ii) Geometrical properties - area, moment of inertia, width and length of piers and connecting beams, effective shear area of connecting beams, story height and distance of center lines of piers.

(iii) Load data -

piecewise trapezoidal loads and points of load application.

(b) The shear moduli k_m of the connecting medium, i. e. the connecting beams is calculated for each interfase. Then the β -matrix is built and inverted by subroutine MINV. The coefficients $\epsilon_{m,v}$ are calculated [Eq. (3.3.1.11)] and from the structural properties the stiffness parameters ϱ_m are determined.

(c) For each n of the Fourier series:

The $\bar{\delta}$ -matrix is built and solved by subroutine SOLVE [Eqs. (3.2.12) - (3.2.14)]. With the resultant coefficients $C_{v,n}$, with Eq. (3.5.6) and with Eqs. (3.4.1), (3.4.3), (3.4.4) and (3.4.6) the reactions $Q_m(x)$ and $N_m^c(x)$ in the connecting beams are calculated. Each set of coefficients is checked with the initial set of coefficients $C_{v,1}$. If for all $\frac{C_{v,n}}{C_{v,1}} \leq \xi = 0.00001$ the accuracy is assumed to be satisfactory. Otherwise the calculation is repeated for $v+1$. The resultant reactions are the sum of reactions for all n .

- (d) From $Q_m(x)$, $N_m^c(x)$ and $M_{o,m}(x)$ the bending moments and normal forces of the piers are determined from equilibrium considerations.
- (e) The deflection of the shear wall is determined for the actual degree of interaction and for comparison for full interaction. A method is used considering the piers loaded with $-\frac{M_m(x)}{EI_m}$. Assuming the fixed and free end exchanged the resultant moments are the deflections.
- (f) Output of stiffness parameters, reactions and deflection.

6.2.1 Limitation on the use of the program

(a) Structural properties -

For each pier moment of inertia, area and width have to be constant all over the shear wall height but may vary from pier to pier. The shear modulus of the connecting medium has to be constant for each interface but can be different for different interfaces: this means that for constant storey height all connecting beams of each interface must have the same properties while for the last connecting beam on the top of the shear wall the effective shear area and moment of inertia must be half of the connecting beams below.

(b) Capacity of the program

The actual capacity is limited to $N1 = 20$ piers and $N3 = 40$ stories, but the capacity can be extended if the storage reservation of the program is enlarged.

C H A P T E R VII

Conclusions

7.1 Conclusions

The multiplier shear wall problem and the multilayer sandwich beam problem have been solved by means of Fourier series. Normal deformation of piers and layers have been taken into account. The mathematical formulation and solution of the problem is easier and less complex than the solutions given by other authors (4), (5), (6), since for the set of linear inhomogeneous differential equations describing the problem, the particular solution already is the complete solution (chap. 3.2). This allows a better insight into the nature of the structure. It was possible to determine stiffness parameters which describe the degree of interaction between the layers or piers. It was found that for $\rho_m = 160$ full interaction for interface m can be assumed (chap. IV). Further, the Fourier solution allows for a great variety of load shapes, as for instance for the piecewise trapezoidal load, which can be used to approximate nearly all other kinds of load shapes as well. The Fourier solution was compared to the results of Beck⁽²⁾ (chap. 3.6) and numerical coincidence was observed. However experiments to confirm the theoretical results for the multiplier shear wall are desirable.

The multilayer sandwich beam problem was analysed to find out, if the propagation of plastic zones in homogeneous beams can be simulated by the multilayer sandwich beam. It was found, that the results can be used to explain the shape of the plastic zones, which deviates from the shape calculated by conventional plastic theory. But in this stage of development it is not clear, whether the multilayer sandwich beam model can be extended to a detailed explanation of the shape phenomenon of the plastic zones in homogeneous beams under two symmetrical point loads or if the multilayered beam model only gives useful suggestions as how to improve the plastic theory.

7.2 Future developments

Shear wall problems have been analysed by different mathematical approaches as for example by the finite difference method and the matrix displacement method. These methods are merely numerical and they do not inform much about the nature of the structure, for instance, they would not be able to trace parameters, which describe certain structural properties, as the continuous method does.

Though the matrix displacement method is very powerful and very complex three dimensional shear wall problems have already been solved, it seems to be desirable to extend the continuous method used here to more complex shear wall problems and structures because of the reasons described above .

Possible future developments could be

- to analyse the multiplier shear wall under vertical loading
- to analyse three dimensional shear wall problems
- to analyse the dynamic response of the multiplier shear wall.

Appendix A

Details of the multilayer sandwich beam computer program

Introduction: The program analyses the simply supported multilayer sandwich beam under two symmetrical point loads.

For sign convention and coordinate axis see Fig. 2.3.1 and Fig. 5.1.1.

Input: Details of input data are given on the following pages

Output: I) Geometrical properties
II) Material properties
III) Load data
IV) Reactions: shear intensity
normal force intensity
singular normal force at layer ends
normal forces, bending moments
V) Strains, slip

Input data

90

1	5	10	15	20	30	40	50	60	70	80
N1	N2	N3								

N1 = number of layers (I-Format)

N2 = number of interfaces (I-Format)

N3 = number of steps for $\chi_{SI} = \frac{\chi}{BL}$ (I-Format) [$0 \leq \chi_{SI} \leq 0.5$]

	EM	BL	P	XSIA		
--	----	----	---	------	--	--

EM = Youngs modulus in kg/cm^2 (E-Format)

BL = Length of beam in cm (F-Format)

P = Point load at x_A in kg (F-Format)

XSIA = Point of load application = $\frac{x_A}{BL}$ (F-Format)

A(1)	A(2)		A(I)	A(N1)	BI(1)	BI(2)
	BI(I)		BI(N1)	H(1)	H(2)	H(I)
	H(N1)	B(1)	B(2)	B(I)		B(N2)

A (I) = Area of layers in cm^2 (F-Format)

BI (I) = Moment of inertia of layers in cm^4 (F-Format)

H (I) = Thickness of layers in cm (F-Format)

B (I) = Distance of center lines of layers in cm (F-Format)

SK(1)	SK(2)		SK(I)	SK(N2)	
-------	-------	--	-------	--------	--

SK (I) = Shear moduls of connecting material in kg/cm^2 (E-Format)

As example the multilayer sandwich beam of chapter 5.2 with $NI = 5$ layers was chosen

5	10	15	20	30	40	50	60	70	80
5	4	20							
		3.00000E+06	200.0	100.0	0.25				
	1.0	1.0	1.0	1.0	1.0	1.0	0.0834	0.0834	0.0834
	0.0834	0.0834	1.0	1.0	1.0	1.0	1.0	1.0	1.0
	1.0	1.0	1.0						
	1.000E+03	1.000E+03	1.000E+03	1.000E+03					

N1=NUMBER OF LAYERS
 N2=N1-1 NUMBER OF INTERFACES
 N3=NUMBER OF STEPS OF XSI,MAX.NUMBER 20
 N=NUMBER OF FOURIERTERMS TO OBTAIN ACCURACY EPS
 EPS=ACCURACY OF FOURIERTERMS
 A(I)=AREA OF LAYER
 BI(I)=MOMENT OF INERTIA OF LAYERS
 EM=YOUNGS MODULUS
 B(I)=DISTANCE BETWEEN CENTERLINES OF LAYERS
 H(I)=THICKNESS OF LAYERS
 SK(I)=SHEARMODULUS OF CONNECTING MATERIAL (F.E.STUDS,GLUE,.....)
 RL=TOTAL LENGTH OF BEAM
 XSI=X/RL COORDINATES COUNTING FROM LEFT END
 XSIA=POINT OF LOADAPPLICATION
 P=POINTLOADS AT XSIA AND 1-XSIA

R E A C T I O N S

V(I,J)=SHEARINTENSITY
 SN(I,J)=NORMALFORCES AT INTERFACES
 SNS(I)=SINGULAR NORMALFORCES AT INTERFACES
 PN(I,J)=NORMALFORCES IN LAYERS
 BM(I,J)=BENDINGMOMENTS IN LAYERS
 STU(I,J)=STRAINS IN UPPER FIBRE OF LAYER
 STL(I,J)=STRAINS IN LOWER FIBRE OF LAYER
 SLIP(I,J)=RELATIVE DISPLACEMENT OF ADJACENT POINTS OF TOUCHING LAYERS

BEGIN STORAGE RESERVATION AND READING OF DATA

DIMENSION A(30),BI(30),B(30),H(30),SK(30),XSI(21),C1(30),C2(30),
 CC1(30),CC2(30),CC3(30),CC4(30),CC5(30),CC6(30),V(30,21),
 SN(30,21),SNS(30),PN(30,21),BM(30,21),STU(30,21),STL(30,21),
 SLIP(30,21),RF(300),F(30,30),D(30,30),LL(30),MM(30),D1(30,30)
 READ(5,2) N1,N2,N3
 2 FORMAT(3(I5))
 READ(5,3) EM,RL,P,XSIA
 3 FORMAT(F20.5,3(F10.0))
 READ(5,4) (A(I),I=1,N1),(BI(I),I=1,N1),(H(I),I=1,N1),
 S(P(I),I=1,N2)
 4 FORMAT(8F10.0)
 READ(5,5) (SK(I),I=1,N2)
 5 FORMAT(8E10.3)

BEGIN BUILD BE-MATRIX,INVERT BE-MATRIX AND BUILD E-MATRIX

DO 9 I=1,N2
 K1=I-1
 K2=I+1
 DO 10 J=1,N2


```

LLL=(J-1)*N2+I
BE(LLL)=0.0
IF(J.EQ.K1) GOTO 11
IF(J.EQ.I) GOTO 12
IF(J.EQ.K2) GOTO 13
GOTO 10
11 BE(LLL)=1.0/BI(I)
GOTO 10
12 BE(LLL)=-1.0/BI(I)-1.0/BI(K2)
GOTO 10
13 BE(LLL)=1.0/BI(K2)
10 CONTINUE
10 CONTINUE
CALL MINV(BE,N2,HH,LL,MM)
DO 19 I=1,N2
DO 20 J=1,N2
K1=J-1
K2=J+1
MM1=(J-1)*N2+I
MM11=(J-2)*N2+I
MM12=J*N2+I
IF(J.EQ.1) GOTO 21
IF(J.EQ.N2) GOTO 22
GOTO 23
21 E(I,J)=-BE(MM1)*0.5*H(J)/BI(J)+(BE(MM1)-BE(MM12))*0.5*H(K2)/BI(K2)
GOTO 20
22 E(I,J)=(BE(MM11)-BE(MM1))*0.5*H(J)/BI(J)+BE(MM1)*0.5*H(K2)/BI(K2)
GOTO 20
23 E(I,J)=(BE(MM11)-BE(MM1))*0.5*H(J)/BI(J)+(BE(MM1)-BE(MM12))*0.5*
H(K2)/BI(K2)
20 CONTINUE
19 CONTINUE

```

MATRIX E IS BUILT
 BEGIN MAIN PART OF PROGRAM=DETERMINE REACTIONS

```

PSI=3.141592654
SUMBI=0.0
DO 30 I=1,N1
SUMBI=SUMBI+BI(I)
30 CONTINUE
DELXSI=0.5/FLOAT(N3)
NM=N3+1
DO 40 I=1,NN
XSI(I)=DELXSI*(FLOAT(I)-1.0)
CONTINUE
BOUND1=XSIA/DELXSI+1.0
D1=P*PL*PL/(4.0*EM*SUMBI)
D2=P*BL/SUMBI
DO 50 I=1,N2
K1=I+1
D3=D2*BI(I)
D4=D1*(H(I)+H(K1))
SNS(I)=0.0
DO 51 J=1,NN
BOUND2=FLOAT(J)
V(I,J)=0.0
SN(I,J)=0.0
RN(I,J)=0.0
IF(BOUND2.GE.BOUND1) GOTO 52
RM(I,J)=D3*XSI(J)
SLIP(I,J)=D4*(XSI(J)*XSI(J)+XSIA*XSIA-XSIA)
GOTO 51
52 RM(I,J)=D3*XSIA
SLIP(I,J)=D4*(2.0*XSIA*XSI(J)-XSIA)
51 CONTINUE
50 CONTINUE
D5=D2*BI(N1)
DO 60 J=1,NN
BOUND2=FLOAT(J)
RN(N1,J)=0.0
IF(BOUND2.GE.BOUND1) GOTO 61
RM(N1,J)=D5*XSI(J)
GOTO 60

```

```

61 BM(N1,J)=D5*XSIA
60 CONTINUE
C
C
C BEGIN TO EVALUATE FOURIERCONSTANTS AND FUNCTIONVALUES
DO 70 I=1,N2
K1=I-1
K2=I+1
DO 71 J=1,N2
IF (J.EQ.K1) GOTO 72
IF (J.EQ.I) GOTO 71
IF (J.EQ.K2) GOTO 73
D1(I,J)=B(J)
GOTO 71
72 D1(I,J)=B(K1)-SUMBI/(A(I)*B(I))
GOTO 71
73 D1(I,J)=B(K2)-SUMBI/(A(K2)*B(I))
71 CONTINUE
70 CONTINUE
C
C
C ALL TERMS OF MATRIX D ARE EVALUATED EXCEPT DIAGONAL TERMS
BEGIN DO-LOOP FOR N
N=1
200 F1=2.0*FLOAT(N)-1.0
F2=PSI*PSI*F1*F1/(BL*BL)
F3=BL/F1
DO 80 I=1,N2
K1=I+1
C2(I)=F3
DO 80 J=1,N2
IF (I.EQ.J) GOTO 79
D(I,J)=D1(I,J)
GOTO 80
79 D(I,J)=B(I)+SUMBI*(1.0/A(I)+1.0/A(K1))/B(I)+SUMBI*EM*F2/(B(I)*
$SK(I))
80 CONTINUE
CALL SOLVE(D,C2,ID,N2,30)
IF (N.GT.1) GOTO 90
DO 89 I=1,N2
C1(I)=C2(I)
89 CONTINUE
90 A1=F1*PSI*XSIA
A2=SIN(A1)
A3=-4.0*P*F1*A2/(BL*BL)
A4=4.0*P*A2/(PSI*BL)
A5=4.0*P*A2/(F1*PSI*PSI)
A8=BL/(EM*PSI*F1)
DO 100 I=1,N2
CC2(I)=0.0
DO 101 J=1,N2
101 CC2(I)=CC2(I)+E(I,J)*C2(J)
CONTINUE
CC1(I)=A4*CC2(I)
CC2(I)=A3*CC2(I)
100 CC3(I)=CC2(I)*A4/A3
CONTINUE
CC4(1)=A5*CC2(1)
CC4(N1)=-A5*CC2(N2)
DO 110 I=2,N2
K=I-1
110 CC4(I)=(C2(I)-C2(K))*A5
CONTINUE
A6=0.0
DO 120 I=1,N2
120 A6=A6+B(I)*C2(I)
CONTINUE
A7=A5*A6/SUMBI
DO 130 I=1,N1
130 CC5(I)=BI(I)*A7
CONTINUE
DO 140 I=1,N2
K=I+1

```

```

CC6(I)=A8*(CC4(I)/A(I)-CC4(K)/A(K)+H(K)*CC5(K)/(2.C*BI(K))+H(I)*
CC5(I)/(2.C*BI(I)))
140 CONTINUE
DO 150 J=1,NN
F4=F1*PSI*XS(I,J)
F5=SIN(F4)
F6=COS(F4)
DO 151 I=1,N1
IF (I.EQ.N1) GOTO 152
V(I,J)=V(I,J)+CC1(I)*F6
SN(I,J)=SN(I,J)+CC2(I)*F5
SLIP(I,J)=SLIP(I,J)+CC6(I)*F6
152 BN(I,J)=BN(I,J)+CC4(I)*F5
BM(I,J)=BM(I,J)-CC5(I)*F5
151 CONTINUE
150 CONTINUE
DO 160 I=1,N2
SNS(I)=SNS(I)+CC3(I)
160 CONTINUE

CHECK ACCURACY OF CONSTANTS C2(I)

K=1
EPS=0.00001
180 IF (C2(K).GT.EPS*C1(K)) GOTO 170
IF (K.FQ.N2) GOTO 190
K=K+1
GOTO 180
170 N=N+1
GOTO 200

CALCULATE STRAINS WITH BN AND BM

190 DO 191 I=1,N1
F7=1.C/(FM*A(I))
F8=0.5*H(I)/(FM*BI(I))
DO 191 J=1,NN
F9=BN(I,J)*F7
F10=BM(I,J)*F8
STU(I,J)=F9-F10
STL(I,J)=F9+F10
191 CONTINUE

DATA OUTPUT FOLLOWS

WRITE(6,210)
21. FORMAT(8HNO. LAYER AREA MOM. OF INERTIA THICKNESS DISTANCE
OF CENTER LAYERSHEARMODULUS //)
DO 220 I=1,N1
IF (I.EQ.N1) GOTO 221
WRITE(6,222) I,A(I),BI(I),H(I),B(I),SK(I)
GOTO 220
221 WRITE(6,223) I,A(I),BI(I),H(I)
220 CONTINUE
222 FORMAT(I6,E12.3,E15.4,E12.4,E19.4,E19.4)
223 FORMAT(I6,E12.3,E15.4,E12.4)
WRITE(6,230)
230 FORMAT(50H1 E-MODUL LOAD LOADPOINT BEAMLENGTH //)
WRITE(6,231) FM,P,XSIA,BL
231 FORMAT(4F12.5)
WRITE(6,240)
240 FORMAT(30H1 R E S U L T S //)
WRITE(6,241) N
241 FORMAT(26HNUMBER OF FOURIER TERMS N=,I3,/)
WRITE(6,250)
250 FORMAT(1H1,*IFACE XSI SHEARINTENSITY NORMLAYFORCE LA
YENDFORCE SLIP*//)
DO 260 I = 1, N2
DO 261 J = 1, NN
WRITE(6,270) I, XSI(J), V(I,J), SN(I,J), SNS(I), SLIP(I,J)
261 CONTINUE
WRITE(6,271)
260 CONTINUE
270 FORMAT (I6, F7.3, 4(F17.6))

```

```
271 FORMAT (1H //)
WRITE (6, 280)
280 FORMAT(1H1,*LAYER      XSI      NORMALFORCE      BENDINGMOMENT      UPPER STR
$AIN      LOWER STRAIN*//)
DO 290 I = 1, N1
DO 291 J = 1, NN
WRITE (6, 292) I, XSI(J) , BN(I,J), BM(I,J),STU(I,J),STL(I,J)
291 CONTINUE
WRITE (6, 271)
290 CONTINUE
292 FORMAT (I7, F8.3, 4(E15.6))
STOP
END
```

CD TOT 0311

Appendix B

Details of the shear wall program with piecewise trapezoidal load

Introduction: The program analyzes the multipier shear wall under piecewise trapezoidal loading.

For sign convention and coordinate axes. Fig. 2.3.1.

Input: Details of the input data are given on the following pages

Output: I) Geometrical properties
II) Material properties
III) Load data
IV) Shear modulus of connecting medium and stiffness parameter
V) Reactions: Shear forces and normal forces in connecting beams, bending moments and normal forces in piers
VI) Deflection for actual and complete interaction, total bending moment

Input data

98

1	5	10	15	20	30	40	50	60	70	80
NP										

NP = number of problems (I-Format)

N1	N2	N3	NN1						
----	----	----	-----	--	--	--	--	--	--

N1 = number of piers (I-Format)

N2 = number of interfaces (I-Format)

N3 = number of stories (I-Format)

NN1 = number of trapezoidal sections (I-Format)

	EM	GE	BL1	AS			
--	----	----	-----	----	--	--	--

EM = Youngs modulus in Mp/m^2 (E-Format)

GE = Ratio of shear modulus to EM (F-Format)

BL1 = Shear wall height (F-Format)

AS = Story height in m (F-Format)

A(1)		A(N1)	BI(1)		BI(N1)	H(1)	
	H(N1)	AB(1)		AB(N2)	BIB(1)		BIB(N2)
BLB(1)		BLB(N2)	B(1)		B(N2)		

A (I) = Area of piers in m^2 (E-Format)

BI (I) = Moment of inertia of piers in m^4 (F-Format)

H (I) = Width of piers in m (F-Format)

AB (I) = Effective shear area of connecting beams in m^2 (F-Format)

BIB (I) = Moment of inertia of connecting beams in m^4 (F-Format)

BLB (I) = Length of connecting beams in m (F-Format)

B (I) = Distance of center lines of piers in m (F-Format)

1	1o	2o	3o	4o	5o	6o	7o	8o
	P1(1)	P2(1)	X1(1)	X2(1)				
	P1(NN1)	P2(NN1)	X1(NN1)	X2(NN1)				

P1 (I) = Load coordinate at XI (I) in Mp/m (F-Format)

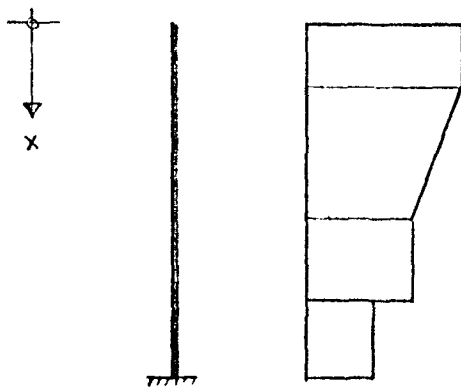
P2 (I) = Load coordinate at X2 (I) in Mp/m (F-Format)

X1 (I) = Begin of trapezoidal section in m (F-Format)

X2 (I) = End of trapezoidal section in m (F-Format)

As example the symmetrical five-pier shear wall of chapter 3.6.2 was chosen.

The load shape is shown below



$x = 0.0 \text{ (m)} \quad q = 7.24 \text{ (Mp/m)}$

$x = 5.2 \text{ (m)} \quad q = 7.24 \text{ (Mp/m)}$

$x = 33.4 \text{ (m)} \quad q = 3.18 \text{ (Mp/m)}$

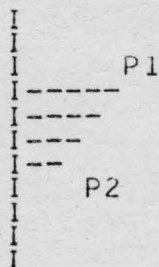
$x = 51.8 \text{ (m)} \quad q = 2.76 \text{ (Mp/m)}$

$x = 70.0 \text{ (m)} \quad q = 2.76 \text{ (Mp/m)}$

1	5	10	15	20	30	40	50	60	70	80
1										
5	4	20	4							
		3.00000 E+06		0.43	70.0	3.5				
	1.0	1.0	1.0	1.0	1.0	1.0	2.1	2.1	2.1	
	2.1	2.1	5.0	5.0	5.0	5.0	5.0	5.0	0.1	
	0.1	0.1	0.1	0.0036	0.0036	0.0036	0.0036	0.0036	1.0	
	1.0	1.0	1.0	6.0	6.0	6.0	6.0			
	7.24	7.24	0.0	5.2						
	7.24	3.18	5.2	33.4						
	3.18	3.18	33.4	51.8						
	2.76	2.76	51.8	70.0						

RUN(S)
 SETINDF.
 REDUCE.
 LGO.

6400 END OF RECORD
 PROGRAM TST (INPUT,OUTPUT,TAPE5=INPUT,TAPE6=OUTPUT)
 MULTIPLIER-SHEARWALL CALCULATED WITH D.E. AND FOURIERSERIES
 LOADCASE PIECEWISE TRAPEZOID LOAD



NP=NUMBER OF PROBLEMS
 N1=NUMBER OF PIERS
 N2=N1-1 NUMBER OF INTERFACES
 N3=NUMBER OF STORIES
 N =NUMBER OF FOURIER TERMS NECESSARY TO OBTAIN ACCURACY EPS
 NN1=NUMBER OF SECTIONS P1-P2
 P1(I),P2(I)=TRAPEZOID LOAD
 X1(I),X2(I)=BEGIN AND END OF TRAPEZOID LOAD

A(I)=AREA OF PIER
 BI(I)=MOMENT OF INERTIA OF PIERS
 AB(I)=EFFECTIVE SHEARAREA OF CONNECTING BEAMS
 BIB(I)=MOMENT OF INERTIA OF CONNECTING BEAMS
 EM=YOUNGS MODULUS
 GE=SHEARMODULUS/EM
 B(I)=DISTANCE BETWEEN CENTERLINES OF PIERS
 H(I)=WIDTH OF PIERS
 BLB(I)=LENGTH OF CONNECTING BEAMS
 AS=STORYHEIGHT
 BL1=HEIGHT OF SHEARWALL
 SK(I)=SHEARMODULUS OF CONNECTING BEAMS

RO(I)=INTERACTIONCOEFFICIENT

R E A C T I O N S

VD(I,J)=SHEARFORCES IN CONNECTING BEAMS (DISCRETE)
 SND(I,J)=NORMAL FORCES IN CONNECTING BEAMS (DISCRETE)
 BN(I,J)=NORMAL FORCES IN PIERS
 BM(I,J)=BENDINGMOMENTS IN PIERS (BELOW CONNECTING BEAM)
 BMU(I,J)=BENDINGMOMENTS IN PIERS (ABOVE CONNECTING BEAM)
 DEFF(I)=DEFLECTION OF SHEARWALL
 DEFC(I)=DEFLECTION OF SHEARWALL (COMPLETE INTERACTIO ASSUMED)

CCC

```

DIMENSION A(20),BI(20),AB(20),BIB(20),B(20),H(20),BLB(20),SK(20),
$ XSI(41),C1(20),C2(20),CC1(20),CC2(20),CC3(20),
$ BN(20,41),BM(20,41),BMO(41),RO(20),
$ VD(20,41),SND(20,41),BMO(20,41),SUMQM(20),SUMQN(20),
$ SUMSND(20),SUMBNM(20),PF(41),PC(41),DEFF(41),DEFC(41),
$ BE(400),E(20,20),D(20,20),D1(20,20),LL(20),MM(20),
$ P1(20),P2(20),X1(20),X2(20),XSI1(20),XSI2(20),X(41)
READ(5,1) NP
1 FORMAT (I5)
DO 400 M=1,NP
READ(5,2) N1,N2,N3,NN1
2 FORMAT (9I5)
READ(5,3) EM,GE,BL1,AS
3 FORMAT (E20.5,3F10.0)
READ(5,4) (A(I),I=1,N1),(BI(I),I=1,N1),(H(I),I=1,N1),
$ (AB(I),I=1,N2),(BIB(I),I=1,N2),(BLB(I),I=1,N2),
$ (B(I),I=1,N2)
4 FORMAT (8F10.0)
WRITE(6,300)
300 FORMAT (1H0,* E-MODULUS G/E SHEARWALLHEIGHT STORYHEI
$GHT*////)
WRITE(6,301) EM,GE,BL1,AS
301 FORMAT (E15.6,3F15.6)
WRITE(6,302)
302 FORMAT (1H1,*PIERNO. PIERAREA MOM.OF INERTIA PIERWIDTH*////)
DO 303 I=1,N1
WRITE(6,304) I,A(I),BI(I),H(I)
303 CONTINUE
304 FORMAT (I7,3E15.6)
WRITE(6,305)
305 FORMAT (1H1,*IFACE CONN.BEAMAREA MOM.OF INERTIA BEAMLENGTH DIST
$ANCE OF PIERCENTERLINES*////)
DO 306 I=1,N2
WRITE(6,307) I,AB(I),BIB(I),BLB(I),B(I)
306 CONTINUE
307 FORMAT (I5,4E15.6)
WRITE(6,310)
310 FORMAT (1H1,* PIECEWISE TRAPEZOID LOAD *////)
DO 320 I=1,NN1
READ(5,325) P1(I),P2(I),X1(I),X2(I)
WRITE(6,330) I,P1(I),P2(I),X1(I),X2(I)
XSI1(I)=0.5*X1(I)/BL1
XSI2(I)=0.5*X2(I)/BL1
320 CONTINUE
325 FORMAT (4F10.0)
330 FORMAT (I5,* P1=*,E15.6,* P2=*,E15.6,* X1=*,F10.4,* X2=*,F10.4)
BL=2.0*BL1
DO 5 I=1,N2
SK(I)=1.0/(AS*BLB(I)**3/(12.0*EM*BIB(I))+AS*BLB(I)/(GE*EM*AB(I)))
WRITE(6,7) I,SK(I)
5 CONTINUE
7 FORMAT (1H0,*SK*,I3,*=*,E15.6)

```

CCC

BEGIN BUILD BE-MATRIX,INVERT BE-MATRIX AND BUILD E-MATRIX

```

DO 9 I=1,N2
K1=I-1
K2=I+1
DO 10 J=1,N2
LLL=(J-1)*N2+I
BE(LLL)=0.0
IF(J.EQ.K1) GOTO 11
IF(J.EQ.I) GOTO 12
IF(J.EQ.K2) GOTO 13
GOTO 10
11 BE(LLL)=1.0/BI(I)
GOTO 10
12 BE(LLL)=-1.0/BI(I)-1.0/BI(K2)
GOTO 10
13 BE(LLL)=1.0/BI(K2)
10 CONTINUE
9 CONTINUE

```

```

CALL MINV(BE,N2,HH,LL,MM)
E(1,1)=BE(1)*(0.5*H(2)/BI(2)-0.5*H(1)/BI(1))
IF (N1.EQ.2) GOTO 25
DO 19 I=1,N2
DO 20 J=1,N2
K1=J-1
K2=J+1
MM1=(J-1)*N2+I
MM11=(J-2)*N2+I
MM12=J*N2+I
IF(J.EQ.1) GOTO 21
IF(J.EQ.N2) GOTO 22
GOTO 23
21 E(I,J)=-BE(MM1)*0.5*(H(J)+BLB(J))/BI(J)+(BE(MM1)-BE(MM12))*0.5*
$(H(K2)+BLB(J))/BI(K2)
GOTO 20
22 E(I,J)=(BE(MM11)-BE(MM1))*0.5*(H(J)+BLB(J))/BI(J)+BE(MM1)*0.5*
$(H(K2)+BLB(J))/BI(K2)
GOTO 20
23 E(I,J)=(BE(MM11)-BE(MM1))*0.5*(H(J)+BLB(J))/BI(J)+(BE(MM1)-
$BE(MM12))*0.5*(H(K2)+BLB(J))/BI(K2)
20 CONTINUE
19 CONTINUE

```

```

MATRIX E IS BUILT
BEGIN MAIN PART OF PROGRAM=DETERMINE REACTIONS

```

```

25 PSI=3.141592654
SUMBI=0.0
DO 30 I=1,N1
SUMBI=SUMBI+BI(I)
30 CONTINUE
DELXSI=0.5/F-OAT(N3)
NN=N3+1
DO 40 I=1,NN
XSI(I)=DELXSI*(FLOAT(I)-1.0)
40 CONTINUE
DO 41 I=1,NN
BMO(I)=0.0
41 CONTINUE
DO 45 I=1,NN1
T1=XSI2(I)-XSI1(I)
T2=BL*BL*(P1(I)-P2(I))/(6.0*T1)
T3=BL*BL*P1(I)/2.0
T4=BL*BL*T1*T1*(P2(I)+2.0*P1(I))/6.0
T5=BL*BL*T1*(P1(I)+P2(I))/2.0
DO 45 J=1,NN
T6=XSI(J)-XSI1(I)
T7=XSI(J)-XSI2(I)
IF (XSI(J).GT.XSI1(I).AND.XSI(J).LT.XSI2(I)) GOTO 46
IF (XSI(J).GE.XSI2(I)) GOTO 47
GOTO 45
46 BMO(J)=BMO(J)+T2*T6**3-T3*T6*T6
GOTO 45
47 BMO(J)=BMO(J)-T4-T5*T7
45 CONTINUE
DO 60 I=1,N1
DO 60 J=1,NN
IF (I.EQ.N1) GOTO 61
VD(I,J)=0.0
SND(I,J)=0.0
61 BN(I,J)=0.0
BM(I,J)=BI(I)*BMO(J)/SUMBI
60 CONTINUE

```

```

BEGIN TO EVALUATE FOURIERCONSTANTS AND FUNCTIONVALUES

```

```

DO 70 I=1,N2
K1=I-1
K2=I+1
RO(I)=SK(I)*BL*BL*(B(I)*B(I)/SUMBI+1.0/A(I)+1.0/A(K2))/(EM*PSI*
$PSI)
DO 71 J=1,N2
IF (J.EQ.K1) GOTO 72

```



```

IF (J.EQ.I) GOTO 71
IF (J.EQ.K2) GOTO 73
D1(I,J)=B(J)
GOTO 71
72 D1(I,J)=B(K1)-SUMBI/(A(I)*B(I))
GOTO 71
73 D1(I,J)=B(K2)-SUMBI/(A(K2)*B(I))
71 CONTINUE
70 CONTINUE

```

ALL TERMS OF MATRIX D ARE EVALUATED EXCEPT DIAGONAL TERMS

BEGIN DO-LOOP FOR N

```

C
C
C
C
C
N=1
Z=1.0
200 F1=2.0*FLOAT(N)-1.0
F2=PSI*PSI*F1*F1/(BL*BL)
F3=BL/F1
F31=F3/PSI
DO 80 I=1,N2
K1=I+1
C2(I)=F3
DO 80 J=1,N2
IF (I.EQ.J) GOTO 79
D(I,J)=D1(I,J)
GOTO 80
79 D(I,J)=B(I)+SUMBI*(1.0/A(I)+1.0/A(K1))/B(I)+SUMBI*EM*F2/(B(I)*
$SK(I))
80 CONTINUE
CALL SOLVE(D,C2,ID,N2,20)
IF (N.GT.1) GOTO 90
DO 89 I=1,N2
C1(I)=C2(I)
89 CONTINUE
90 DO 91 I=1,N2
CC1(I)=0.0
91 CONTINUE
Z=Z*(-1.0)
DO 95 I=1,NN1
R1=XSI2(I)-XSI1(I)
R2=P2(I)-P1(I)
R3=P1(I)*XSI1(I)-R2*XSI1(I)*XSI1(I)/(R1*R1)
R4=-P1(I)+R2*XSI1(I)/R1
R5=0.5*R2/R1
R6=0.5*(P2(I)+P1(I))*R1
R7=4.0/PSI
G1=R7*(R3+R4*XSI2(I)+R5*XSI2(I)*XSI2(I)-R6
G2=2.0*R7*R5/(PSI*PSI)
G3=R7*(R3+R4*XSI1(I)+R5*XSI1(I)*XSI1(I))
G4=R7*(R4+2.0*XSI2(I)*R5)/PSI
G5=R7*(R4+2.0*XSI1(I)*R5)/PSI
R8=F1*PSI*XSI1(I)
R9=F1*XSI2(I)
G6=G2/(F1*F1)
R10=(G1-G6)*SIN(R9)-(G3-G6)*SIN(R8)+G4*COS(R9)/F1-G5*COS(R8)/F1
$-Z*4.0*R6/PSI
DO 95 J=1,N2
CC1(J)=CC1(J)+R10*C2(J)
95 CONTINUE
R11=(-F1)*PSI/BL
DO 104 I=1,N2
CC3(I)=0.0
DO 105 J=1,N2
CC3(I)=CC3(I)+E(I,J)*CC1(J)
105 CONTINUE
CC2(I)=R11*CC3(I)
104 CONTINUE
DO 150 J=1,NN
IF (J.EQ.1) GOTO 152
IF (J.EQ.NN) GOTO 153
F41=F1*PSI*(XSI(J)+0.5*DELXSI)
F42=F1*PSI*(XSI(J)-0.5*DELXSI)
GOTO 154

```

```

152 F41=F1*PSI*0.5*DELXSI
    F42=0.0
    GOTO 154
153 F41=F1*PSI*XSI(J)
    F42=F1*PSI*(XSI(J)-0.5*DELXSI)
154 F51=F31*(SIN(F41)-SIN(F42))
    F61=F31*(COS(F42)-COS(F41))
    DO 151 I=1,N2
    VD(I,J)=VD(I,J)+CC1(I)*F51
    SND(I,J)=SND(I,J)+CC2(I)*F61
151 CONTINUE
150 CONTINUE
    DO 160 I=1,N2
    SND(I,1)=SND(I,1)+CC3(I)
160 CONTINUE

```

105

```

C
C
C CHECK ACCURACY OF CONSTANTS C2(I)

```

```

    K=1
    EPS=0.00001
165 IF(C2(K).GT.EPS*C1(K)) GOTO 170
    IF (K.EQ.N2) GOTO 162
    K=K+1
    GOTO 165
170 N=N+1
    GOTO 200
162 SUMA=0.0
    DO 186 I=1,N1
    SUMA=SUMA+A(I)
186 CONTINUE
    YS=0.0
    SUMB=0.0
    DO 187 I=1,N2
    K=I+1
    SUMB=SUMB+B(I)
    YS=YS+SUMB*A(K)
187 CONTINUE
    YS=YS/SUMA
    BITOT=SUMBI+YS*YS*A(1)
    DIST=YS
    DO 188 I=2,N1
    K=I-1
    DIST=DIST-B(K)
    BITOT=BITOT+DIST*DIST*A(I)
188 CONTINUE

```

```

C
C
C CALCULATE BENDINGMOMENTS AND NORMALFORCES IN PIERS

```

```

    DO 192 I=1,N1
    SUMQM(I)=0.0
    SUMQN(I)=0.0
    SUMSND(I)=0.0
    SUMBNM(I)=0.0
192 CONTINUE
    DO 196 I=1,N1
    K=I-1
    DO 196 J=1,NN
    BMU(I,J)=BM(I,J)+SUMQM(I)+SUMBNM(I)
    IF (I.EQ.1) GOTO 193
    IF (I.EQ.N1) GOTO 194
    IF (J.EQ.NN) GOTO 197
    SUMQM(I)=SUMQM(I)-0.5*(H(I)+BLB(I))*VD(I,J)-0.5*(H(I)+BLB(K))*
    $VD(K,J)
197 SUMSND(I)=SUMSND(I)+SND(I,J)-SND(K,J)
    SUMQN(I)=SUMQN(I)+VD(I,J)-VD(K,J)
    GOTO 195
193 IF (J.EQ.NN) GOTO 198
    SUMQM(I)=SUMQM(I)-0.5*(H(I)+BLB(I))*VD(I,J)
198 SUMSND(I)=SUMSND(I)+SND(I,J)
    SUMQN(I)=SUMQN(I)+VD(I,J)
    GOTO 195
194 IF (J.EQ.NN) GOTO 199
    SUMQM(I)=SUMQM(I)-0.5*(H(I)+BLB(K))*VD(K,J)
199 SUMSND(I)=SUMSND(I)-SND(K,J)

```

```

SUMQN(I)=SUMQN(I)-VD(K,J)
195 BM(I,J)=BM(I,J)+SUMQM(I)+SUMBNM(I)
IF (J.EQ.NN) GOTO 201
BN(I,J)=BN(I,J)+SUMQN(I)
GOTO 202
201 BN(I,J)=BN(I,N3)
202 SUMBNM(I)=SUMBNM(I)+SUMSND(I)*AS
196 CONTINUE

```

106

C
C
C
CALCULATE DEFLECTION

```

DEFF(NN)=0.0
DEFC(NN)=0.0
SUMPF=0.0
SUMPC=0.0
DO 205 I=1,N3
K=I+1
PF(I)=-AS*0.5*(BMU(1,K)+BM(1,I))/(EM*BI(1))
PC(I)=-0.5*AS*(BMO(K)+BMO(I))/(EM*BITOT)
205 CONTINUE
DO 206 I=1,N3
K1=NN-I
K2=K1+1
DEFF(K1)=DEFF(K2)+SUMPF+0.5*AS*PF(K1)
DEFC(K1)=DEFC(K2)+SUMPC+0.5*AS*PC(K1)
SUMPF=SUMPF+AS*PF(K1)
SUMPC=SUMPC+AS*PC(K1)
206 CONTINUE

```

C
C
C
OUTPUT OF RESULTS

```

WRITE(6,210)
210 FORMAT(1H1,*          R E S U L T S *////)
WRITE(6,215) N,EPS
215 FORMAT(1HC,*NUMBER OF FOURIER TERMS N=*,I3,*   WITH ACCURACY EPS=*,
$F11.7,////)
DO 216 I=1,N2
WRITE(6,217) I,RO(I)
216 CONTINUE
217 FORMAT(1HU,*RO*,I3,*=*,E15.6)
240 FORMAT(////)
WRITE(6,245)
245 FORMAT(1H1,*IFACE   X          SHEAR IN CONN.BEAMS NORMAL FORCE IN CON
$N.BEAM*////)
DO 250 I=1,N2
DO 255 J=1,NN
WRITE(6,260) I,X(J), VD(I,J),SND(I,J)
255 CONTINUE
WRITE(6,240)
250 CONTINUE
260 FORMAT(I6,F8.3,2E20.6)
WRITE(6,265)
265 FORMAT(1H1,*PIERNO.   X   BENDINGMOMENT          BENDINGMOMENT
$NORMALFORCE IN PIER*)
WRITE(6,266)
266 FORMAT(1HU,*          ABOVE CONNECT.BEAM  BELOW CONNECT.BEAM*/
$///)
DO 270 I=1,N1
DO 272 J=1,NN
WRITE(6,275) I,X(J), BMU(I,J),BM(I,J),BN(I,J)
272 CONTINUE
WRITE(6,240)
270 CONTINUE
275 FORMAT(I6,F8.3,3E20.6)
WRITE(6,280)
280 FORMAT(1H1,*          X   DEFLECTION SHEARWALL DEFL.(COMPL.INTERACT.)
$          BMO*////)
DO 285 J=1,NN
WRITE(6,290) X(J), DEFF(J),DEFC(J),BMO(J)
285 CONTINUE
290 FORMAT(F8.3,3E20.6)
400 CONTINUE
STOP
END

```


- (1) Beck, H. "Ein neues Berechnungsverfahren für gegliederte Scheiben, dargestellt am Beispiel des Vierendeelträgers", Der Bauingenieur, 1956, Vol. 31, pp. 436-443.
- (2) Beck, H. "Ein Beitrag zur Berücksichtigung der Dehnungsverformung bei Rahmen mit schlanken und gedrunenen Konstruktionsgliedern", Die Bautechnik, 1959, Vol. 36, pp. 178-184.
- (3) Beck, H. "Ein Beitrag zur Berechnung regelmäßig gegliederter Scheiben", Ingenieur Archiv, 1958, Vol. 36, pp. 343-357.
- (4) Eriksson, O. "Analysis of Wind Bracing Walls in Multi-Storey Housing". Ingeniøren-International Edition, 1961, Vol. 5, pp. 115-124
- (5) Eisert, H. D. " Ein Beitrag zur Berechnung mehrfeldriger Windrahmen als gegliederte Scheiben", Phd-thesis, 1967, Faculty of Civil Engineering, TH Darmstadt.

- (6) Despeyroux, J. "Analyse statique et dynamique des contreventements par consoles élémentaires solidarisée par des milieux élastiques", International Association for Bridge and Structural Engineering publications, 1969, Vol. 29-II, pp. 53-66.
- (7) Adekola, A. O. "Partial interaction between elastically connected elements of a composite beam", Int. J. Solids Structures, 1968, Vol. 4, pp. 1125-1135.